Title	Studies on Separation and Purification Processes of Rare Metals Using Advanced Liquid-Liquid Extraction Systems
Author(s)	西浜, 章平
Citation	大阪大学, 2001, 博士論文
Version Type	VoR
URL	https://doi.org/10.11501/3184158
rights	
Note	

Studies on Separation and Purification Processes of Rare Metals Using Advanced Liquid-Liquid Extraction Systems

SYOUHEI NISHIHAMA

Department of Chemical Science and Engineering
Graduate School of Engineering Science
Osaka University
2001

Preface

This dissertation work was carried out under the joint supervision of Professor Dr. Isao Komasawa and Associate Professor Dr. Takayuki Hirai at the Department of Chemical Science and Engineering, Graduate School of Engineering Science, Osaka University from 1996 to 2001.

The objective of this thesis is to develop the advanced liquid-liquid extraction system for the separation and purification of rare metals. The design of the extraction process, based on the equilibrium theories and precise material balance, was firstly carried out. Two types of the advanced extraction systems, combined with the masking reaction or photochemical reduction, were then employed. The variation in the distribution ratio can be predicted by the proposed extraction scheme, enabling the separation process of the rare metals to be designed. The author hopes that the results obtained in this work give some suggestions for the design of liquid-liquid extraction system for the separation of rare metals on the industrial scale.

Syouhei Nishihama

Department of Chemical Science and Engineering

Graduate School of Engineering Science

Osaka University

Toyonaka 560-8531, Japan

Contents

General Introduction

Liquid-liquid extraction is one of the major methods for separation, purification, and recovery of rare metals on industrial scale. The demand for rare metals, especially having high purity, becomes higher in recent years, and thus the construction of high selective separation process using liquid-liquid extraction technique becomes an important problem. There are many investigations of the separation processes using the liquid-liquid extraction, and the results have been summarized in several reviews.[1-10] The liquid-liquid extraction technique is based on the difference in the ability for the complex formation between the extractant and the metals, and thus, the extractability and separation ability depend on the structure of the extractant, especially the steric effect.[11-19] Recently, molecular modeling for the extracted species using molecular mechanics (MM) calculation has been investigated.[20-23] The knowledge obtained from these investigations is expected to develop the new extractants with effective ligands for the separation of rare metals. In recent years, macrocyclic ligands having the ion size selectivity, such as crown ethers[24] and calixarenes,[25,26] have been studied as possible candidates for the extractant in the industrial process.

The determination of the extraction equilibrium formulations is important for design of the extractive separation process based on the equilibrium theory. One of the major methods for the determination of the formulations is the slope analysis method. This method, however, can only be used under conditions: (1) no polymeric species are formed in either phase, (2) activity coefficients of the species are essentially constant, (3) the formation of intermediate non-extractable complex can be neglected, (4) no adduct formation between complexes and undissociated extractant molecules or the organic diluent or modifier takes place, and (5) all hydrolysis reactions are insignificant.[27] However, the formation of aggregated species, at the high loading ratios of the extractant, was pointed out in 1976.[28] There are few reports concerning the extraction equilibrium in such a high loading region, although it is very important from the industrial point of view.[29,30] In the industrial extractive separation process, a mixer-settler cascade is mainly used as the extraction equipment.[31] There are two ways for the design of the separation process with the mixer-settler cascade, that is, the McCabe-Thiele method and a simulation method. In the cation-exchange type extractant system, however, two-dimensional coordinate cannot be used, because the extraction curve changes with the equilibrium pH value, and three-dimensional coordinate must be used

1

in the McCabe-Thiele diagram.[2] The simulation method can be easily applied to the design of extractive separation process in all extraction system, because it is based on the extraction equilibrium formulations determined. The effect of the magnitude of the extraction equilibrium constant[32] and the effect of the each equilibrium constant in the system[33] have been reported. Goto has investigated the simulation method based on the extraction equilibrium formulations in a low loading region.[34] The simulation method for the design of industrial separation processes, however, should be carried out based on the extraction equilibrium formulations over whole range of the loading ratios, which cover the conditions from inlet to outlet of the mixer-settler cascade.

There are some metals for which a separation using such extraction system based on the equilibrium theory is difficult. In these cases, the conversion of both aqueous- or organic-phase species by functional chemical reaction during actual extraction has proved very effective in improving the separation obtained for such metal species. In the case of the aqueous phase species, (1) a redox reaction of the metal ions, (2) a masking reaction with water-soluble complexing agents, and (3) a complexing reaction with salting out agents are all possible feasible solutions. The redox reaction for metal ions has been widely applied in the separation of U/Pu in the Purex process, employed commercially in the nuclear industry.[35] Such reactions are based on the principle that metal ions, having different valences, behave like different elements with respect to their extractability. In the case of the masking reaction for the metal ions with a water-soluble complexing agent, a part of the metals in the aqueous phase is complexed and thus hindered in the extraction. There are two ways for improving the separation by combining the masking reaction with water-soluble complexing agent: (1) in equilibrium state and (2) in non-equilibrium state. The separation abilities are based on the difference in the ability for the complex formation between the metals and the agent in the equilibrium state, and on the difference in the rate of complexing reaction in the non-equilibrium state. Matsuyama et al. have briefly reviewed such extraction system, in the presence of complexing agents, for separation of rare earth metals.[36] Salting out agents are generally used in amine and ammonium salt extractant systems, as a high selective separation can be also achieved by a modification of the metal ion, using the salting out agent. A typical extraction process consists of the separation of Co/Ni from chloride solution, with tri-n-octyl amine (TOA).[37] In this system, the extraction of Ni with TOA does not progress, since the Ni

2

does not form an anionic chloro complex. The selective separation of Co/Ni, therefore, is achieved from the aqueous solution of high chloride concentration.

In the case of the treatment in the organic phase, there three differing reaction possibilities may exist. These are (1) modification of the extractant or of the extracted species, using the diluents and modifiers, (2) a synergistic effect, obtained by adding additional extractants, and (3) a redox reaction for the extracted species. A diluent is normally employed to decrease the viscosity of the extractant solution, to provide a suitable concentration for the extractant, to decrease the emulsion-forming tendencies of the extractant, and/or to improve the dispersion and coalescence properties of the solvent. A modifier may also be used in order to overcome the formation of a third phase, of which formation is essentially a solubility problem of the diluent. Both the diluent and modifier affect the extractant and extracted species, such that the extractability or extraction equilibrium formulation is often made to change dramatically. Synergistic extraction systems have been investigated widely in attempts to take advantage of the synergistic effect, especially in the nuclear field with bis(2-ethylhexyl)phosphoric acid (D2EHPA)/tri-n-butyl phosphate (TBP) and thenoyltrifluoroacetone (Htta)/TBP.[38] The system was summarized in several reviews.[39-43] The redox reaction for the extracted species was recently paid attention for the separation of rare metals.

The main purpose of this thesis is to develop the advanced liquid-liquid extraction system for the separation and purification of rare metals by combining the functional chemical reactions. Firstly, the method for the design of the liquid-liquid extraction process based on the equilibrium theory was investigated. The advanced extraction systems, combined with the masking reaction or photochemical reduction, were then employed for more selective separation of the rare metals.

The thesis consists of the following three chapters.

In chapter I, the method for the design of the liquid-liquid extraction process with the simulation method based on the extraction equilibrium formulations which are properly determined is investigated. The separation and recovery of Ga and In from zinc refinery residue is investigated as a case study. In the extraction of Ga and In, the co-extraction of anions in the aqueous phase, chloride and hydroxyl ions, should be considered. The extraction equilibrium formulations for the two rare metals, in which the effect of chloride and hydroxyl ions is taken into account, are determined up to high loading ratios. The interaction

3

between the metals in the binary metal system was also investigated. The separation and recovery process of the two metals from the zinc refinery residue with the counter-current mixer-settler cascade is then investigated by using the simulation based in the extraction equilibrium formulations and material balance.

In chapter II, the liquid-liquid extraction system, combined with the masking reaction with water-soluble complexing agent, is investigated. The method for the determination of the extraction equilibrium formulation is investigated, by considering the complexing reaction between the metals and the agents. The design of the extraction process in the presence of the water-soluble complexing agent is then carried out. In this work, the separation of rare earth metals is carried out as a case study, employing ethylenediaminetetraacetic acid (EDTA) and diethylenetriaminepentaacetic acid (DTPA) as the agent.

In chapter III, the liquid-liquid extraction system combined with the photochemical reduction of the target metals is investigated. The mechanism of the extraction system is made clear based on the kinetic studies, enabling the variation of the distribution ratio with the photoirradiation to be quantitatively expressed. In this work, the photoreductive stripping of Fe(III) and photoreductive extraction of V(V) are carried out as case studies. In addition, the applications of the extraction system for the selective separation of the Fe and the stripping of Co, which is difficult in the stripping due to its auto-oxidation in the organic phase, are then investigated for the demonstration of the usefulness of the photochemical reduction.

The results obtained in this work are summarized in general conclusions.

Chapter I

Design of the Liquid-Liquid Extraction Process

Based on the Equilibrium Theory

~ Separation and Recovery of Ga and In from Zinc Refinery Residue ~

1. Introduction

For the design of the liquid-liquid extraction process based on the equilibrium theory, with the simulation method, the extraction equilibrium must be formulated under the proper ranges, which cover the commercial operations. The formulations, therefore, should be determined up to high loading ratios. In addition, the interactions among the metals, such as the co-extraction of metal species and other ions, should be included in the extraction equilibrium formulations. In this chapter, the determination of the extraction equilibrium formulations, which include the interaction between the metals in the binary metal system, up to high loading ratios is firstly investigated. The design of the liquid-liquid extraction process with the simulation method, based on the extraction equilibrium formulations, is then carried out.

The separation and recovery of Ga and In from zinc refinery residue is selected as a case study. The demands for Ga and In have increased in recent years because of their use as semiconductor materials such as GaAs or InP. Kikuchi et al. investigated extraction from sulfuric acid solution using octylphenyl phosphoric acid as extractant, and reported that the optimum separation factor for Ga/In was 600 under appropriate conditions.[44] Inoue investigated the extraction of Ga and In from nitrate solution using several acidic organophosphorus compounds as extractants.[45] Extraction equilibrium formulations for each metal and extractant were established at low loading ratios, and it was found that In was extracted as $\overline{InR_3 3(RH)}$ with all extractants, and Ga was extracted as $\overline{GaR_3(RH)}$ with acidic phosphate and phosphonate while as $\overline{GaR_3}$ with acidic phosphinate. Sato et al. conducted the extraction of Ga and In from hydrochloric acid solution with bis(2-ethylhexyl)phosphoric acid and pointed out that Ga extraction proceeds according to a cation exchange reaction at low aqueous acidity, and a solvating reaction at very high acidity, as expected.[46]

One source for the two metals is zinc refinery residue, because both metals are contained as minor components.[47,48] The separation and recovery process of Ga and In from the residue by liquid-liquid extraction has been considered for the commercial application. A recovery process of the two rare metals from the Black Ore types of deposits (a mixture of zinc blende, galena, and others) was considered.[49] In this process, the leach liquor of the residue is treated firstly using H_2S gas to remove copper and arsenic, O_2 gas to remove Fe as hematite, and then NH_3 gas to remove Al. The resulting liquor is extracted with Versatic 10 for the recovery of Ga and In. The recovered Ga is separated from other metals by extraction with ether, and In separated with TBP. This extraction process is rather complicated, and many operations are combined. A simpler recovery process linked to a commercial application must be studied.

In this chapter, the extraction of Ga and In with several acid organophosphorus compounds, such as bis(2-ethylhexyl)phosphoric acid (D2EHPA), 2-ethylhexyl phosphonic acid mono-2-ethylhexyl ester (EHPNA), and bis(2-ethylhexyl)phosphinic acid (PIA-226), was investigated and the extraction equilibrium formulations were determined up to high loading ratios, which is practical importance, by considering the formation of aggregated species. The interaction between the two rare metals in the binary metal extraction systems was also investigated. The scrubbing effect of the metal-loaded organic solution was carried out, and the application of the extraction equilibrium formulations for the scrubbing treatment was investigated. The separation and recovery of the two rare metals was then investigated, based on the formulations which are verified experimentally. Major metal components other than Zn can be removed from leach liquor by extraction with TBP. The remaining liquor then contains the rare metals, Ga and In, and Zn. On the basis of the above equilibrium studies, a simulation study for the separation and recovery of Ga and In from zinc refinery residue was also carried out.

2. Experiment

2.1 Reagents.

Tri-*n*-butyl phosphate (TBP, marketed as TBP), bis(2-ethylhexyl)phosphoric acid (D2EHPA, marketed as DP-8R), 2-ethylhexyl phosphonic acid mono-2-ethylhecxyl ester (EHPNA, marketed as PC-88A) were supplied by Daihachi Chemical Ind. Co., Ltd., Osaka,

Japan, and used without further purification. Bis(2-ethylhexyl)phosphinic acid (PIA-226), having a purity of 97 wt%, was synthesized as reported.[50] D2EHPA, EHPNA, and PIA-226 were diluted in kerosene. It has been shown by a vapor phase osmometric study that the majority of acidic organophosphorus compounds are dimerized in nonpolar diluents such as kerosene.[11,51] The resultant extractant concentration was determined by potentiometric titration method using an automatic titration apparatus (Hiranuma Comtite-550). All inorganic chemicals were supplied by Wako Pure Chemical Industry as analytically pure reagent-grade materials. Deionized water was purified by simple distillation. Aqueous solutions of Ga, In, and Zn were prepared by dissolving $GaCl_3$, $InCl_3 \cdot 4H_2O$ and $ZnCl_2$, respectively, in (Na,H)Cl solution with ionic strength of 1.0 mol/l. For the five metals system, aqueous feed solutions, containing Ga, In, Zn, Fe(II), and Al, were prepared by the dissolution of $GaCl_3$, $InCl_3 \cdot 4H_2O$, $ZnCl_2$, $FeCl_2 \cdot 4H_2O$ and $AlCl_3 \cdot 6H_2O$ into water, without consideration of ionic strength.

2.2 Procedure.

2.2.1 Extraction of Ga, In, and Zn.

Organic and aqueous solutions having an organic/aqueous volume ratio (O/A) of 1 were shaken for 2 hours at 298 K. The metal-loaded organic solutions were stripped using 6 mol/l HCl for the case of D2EHPA, and 3 mol/l HCl for the cases of EHPNA and PIA-226 at an O/A volume ratio of 0.5. The resulting aqueous samples were analyzed by ICP-AES. Equilibrium aqueous pH values were measured using an Orion 920A pH meter equipped with a glass combination electrode. The chloride ion concentration in the organic phase was measured by a potentiometric titration method with $AgNO_3$ after stripping with H_2SO_4. Infrared spectra of the metal loaded organic phase were recorded on an FT/IR-410 infrared spectrometer (Japan Spectroscopic Co., Ltd.) at room temperature in an IR cell with TlBr/TlI windows (KRS-5; Shimadzu). The loading ratio was defined as $[\overline{M}]/[\overline{(RH)_2}]_{feed}$.

2.2.2 Removal of Fe(II) and Al with TBP.

TBP was saturated with water prior to use, owing to its extractability of water.[52,53] Organic and aqueous solutions having O/A volume ratios of 0.5, 1, and 2 were shaken for 6 hours at 298 K. The concentrations of each metal in the aqueous phase were analyzed by using ICP-AES. The corresponding organic phase concentrations were determined by mass

balance.

3. Results and Discussion

3.1 Extraction and Separation of Ga and In.

3.1.1 Single Metal System.

3.1.1.1 Analytical Composition of the Extracted Species.

The analytical composition of the extracted species was investigated. This was met only at high loadings of the extractant. The maximum loading of the extractant was achieved by raising the equilibrium pH levels through adding NaOH solution. The maximum loading ratios approached about 1.0 for the three extractants, suggesting that a complex containing the dimeric extractant and the metal with the mole ratio of 1 : 1 may be formed at the extreme conditions of maximum loading ratios of the extractants, and anions in the aqueous phase may be co-extracted into the organic phase to compensate the positive charge of the metals. The amount of chloride ion was determined from the observed chloride ion concentration, corrected for the contribution of acid dissolved in the diluent. The ratios of $[\overline{Cl}]/[\overline{M}]$ are plotted in **Figure 1-1**.
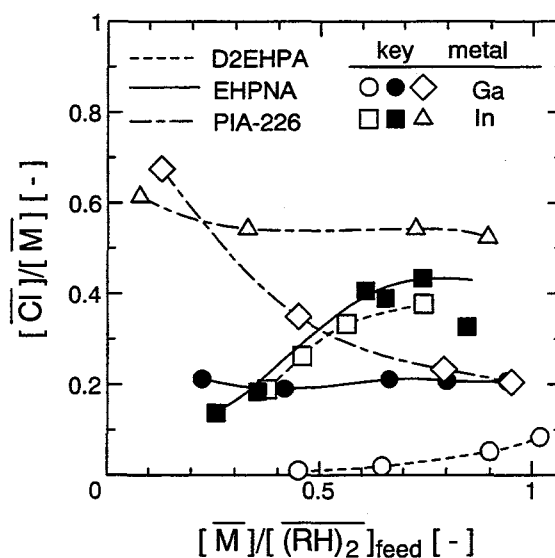
Figure 1-1   Effect of loading ratios on the ratio of chloride to metal in the organic phase.

8

For PIA-226 system, the ratio is rather high in the very low loading region, indicating a comparable amount of chloride ion is accompanied with the metal. The ratio decreases with increasing loading ratio. For Ga extraction with the three extractants, the ratios approach around 0.25, implying the ratio of chloride ion to metal to be 1 : 4. For In, the ratios approach around 0.5, implying the ratio of chloride ion to metal to be 1 : 2. The behavior of chloride ion in Ga extraction is different from that in In extraction at high loadings of the extractant, which is practical importance.

The loaded organic solutions were also studied by the infrared spectra. **Figure 1-2** shows the IR spectra in the region of OH groups in the D2EHPA/Ga system. It is known that the metal-OH is characterized by a sharp band at 3700-3500 cm^{-1}.[54]
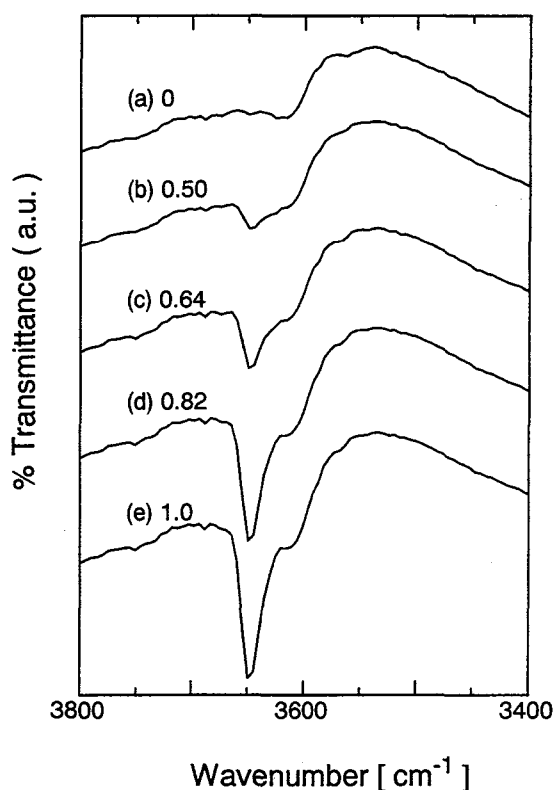
Figure 1-2 Infrared spectra for metal loaded organic solution in D2EHPA/Ga system. $[\overline{Ga}]/[\overline{(RH)_2}]_{feed}$ = (a) 0, (b) 0.50, (c) 0.64, (d) 0.82, and (e) 1.0.

The Ga-OH stretching band appears at 3647 cm^{-1} in the range of loading ratios greater than 0.5. The hydroxyl ion is actually involved in the extract entities in the range of high loading ratios. The ion may compensate the positive charge of the metal. Consequently, the stoichiometric relations between the metal and other elements under extreme conditions of maximum loading of extractant are most likely to be $\overline{Ga_4R_8Cl(OH)_3}$ and $\overline{In_2R_4Cl(OH)}$.

3.1.1.2 Extraction Equilibrium at Low Loading Ratios.

The slope analysis method was applied to determine the overall extraction equilibria of Ga and In with organophosphorus acids. **Figure 1-3** shows the effect of equilibrium pH values on the distribution ratios of these metals. Straight lines with slopes of 3 are obtained with D2EHPA and EHPNA. In the case of PIA-226, however, the slope is about 2, and the positive charge of the metals is not compensated for by the anionic species of PIA-226 alone. It is considered from the comparison with the results shown in Figure 1-1 that one chloride ion is possibly involved in their extract entities to compensate the positive charge of the metal. The PIA-226 extractant has the largest pK_a value in the present three extractants, and is, therefore, less dissociative than the other two.
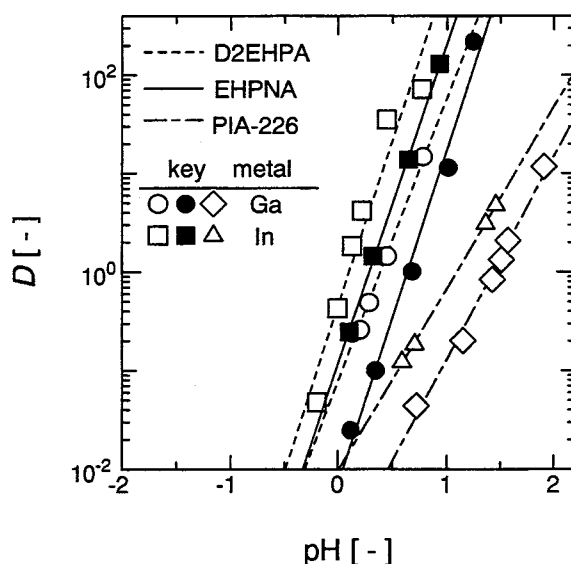
Figure 1-3   Effect of aqueous pH value on the distribution ratio. $[\overline{(RH)_2}]_{feed} = 5.0 \times 10^{-1}$ mol/l and $[M]_{feed} = 1.0 \times 10^{-2}$ mol/l.

The other anion, such as chloride, may be involved in the metal-PIA-226 complex in the present chloride ion system. This behavior differs from that reported for the extraction of In[55] and Ga[56] with the acidic phosphinate type extractant from the aqueous nitrate solution. This may arise from the difference of the media in the aqueous solutions.

As for D2EHPA and EHPNA, the extraction of Ga and In can be described by the following extraction equilibrium formulation.

$$M^{3+} + \frac{3+n}{2}\overline{(RH)_2} \leftrightarrow \overline{MR_3(RH)_n} + 3H^+ \tag{1-1}$$
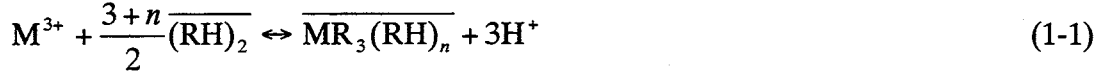
The distribution ratio can be described as Eq. (1-2).

$$D = K_{ex}[\overline{(RH)_2}]^{\frac{3+n}{2}} /[H^+]^3 \tag{1-2}$$

The variation of $D[H^+]^3$ with $[\overline{(RH)_2}]$ is shown in **Figure 1-4**.
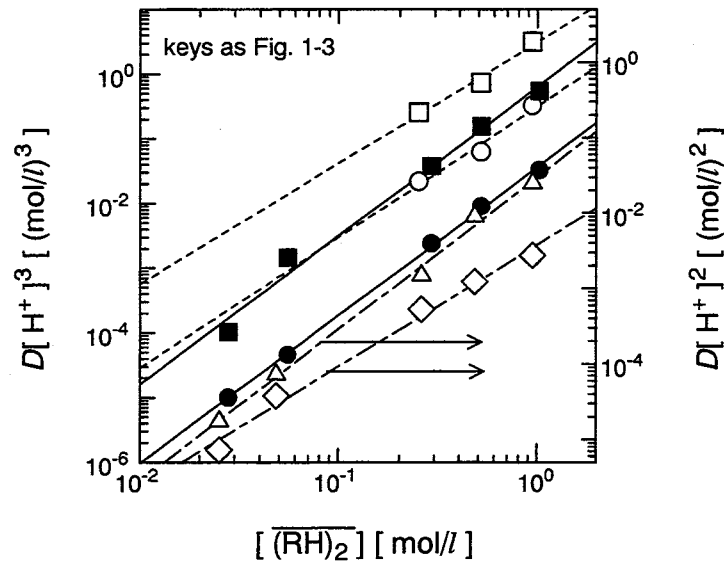
Figure 1-4 Effect of the concentration of dimeric extractants on normalized distribution ratio. $[M]_{feed} = 1.0 \times 10^{-2}$ mol/l.

Straight lines with slopes of about 2 are obtained, indicating that the extracted species is $\overline{MR_3(RH)}$. The dominant extraction equilibria of Ga and In with D2EHPA and EHPNA in low loading ratios can, therefore, be formulated as follows.

11

$$M^{3+} + 2\overline{(RH)_2} \leftrightarrow \overline{MR_3(RH)} + 3H^+ \qquad ; K_{ex,1} \qquad (1\text{-}3)$$

As for PIA-226, a metal-chloro complex, such as MCl^{2+}, is likely to be extracted, and the extraction equilibrium formulation is as shown in Eq. (1-4).

$$MCl^{2+} + \frac{2+n}{2}\overline{(RH)_2} \leftrightarrow \overline{MR_2Cl(RH)_n} + 2H^+ \qquad (1\text{-}4)$$

The distribution ratio can be described as Eq. (1-5).

$$D = K_{ex}\overline{[(RH)_2]}^{\frac{2+n}{2}} /[H^+]^2 \qquad (1\text{-}5)$$

The variation of $D[H^+]^2$ with $\overline{[(RH)_2]}$ is shown in Figure 1-4. Straight lines with slopes of about 2 are obtained, indicating that the extracted species is $\overline{[MR_2Cl(RH)_2]}$. The extraction equilibrium with PIA-226 at low loading ratios can, therefore, be formulated by Eq. (1-6).

$$MCl^{2+} + 2\overline{(RH)_2} \leftrightarrow \overline{MR_2Cl(RH)_2} + 2H^+ \quad ; K_{ex,1} \qquad (1\text{-}6)$$

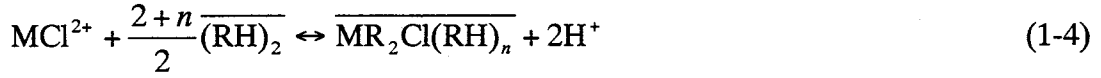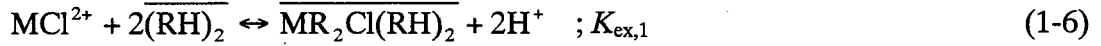This means that the metal to chloride ion ratio in the organic phase approaches to 1 in the low loading region.

3.1.1.3 Extraction Equilibrium at High Loading Ratios.

The high loadings of extractants were brought about by increasing the feed metal concentration and raising the equilibrium pH value. The distribution ratios are plotted against equilibrium pH values in **Figure 1-5**. The distribution ratios are seen to approach maximum values of 1.0 with all three extractants. The extracted species is now defined as $\overline{GaR_3(RH)}$ at low loading ratios, and as $\overline{Ga_4R_8Cl(OH)_3}$ at high loading ratios for the extraction of Ga with D2EHPA and EHPNA. It is necessary to express the extraction equilibrium formulation to cover the whole range from low loading to maximum loading. The aggregated species, $\overline{Ga_4R_8Cl(OH)_3}$, is assumed to be formed from $\overline{GaR_3(RH)}$ as follows.

$$Ga^{3+} + GaCl^{2+} + 3OH^- + 2\overline{GaR_3(RH)} \leftrightarrow \overline{Ga_4R_8Cl(OH)_3} + 2H^+ \qquad ; K_{ex,2} \quad (1\text{-}7)$$
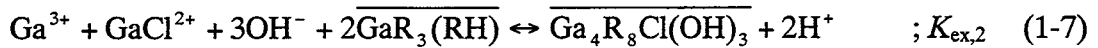
Considering the formation of metal-chloro complexes as shown in **Table 1-1**, total concentrations of dimeric extractant $([\overline{(RH)_2}]_{feed})$, total chloride $([Cl]_t)$, and extracted Ga $([\overline{Ga}])$ can be described as follows. In this calculation, the metal-chloro complexes in the aqueous phase are estimated by using literature values listed in Table 1-1.[57]

12
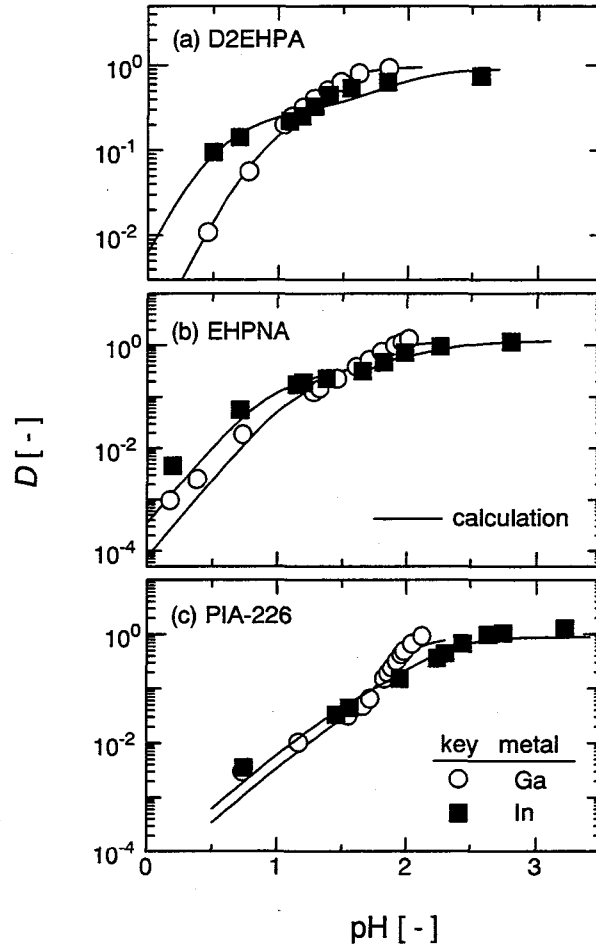
Figure 1-5 Effect of aqueous pH value on the distribution ratio of Ga and In in single metal system with (a) D2EHPA, (b) EHPNA, and (c) PIA-226. Comparison of observed data with prediction shown by solid lines.

$\overline{[(RH)_2]}_{feed} = 5.0 \times 10^{-2}$ mol/l and $[M]_{feed} = 1.0 \times 10^{-1}$ mol/l.

Table 1-1 Formation of metal-chloro complexes and its overall formation constants

$Ga^{3+} + Cl^- \leftrightarrow GaCl^{2+}$; $\log K_{a,1,Ga} = -0.64$	$In^{3+} + Cl^- \leftrightarrow InCl^{2+}$; $\log K_{a,1,In} = 2.49$
$Ga^{3+} + 2Cl^- \leftrightarrow GaCl_2^+$; $\log K_{a,2,Ga} = -2.18$	$In^{3+} + 2Cl^- \leftrightarrow InCl_2^+$; $\log K_{a,2,In} = 4.03$
$Ga^{3+} + 3Cl^- \leftrightarrow GaCl_3$; $\log K_{a,3,Ga} = -3.90$	$In^{3+} + 3Cl^- \leftrightarrow InCl_3$; $\log K_{a,3,In} = 3.53$
$Ga^{3+} + 4Cl^- \leftrightarrow GaCl_4^-$; $\log K_{a,4,Ga} = -5.74$	

$$[\overline{(RH)_2}]_{feed} = S + 2[\overline{GaR_3(RH)}] + 4[\overline{Ga_4R_8Cl(OH)_3}]$$

$$= S + \frac{2K_{ex,1}[Ga]S^2}{T[H^+]^3} + \frac{4K_{ex,1}^{\ 2}K_{ex,2}K_{a,1}[Ga]^4[Cl^-][OH^-]^3S^4}{T^4[H^+]^8} \tag{1-8}$$

$$[Cl]_t = [Cl^-] + [GaCl^{2+}] + 2[GaCl_2^+] + 3[GaCl_3] + 4[GaCl_4^-] + [\overline{Ga_4R_8Cl(OH)_3}]$$

$$= [Cl^-] + \frac{T'[Ga][Cl^-]}{T} + \frac{K_{ex,1}^{\ 2}K_{ex,2}K_{a,1}[Ga]^4[Cl^-][OH^-]^3S^4}{T^4[H^+]^8} \tag{1-9}$$

$$[\overline{Ga}] = [\overline{GaR_3(RH)}] + 4[\overline{Ga_4R_8Cl(OH)_3}]$$

$$= \frac{K_{ex,1}[Ga]S^2}{T[H^+]^3} + \frac{4K_{ex,1}^{\ 2}K_{ex,2}K_{a,1}[Ga]^4[Cl^-][OH^-]^3S^4}{T^4[H^+]^8} \tag{1-10}$$

where [Ga], T and T' is expressed as Eqs. (1-11)-(1-13).

$$[Ga] = [Ga^{3+}] + [GaCl^{2+}] + [GaCl_2^+] + [GaCl_3] + [GaCl_4^-] \tag{1-11}$$

$$T = 1 + K_{a,1}[Cl^-] + K_{a,2}[Cl^-]^2 + K_{a,3}[Cl^-]^3 + K_{a,4}[Cl^-]^4 \tag{1-12}$$

$$T' = \frac{dT}{d[Cl^-]} = K_{a,1} + 2K_{a,2}[Cl^-] + 3K_{a,3}[Cl^-]^2 + 4K_{a,4}[Cl^-]^3 \tag{1-13}$$

The most likely values of $K_{ex,1}$ and $K_{ex,2}$ are determined by the nonlinear least squares method based on Eqs. (1-8)-(1-10) to fit the experimental results. The results are shown in **Table 1-2**. With these constants, and by use of Eqs. (1-8) and (1-9), the values of [Cl⁻] and the concentration of free dimeric extractant, S, can then be calculated for each run, enabling the distribution ratio and the metal concentration in the organic phase to be calculated by use of Eq. (1-10).

For the extraction of In with D2EHPA and EHPNA, the aggregated species, $\overline{In_2R_4Cl(OH)}$, is assumed to be formed from $\overline{InR_3(RH)}$. For the extraction of Ga and In with PIA-226, the aggregated species, $\overline{Ga_4R_8Cl(OH)_3}$ and $\overline{In_2R_4Cl(OH)}$, are assumed to be formed from $\overline{GaR_2Cl(RH)_2}$ and $\overline{InR_2Cl(RH)_2}$, respectively. The values of extraction constants were determined by the same procedures employed for the extraction of Ga with D2EHPA and EHPNA. The results are summarized in Table 1-2. The calculated distribution ratios are shown by solid lines in Figure 1-5, and the experimental data are seen to cluster on the respective lines. The extraction behavior of these metals with D2EHPA,

EHPNA and PIA-226 can be expressed up to high loading ratios by the proposed extraction schemes.

Table 1-2 Extraction equilibrium formulations and extraction equilibrium constants

extractant	metal	extraction equilibrium	extraction equilibrium constant
D2EHPA	Ga	$Ga^{3+} + 2\overline{(RH)_2} \leftrightarrow \overline{GaR_3(RH)} + 3H^+$	$K_{ex,1,Ga} = 2.54 \times 10^{-1}$
		$Ga^{3+} + GaCl^{2+} + 3OH^- + 2\overline{GaR_3(RH)} \leftrightarrow \overline{Ga_4R_8Cl(OH)_3} + 2H^+$	$K_{ex,2,Ga} = 2.95 \times 10^{40}$
	In	$In^{3+} + 2\overline{(RH)_2} \leftrightarrow \overline{InR_3(RH)} + 3H^+$	$K_{ex,1,In} = 9.49 \times 10^3$
		$InCl^{2+} + OH^- + \overline{InR_3(RH)} \leftrightarrow \overline{In_2R_4Cl(OH)} + H^+$	$K_{ex,2,In} = 7.87 \times 10^{12}$
EHPNA	Ga	$Ga^{3+} + 2\overline{(RH)_2} \leftrightarrow \overline{GaR_3(RH)} + 3H^+$	$K_{ex,1,Ga} = 2.86 \times 10^{-2}$
		$Ga^{3+} + GaCl^{2+} + 3OH^- + 2\overline{GaR_3(RH)} \leftrightarrow \overline{Ga_4R_8Cl(OH)_3} + 2H^+$	$K_{ex,2,Ga} = 3.52 \times 10^{38}$
	In	$In^{3+} + 2\overline{(RH)_2} \leftrightarrow \overline{InR_3(RH)} + 3H^+$	$K_{ex,1,In} = 3.59 \times 10^2$
		$InCl^{2+} + OH^- + \overline{InR_3(RH)} \leftrightarrow \overline{In_2R_4Cl(OH)} + H^+$	$K_{ex,2,In} = 2.84 \times 10^{12}$
PIA-226	Ga	$GaCl^{2+} + 2\overline{(RH)_2} \leftrightarrow \overline{GaR_2Cl(RH)_2} + 2H^+$	$K_{ex,1,Ga} = 1.10 \times 10^{-1}$
		$3Ga^{3+} + 3OH^- + \overline{GaR_2Cl(RH)_2} + 2\overline{(RH)_2} \leftrightarrow \overline{Ga_4R_8Cl(OH)_3} + 6H^+$	$K_{ex,2,Ga} = 6.31 \times 10^{31}$
	In	$InCl^{2+} + 2\overline{(RH)_2} \leftrightarrow \overline{InR_2Cl(RH)_2} + 2H^+$	$K_{ex,1,In} = 5.64 \times 10^{-1}$
		$In^{3+} + OH^- + \overline{InR_2Cl(RH)_2} \leftrightarrow \overline{In_2R_4Cl(OH)}$	$K_{ex,2,In} = 1.98 \times 10^{12}$

3.1.2 Binary Metal System.

The extraction of binary metal systems is firstly investigated on the assumption of no interaction between Ga and In. The extraction of Ga and In is assumed to be expressed by the extraction equilibrium formulations determined in the single metal system. The experimental D values in binary metal systems are plotted against equilibrium pH values in **Figure 1-6**, and compared with the values calculated with the assumption of negligible interaction between the two metals shown by the dotted lines. Only in the extraction with D2EHPA, experimental distribution ratios are seen to cluster on the calculation lines, indicating that the extraction from binary metal solution can be expressed by the extraction equilibrium formulations obtained with the single metal systems.

15
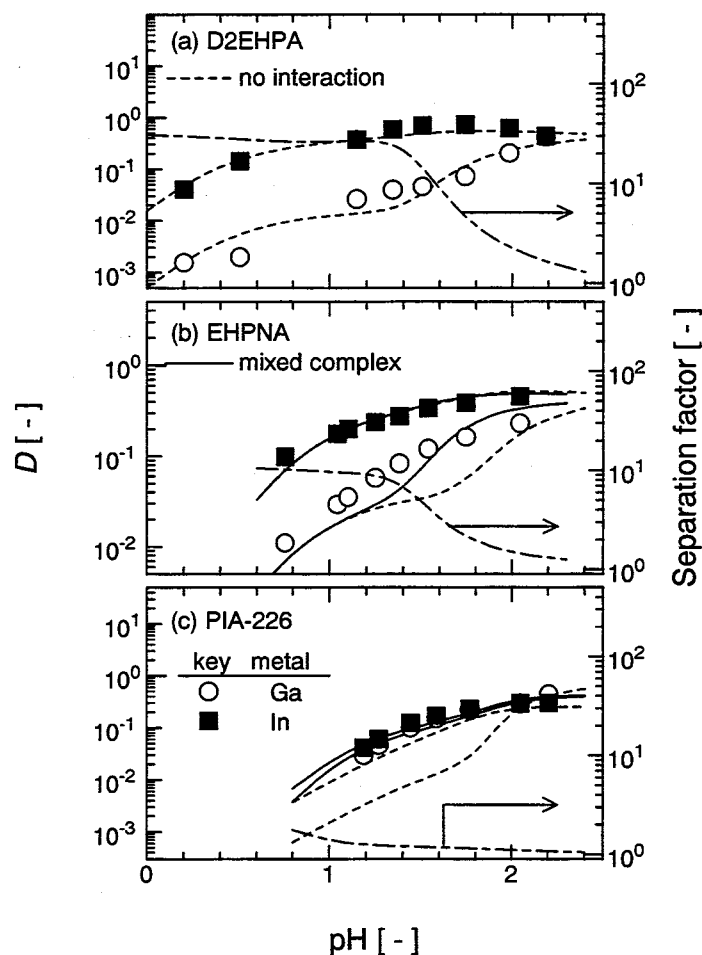
Figure 1-6 Effect of aqueous pH value on the distribution ratio of Ga and In, and on the calculated separation factor in binary metal system with (a) D2EHPA, (b) EHPNA, and (c) PIA-226. Comparison of observed data with predictions. Solid lines: mixed complex considered, dotted lines: single metal species alone considered. $[\overline{(RH)_2}]_{feed}$ = 5.0 × 10^{-2} mol/l and $[M_i]_{feed}$ = 8.0 × 10^{-2} mol/l.

For extraction with the EHPNA and PIA-226 systems, however, the experimental D values are greater than those calculated with the assumption of negligible interaction, especially, at high loading ratios. For extraction with PIA-226, the experimental D values are greater than those calculated over the whole range of loading ratios. The deviation is likely to be caused by formation of the mixed complex, in addition to the complex containing Ga or In alone, at low loadings, as well as high loadings. Ga and In are possibly co-extracted by forming mixed

16

complexes in the binary metal systems.

It is now necessary to have knowledge on the composition of the mixed complex. One of the most popular approaches for the study of the composition of co-extracted species is Job's method.[58] This method, however, can be applied only in the range of low loading ratios, where the metals in the feed solution are perfectly extracted. Therefore, a continuous variation method similar to Job's method was employed. The mole ratios in the aqueous feed solutions, of which total concentration of metals was kept constant, varied continuously, and the metals were extracted to the maximum loading. If only a single complex is formed, the quantity of extracted Ga into the organic phase may increase, and that of extracted In into the organic phase may decrease with increasing mole ratio of Ga/In in the aqueous feed solution. However, as shown in **Figure 1-7**, two straight lines with different slopes are actually seen with the rise of mole fraction of Ga in aqueous feed solution.

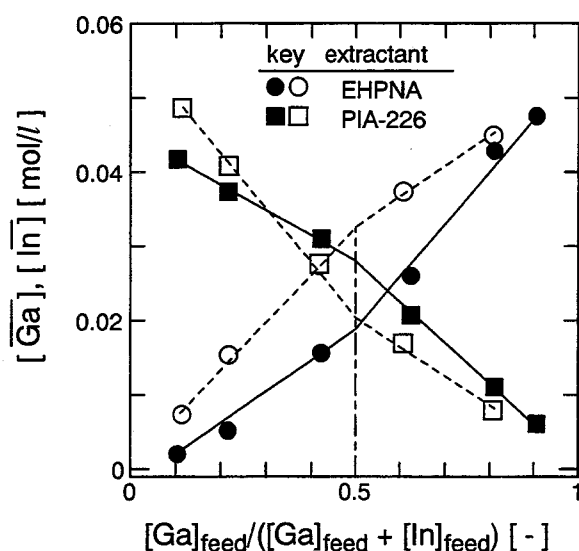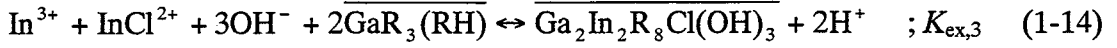**Figure 1-7** Determination of composition of mixed complexes containing both Ga and In by continuous variation method at maximum loadings. $[\overline{(RH)_2}]_{feed}$ = 5.0 × 10^{-2} mol/l and $[M]_t$ = 1.0 × 10^{-1} mol/l.

The inflection point of the plots of organic Ga and In concentrations and mole fraction of Ga in aqueous feed solution can be related with the composition of Ga and In in the mixed complex.

The mole fractions of Ga in the aqueous feed solution corresponding to the inflection points are 0.5 for the systems. Thus, mixed complexes with the mole ratio of Ga : In = 1 : 1 are considered to be formed.

As for the EHPNA system, the formation of mixed species in the organic phase is, therefore, assumed to be as shown by Eq. (1-14).

$$\mathrm{In^{3+} + InCl^{2+} + 3OH^- + 2\overline{GaR_3(RH)} \leftrightarrow \overline{Ga_2In_2R_8Cl(OH)_3} + 2H^+} \quad ; K_{ex,3} \quad (1\text{-}14)$$

Total concentrations of dimeric extractant ($[\overline{(RH)_2}]_{feed}$), total chloride ($[Cl]_t$) and the concentrations of Ga and In in the organic phase ($[\overline{Ga}]$ and $[\overline{In}]$) can be described as follows.

$$[\overline{(RH)_2}]_{feed} = S + 2[\overline{GaR_3(RH)}] + 4[\overline{Ga_4R_8Cl(OH)_3}] + 2[\overline{InR_3(RH)}]$$

$$+ 2[\overline{In_2R_4Cl(OH)}] + 4[\overline{Ga_2In_2R_8Cl(OH)_3}]$$

$$= S + \frac{2K_{ex,1,Ga}[Ga]S^2}{T_{Ga}[H^+]^3} + \frac{4K_{ex,1,Ga}{}^2 K_{ex,2,Ga}K_{a,1,Ga}[Ga]^4[Cl^-][OH^-]^3 S^4}{T_{Ga}{}^4[H^+]^8}$$

$$+ \frac{2K_{ex,1,In}[In]S^2}{T_{In}[H^+]^3} + \frac{2K_{ex,1,In}K_{ex,2,In}K_{a,1,In}[In]^2[Cl^-][OH^-]S^2}{T_{In}{}^2[H^+]^4}$$

$$+ \frac{4K_{ex,1,Ga}{}^2 K_{ex,3}K_{a,1,In}[Ga]^2[In]^2[Cl^-][OH^-]^3 S^4}{T_{Ga}{}^2 T_{In}{}^2[H^+]^8} \quad (1\text{-}15)$$

$$[Cl]_t = [Cl^-] + [GaCl^{2+}] + 2[GaCl_2{}^+] + 3[GaCl_3] + 4[GaCl_4{}^-] + [\overline{Ga_4R_8Cl(OH)_3}]$$

$$+ [InCl^{2+}] + 2[InCl_2{}^+] + 3[InCl_3] + 4[InCl^-] + [\overline{In_2R_4Cl(OH)}]$$

$$+ 4[\overline{Ga_2In_2R_8Cl(OH)_3}]$$

$$= [Cl^-] + \sum_i \frac{T_i'[M_i][Cl^-]}{T_i} + \frac{K_{ex,1,Ga}{}^2 K_{ex,2,Ga}K_{a,1,Ga}[Ga]^4[Cl^-][OH^-]^3 S^4}{T_{Ga}{}^4[H^+]^8}$$

$$+ \frac{K_{ex,1,In}K_{ex,2,In}K_{a,1,In}[In]^2[Cl^-][OH^-]S^2}{T_{In}{}^2[H^+]^4}$$

$$+ \frac{K_{ex,1,Ga}{}^2 K_{ex,3}K_{a,1,In}[Ga]^2[In]^2[Cl^-][OH^-]^3 S^4}{T_{Ga}{}^2 T_{In}{}^2[H^+]^8} \quad (1\text{-}16)$$

$$\overline{[Ga]} = \overline{[GaR_3(RH)]} + 4\overline{[Ga_4R_8Cl(OH)_3]} + 2\overline{[Ga_2In_2R_8Cl(OH)_3]}$$

$$= \frac{K_{ex,1}[Ga]S^2}{T[H^+]^3} + \frac{4K_{ex,1}{}^2 K_{ex,2}K_{a,1}[Ga]^4[Cl^-][OH^-]^3 S^4}{T^4[H^+]^8}$$

$$+ \frac{2K_{ex,1,Ga}{}^2 K_{ex,3}K_{a,1,In}[Ga]^2[In]^2[Cl^-][OH^-]^3 S^4}{T_{Ga}{}^2 T_{In}{}^2[H^+]^8} \qquad (1\text{-}17)$$

$$\overline{[In]} = \overline{[InR_3(RH)]} + 2\overline{[In_2R_4Cl(OH)]} + 2\overline{[Ga_2In_2R_8Cl(OH)_3]}$$

$$= \frac{K_{ex,1,In}[In]S^2}{T_{In}[H^+]^3} + \frac{2K_{ex,1,In}K_{ex,2,In}K_{a,1,In}[In]^2[Cl^-][OH^-]S^2}{T_{In}{}^2[H^+]^4}$$

$$+ \frac{2K_{ex,1,Ga}{}^2 K_{ex,3}K_{a,1,In}[Ga]^2[In]^2[Cl^-][OH^-]^3 S^4}{T_{Ga}{}^2 T_{In}{}^2[H^+]^8} \qquad (1\text{-}18)$$

The most likely value of $K_{ex,3}$ is then determined, by use of Eqs. (1-15)-(1-18) and extraction equilibrium constants determined in single metal systems, to fit the experimental results and the results are shown in **Table 1-3**.

Table 1-3 Extraction equilibrium formulations and extraction equilibrium constants in binary systems for mixed species

Extractant	Extraction equilibrium	Extraction equilibrium constant
EHPNA	$In^{3+} + InCl^{2+} + 3OH^- + 2\overline{GaR_3(RH)} \leftrightarrow \overline{Ga_2In_2R_8Cl(OH)_3} + 2H^+$	$K_{ex,3} = 7.86 \times 10^{43}$
PIA-226	$GaCl^{2+} + InCl^{2+} + 4\overline{(RH)_2} \leftrightarrow \overline{GaInR_4Cl_2(RH)_4} + 4H^+$	$K_{ex,3} = 1.18 \times 10^3$
	$Ga^{3+} + OH^- + \overline{InR_2Cl(RH)_2} \leftrightarrow \overline{GaInR_4Cl(OH)} + 2H^+$	$K_{ex,4} = 3.94 \times 10^{10}$

In the case of PIA-226, the experimental D values are greater than those calculated over the whole range of loading ratios, indicating that the mixed complexes are formed at low loading ratios as well as at high loading ratios, and the extraction equilibria are assumed as Eqs. (1-19) and (1-20).

$$GaCl^{2+} + InCl^{2+} + 4\overline{(RH)_2} \leftrightarrow \overline{GaInR_4Cl_2(RH)_4} + 4H^+ \qquad ; K_{ex,3} \qquad (1\text{-}19)$$

$$Ga^{3+} + OH^- + \overline{InR_2Cl(RH)_2} \leftrightarrow \overline{GaInR_4Cl(OH)} + 2H^+ \qquad ; K_{ex,4} \qquad (1\text{-}20)$$
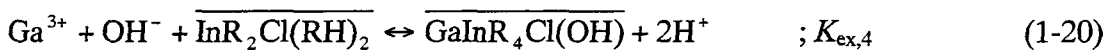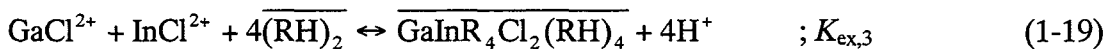
The most likely values of $K_{ex,3}$ and $K_{ex,4}$ are determined by the same method for the EHPNA system. The proposed extraction scheme in binary metal systems and extraction equilibrium

constants are summarized in Table 1-3. The calculated values are shown by solid lines in Figure 1-6 (b) and (c), together with the calculated separation factor, defined as D_{In}/D_{Ga}, for the EHPNA and PIA-226 systems, respectively. The extraction behavior of the metals with D2EHPA, EHPNA and PIA-226 is expressed up to high loading ratios by the proposed extraction schemes. D2EHPA is most suitable for the separation of Ga and In, excepting at very high loadings.

3.2 Design of the Separation and Recovery Process of Ga and In.

3.2.1 Removal of Major Components.

The extraction of Ga and In from the leach liquor was attempted at first using TBP. A typical composition of the liquor then available for liquid-liquid extraction is reported to be $(3.0\text{-}4.3) \times 10^{-3}$ mol/l Ga, $(9.0\text{-}9.6) \times 10^{-3}$ mol/l In, $(2.3\text{-}4.6) \times 10^{-1}$ mol/l Zn, $(3.7\text{-}5.6) \times 10^{-1}$ mol/l Al, and $(1.8\text{-}3.6) \times 10^{-1}$ mol/l Fe.[49] The imitated liquor was first extracted with TBP to move the two rare metals together with Zn into the organic phase, leaving other major impurities in the raffinate solution. Al and Fe(II) are expected to be separated from the two rare metals with TBP.[59,60]
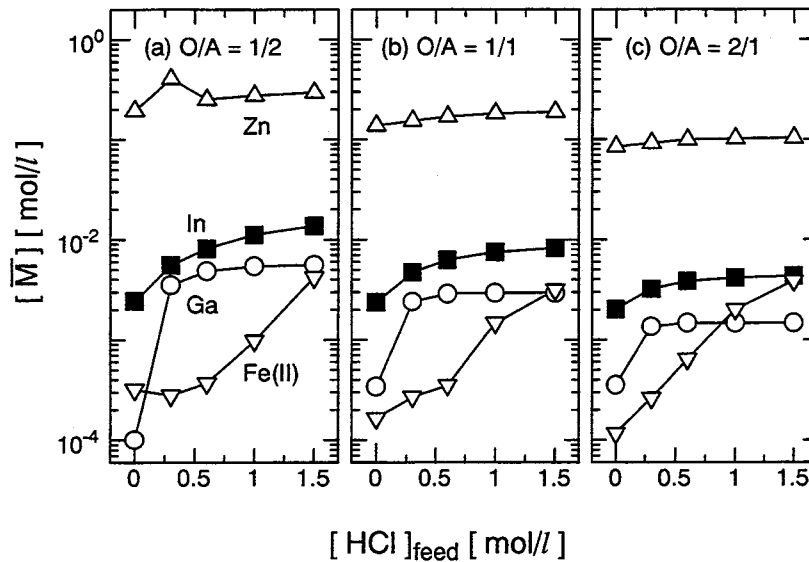
Figure 1-8. Extraction behavior for Ga, In, Zn, Fe(II), and Al with TBP extractant. $[Ga]_{feed} = 3.0 \times 10^{-3}$ mol/l, $[In]_{feed} = 9.0 \times 10^{-3}$ mol/l, $[Zn]_{feed} = 2.3 \times 10^{-1}$ mol/l, $[Fe(II)]_{feed} = 1.8 \times 10^{-1}$ mol/l, and $[Al]_{feed} = 3.7 \times 10^{-1}$ mol/l. Al extraction: null

20

Figure 1-8 shows the effect of the HCl concentration in the aqueous feed solution on the resultant concentrations of each metal in the organic phase for experimental O/A volume ratios of 0.5, 1, and 2. Al was not extracted to the organic phase with TBP at all. The extractability of Fe(II) was extremely low in the low range of the HCl concentration. Thus, Fe(II) and Al may be expected to be removed easily by TBP at a condition of low concentration of HCl. Thus, Zn may be considered to be the only major impurity affecting the separation and recovery of Ga and In in the succeeding operations.

3.2.2 Extraction of Zn with D2EHPA.

3.2.2.1 Extraction at Low Loading Ratios.

The slope analysis method was applied to determine the extraction equilibrium for Zn at low loading ratios. The effect of both pH and D2EHPA concentration on the distribution ratio is shown in **Figure 1-9**.
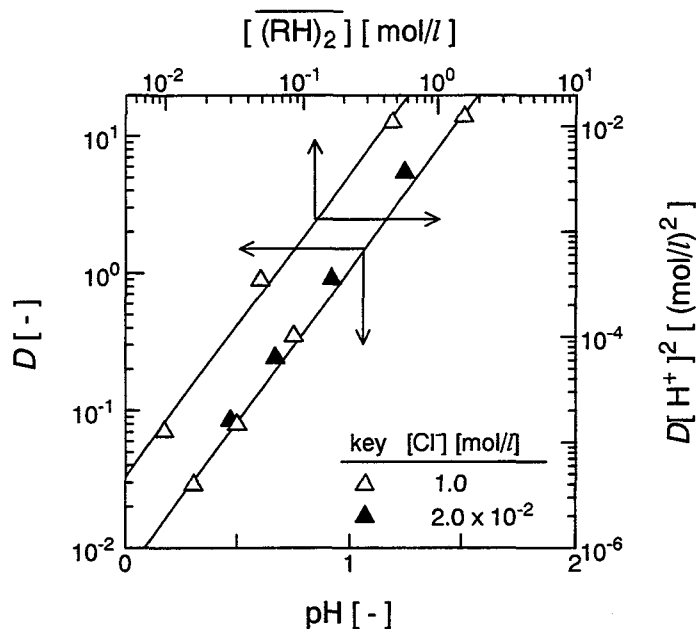
Figure 1-9   Extraction equilibrium for Zn at low loading ratios with D2EHPA.
$[Zn]_{feed} = 1.0 \times 10^{-2}$ mol/l.

For pH, a straight line with a slope of 2 was obtained, with the slope being independent of the chloride ion concentration in the aqueous feed solution. The effect of dimeric D2EHPA

concentration ($[\overline{(RH)_2}]$) on the $D[H^+]^2$ also was given by a straight line relationship with a slope of 2, thus indicating the extraction equilibrium formulation of Zn at low loading to be as follows.

$$Zn^{2+} + 2\overline{(RH)_2} \leftrightarrow \overline{ZnR_2(RH)_2} + 2H^+ \tag{1-21}$$

$$K_{cx,1,Zn} = \frac{[\overline{ZnR_2(RH)_2}][H^+]^2}{[Zn^{2+}][\overline{(RH)_2}]^2} \tag{1-22}$$

3.2.2.2 Extraction at High Loading Ratios.

High extractant loading was brought about by increasing the feed metal concentration and raising the equilibrium pH value. The experimental loading ratios obtained are plotted against the corresponding equilibrium pH values in **Figure 1-10**.
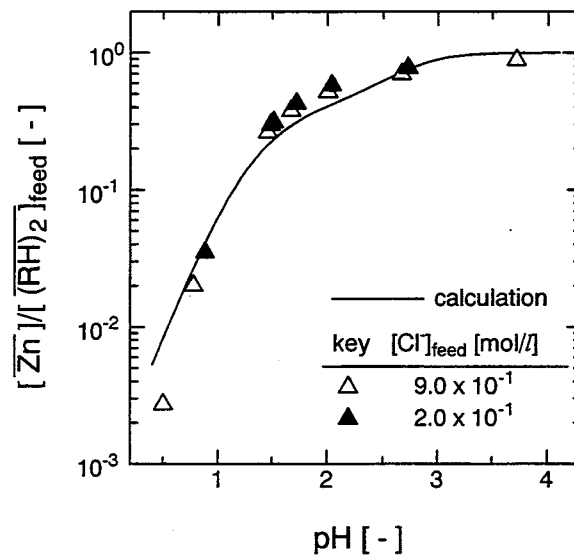
Figure 1-10 Effect of aqueous pH value on the distribution ratio for Zn with D2EHPA. Comparison of observed data with prediction shown by solid lines. $[\overline{(RH)_2}]_{feed}$ = 5.0 × 10^{-2} mol/l and $[Zn]_{feed}$ = 1.0 × 10^{-1} mol/l.

The loading ratios are seen to approach an asymptotic value of 1.0 at high pH, thus indicating the molar ratio of Zn to dimeric D2EHPA in the extract species to be 1. No significant difference is seen between the data obtained for chloride ion concentration of $[Cl^-]$ = 2.0 × 10^{-1}

mol/l and 9.0×10^{-1} mol/l, in agreement with the previous results for the low loading ratio range. An aggregated species is likely to occur with increasing loading ratios as well as in the case of Ga and In. The extraction equilibrium formulation for Zn at high loading ratio is, therefore, assumed as follows.

$$Zn^{2+} + \overline{ZnR_2(RH)_2} \leftrightarrow \overline{Zn_2R_4} + 2H^+ \tag{1-23}$$

$$K_{ex,2,Zn} = \frac{[\overline{Zn_2R_4}][H^+]^2}{[Zn^{2+}][\overline{ZnR_2(RH)_2}]} \tag{1-24}$$

The total Zn concentration in the organic phase ($[\overline{Zn}]$) and total concentration of dimeric D2EHPA are expressed by Eqs. (1-25) and (1-26), respectively, where the symbol S denotes the dimeric concentration of free D2EHPA.

$$[\overline{Zn}] = \frac{K_{ex,1,Zn}[Zn^{2+}]S^2}{[H^+]^2} + \frac{2K_{ex,1,Zn}K_{ex,2,Zn}[Zn^{2+}]^2S^2}{[H^+]^4} \tag{1-25}$$

$$[\overline{(RH)_2}]_{feed} = S + \frac{2K_{ex,1,Zn}[Zn^{2+}]S^2}{[H^+]^2} + \frac{2K_{ex,1,Zn}K_{ex,2,Zn}[Zn^{2+}]^2S^2}{[H^+]^4} \tag{1-26}$$

The most likely values for the extraction equilibrium constants were determined by the nonlinear least square method, based on Eqs. (1-25) and (1-26) to fit the experimental results, as $K_{ex,1,Zn} = 1.90 \times 10^{-1}$ and $K_{ex,2,Zn} = 8.39 \times 10^{-5}$. With these constants and the use of Eqs. (1-25) and (1-26), the loading ratios for Zn in the organic phase may be calculated. The calculated loading ratios are shown in Figure 1-10 by the solid line. The experimental results are seen to cluster very close to the prediction line, thus indicating that the extraction behavior of Zn, up to the high loadings, is expressed successfully by the proposed scheme.

3.2.3 Extraction in Binary and Ternary Systems.

3.2.3.1 Ga/Zn Binary System.

Figure 1-11 shows the effect of the equilibrium pH value on the distribution ratio. If negligible interaction between Ga and Zn is assumed, the concentration of Zn in the organic phase ($[\overline{Zn}]$) is given by Eq. (1-25) and that of Ga ($[\overline{Ga}]$) is expressed as Eq. (1-27) using the established formulations.

23

Figure 1-11 Effect of aqueous pH value on the distribution ratio of Ga and Zn in the binary system. Comparison of observed data with prediction shown by solid lines. $[\overline{(RH)_2}]_{feed} = 5.0 \times 10^{-2}$ mol/l and $[M_i]_{feed} = 1.1 \times 10^{-1}$ mol/l.

$$[\overline{Ga}] = [\overline{GaR_3(RH)}] + 4[\overline{Ga_4R_8Cl(OH)_3}]$$

$$= \frac{K_{ex,1,Ga}[Ga]S^2}{T_{Ga}[H^+]^3} + \frac{4K_{ex,1,Ga}{}^2 K_{ex,2,Ga}K_{a,1,Ga}[Ga]^4[Cl^-][OH^-]^3 S^4}{T_{Ga}{}^4[H^+]^8} \tag{1-27}$$

The feed concentration of dimeric D2EHPA can be expressed as Eq. (1-28).

$$[\overline{(RH)_2}]_{feed} = S + 2[\overline{GaR_3(RH)}] + 4[\overline{Ga_4R_8Cl(OH)}] + 2[\overline{ZnR_2(RH)_2}] + 2[\overline{Zn_2R_4}]$$

$$= S + \frac{2K_{ex,1,Ga}[Ga]S^2}{T_{Ga}[H^+]^3} + \frac{4K_{ex,1,Ga}{}^2 K_{ex,2,Ga}K_{a,1,Ga}[Ga]^4[Cl^-][OH^-]^3 S^4}{T_{Ga}{}^4[H^+]^8}$$

$$+ \frac{2K_{ex,1,Zn}[Zn^{2+}]S^2}{[H^+]^2} + \frac{2K_{ex,1,Zn}K_{ex,2,Zn}[Zn^{2+}]^2 S^2}{[H^+]^4} \tag{1-28}$$

The chloride ion concentration can be expressed as Eq. (1-29)

$$[Cl]_t = [Cl^-] + [GaCl^{2+}] + 2[GaCl_2{}^+] + 3[GaCl_3] + 4[GaCl_4{}^-] + [\overline{Ga_4R_8Cl(OH)}]$$

$$= [Cl^-] + \frac{T'_{Ga}[Ga][Cl^-]}{T_{Ga}} + \frac{K_{ex,1,Ga}{}^2 K_{ex,2,Ga}K_{a,1,Ga}[Ga]^4[Cl^-][OH^-]^3 S^4}{T_{Ga}{}^4[H^+]^8} \tag{1-29}$$

The calculated distribution ratios are shown in Figure 1-11 by the solid lines. The observed data are seen to cluster on the prediction lines, indicating that negligible interaction between Ga and Zn occurs in the extraction of either species from the mixture.

3.2.3.2 In/Zn Binary System.

The combination of In and Zn was then investigated. **Figure 1-12** shows the effect of the equilibrium pH value on the distribution ratio, together with the predictions, based on the assumption of negligible interaction between In and Zn, as shown by the dotted lines. The values of the experimental distribution ratios for Zn are greater than those calculated assuming negligible interaction, especially, at high loading ratios. In the case of In, zero deviation is observed even at high loading ratios, with In extraction being about 100 times greater than the values for Zn extraction. The deviation in the case for Zn is likely to be caused by the formation of a mixed complex of In and Zn at high loading ratios, in addition to the complex containing Zn alone.
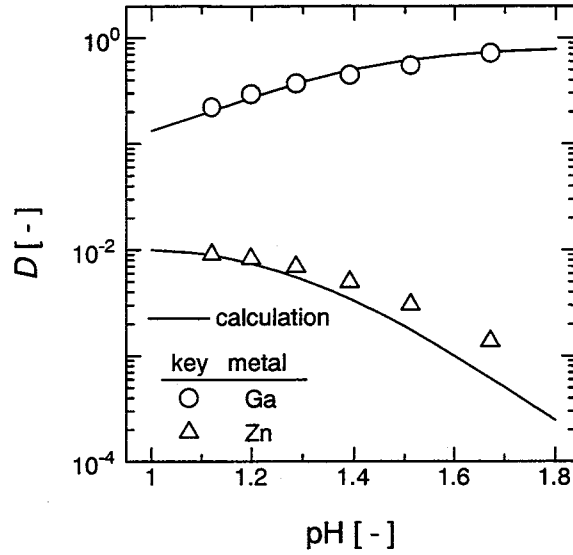

Figure 1-12 Effect of aqueous pH value on the distribution ratio of Ga and Zn in the binary system. Comparison of observed data with prediction shown by solid lines. The dotted lines are based on the assumption of zero interaction between the two metals. $[\overline{(RH)_2}]_{feed} = 5.0 \times 10^{-2}$ mol/l and $[M_i]_{feed} = 1.1 \times 10^{-1}$ mol/l.

The composition of the mixed complex was investigated by the continuous variation method, and a mixed complex with a mole ratio of In : Zn = 1 : 1 is considered to be most likely formed.   The formation of the mixed species in the organic phase is, therefore, assumed to occur as shown by Eq. (1-30).

$$InCl^{2+} + \overline{ZnR_2(RH)_2} \leftrightarrow \overline{InZnR_4Cl} + 2H^+ \tag{1-30}$$
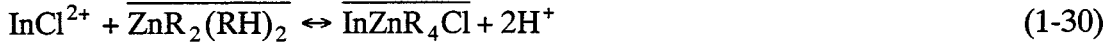
$$K_{ex,3,In/Zn} = \frac{[\overline{InZnR_4Cl}][H^+]^2}{[InCl^{2+}][\overline{ZnR_2(RH)_2}]} \tag{1-31}$$

The concentrations of In ($[\overline{In}]$) and Zn ($[\overline{Zn}]$) in the organic phase may be expressed as Eqs. (1-32) and (1-33), respectively.

$$[\overline{In}] = [\overline{InR_3(RH)}] + 2[\overline{In_2R_4Cl(OH)}] + [\overline{InZnR_4Cl}]$$

$$= \frac{K_{ex,1,In}[In]S^2}{T_{In}[H^+]^3} + \frac{2K_{ex,1,In}K_{ex,2,In}K_{a,1,In}[In]^2[Cl^-][OH^-]S^2}{T_{In}{}^2[H^+]^4}$$

$$+ \frac{K_{ex,1,Zn}K_{ex,3,In/Zn}K_{a,1,In}[In][Zn^{2+}][Cl^-]S^2}{T_{In}[H^+]^4} \tag{1-32}$$

$$[\overline{Zn}] = [\overline{ZnR_2(RH)_2}] + 2[\overline{Zn_2R_4}] + [\overline{InZnR_4Cl}]$$

$$= \frac{K_{ex,1,Zn}[Zn^{2+}]S^2}{[H^+]^2} + \frac{2K_{ex,1,Zn}K_{ex,2,Zn}[Zn^{2+}]^2S^2}{[H^+]^4}$$

$$+ \frac{K_{ex,1,Zn}K_{ex,3,In/Zn}K_{a,1,In}[In][Zn^{2+}][Cl^-]S^2}{T_{In}[H^+]^4} \tag{1-33}$$

The feed dimeric D2EHPA concentration can be expressed as Eq. (1-34).

$$[\overline{(RH)_2}]_{feed} = S + 2[\overline{InR_3(RH)}] + 2[\overline{In_2R_4Cl(OH)}] + 2[\overline{ZnR_2(RH)_2}]$$

$$+ 2[\overline{Zn_2R_4}] + 2[\overline{InZnR_4Cl}]$$

$$= S + \frac{2K_{ex,1,In}[In]S^2}{T_{In}[H^+]^3} + \frac{2K_{ex,1,In}K_{ex,2,In}K_{a,1,In}[In]^2[Cl^-][OH^-]S^2}{T_{In}{}^2[H^+]^4}$$

$$+ \frac{2K_{ex,1,Zn}[Zn^{2+}]S^2}{[H^+]^2} + \frac{2K_{ex,1,Zn}K_{ex,2,Zn}[Zn^{2+}]^2S^2}{[H^+]^4}$$

$$+ \frac{2K_{ex,1,Zn}K_{ex,3,In/Zn}K_{a,1,In}[In][Zn^{2+}][Cl^-]S^2}{T_{In}[H^+]^4} \tag{1-34}$$

The chloride ion concentration can be expressed as Eq. (1-35).

$$[Cl]_t = [Cl^-] + [InCl^{2+}] + 2[InCl_2^+] + 3[InCl_3] + \overline{[In_2R_4Cl(OH)]} + \overline{[InZnR_4Cl]}$$

$$= [Cl^-] + \frac{T_{In}'[In][Cl^-]}{T_{In}} + \frac{2K_{ex,1,In}K_{ex,2,In}K_{a,1,In}[In]^2[Cl^-][OH^-]S^2}{T_{In}^2[H^+]^4}$$

$$+ \frac{K_{ex,1,Zn}K_{ex,3,In/Zn}K_{a,1,In}[In][Zn^{2+}][Cl^-]S^2}{T_{In}[H^+]^4} \tag{1-35}$$

The most likely value for the constant $K_{ex,3,In/Zn}$ was then determined by the nonlinear least square method using Eqs. (1-32)-(1-35) and the extraction equilibrium constants determined in the single-metal systems, to fit the experimental results, as $K_{ex,3,In/Zn} = 1.49$. Using the extraction equilibrium formulations for the single-metal and binary systems, the distribution ratios for In and Zn can be calculated, and these are shown in Figure 1-12 by the solid lines. The experimental values for both species are now seen to cluster excellently on the prediction line, indicating that the proposed scheme when allowing for a mixed complex does express the extraction behavior in the binary system well.

3.2.3.3 Ga/In/Zn Ternary System.

Figure 1-13 shows the effect of the aqueous equilibrium pH value on the distribution ratio for Ga, In, and Zn from an aqueous solution, containing the three metals with identical concentrations of 7.0×10^{-2} mol/l. The prediction lines are calculated on the assumption of zero interaction among the three metals, and these are shown to be applicable to the extraction schemes, determined in each binary system. There is, thus, no interaction between the three metals, and the extraction schemes for the binary systems are, therefore, applicable to the ternary system.
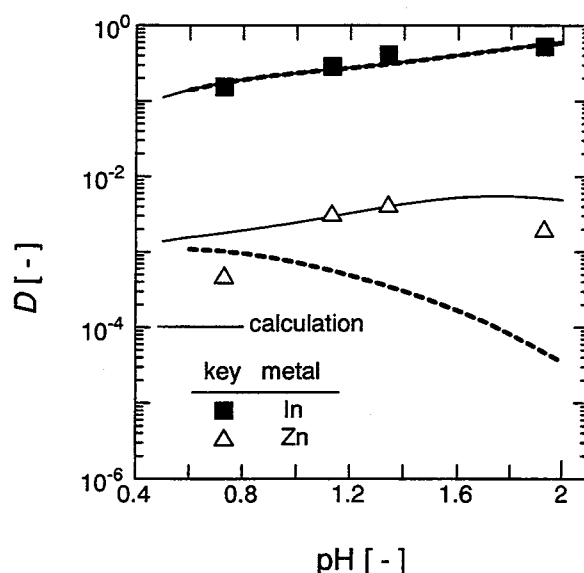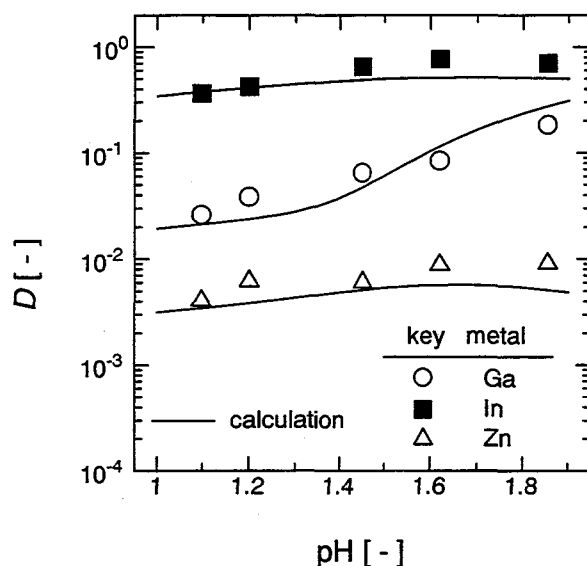
Figure 1-13 Effect of aqueous pH value on the distribution ratio for Ga, In, and Zn in the ternary system. Comparison of observed data with prediction shown by solid lines. $[\overline{(RH)_2}]_{feed} = 5.0 \times 10^{-2}$ mol/l and $[M_i]_{feed} = 7.0 \times 10^{-2}$ mol/l.

3.2.3.4 Scrubbing Effect of Metal-Loaded Organic Solution.

Figure 1-14 shows the experimental loading ratios in the organic phase for the three metals after scrubbing with (a) metal-free and (b) metal-containing aqueous solutions. Comparative values according to the proposed extraction scheme are shown by means of solid lines. The results show that with a metal-free solution both Ga and Zn are scrubbed off into the aqueous phase, with most of the In remaining in the organic phase. With a metal-containing solution, the metal-exchange reaction between Ga and Zn in the organic phase and In in the aqueous phase is shown very well by comparison with the concentration of the three metals in the organic feed solution. The extraction of the more extractable In reduces the concentration of the free extractant, thus causing a decrease in the extraction of the less extractable Ga and Zn. This effect is, thus, notable at the high loading region for the extractant. The experimental data are seen to cluster on the prediction lines, indicating that the proposed extraction scheme is equally applicable to the scrubbing treatment as well.
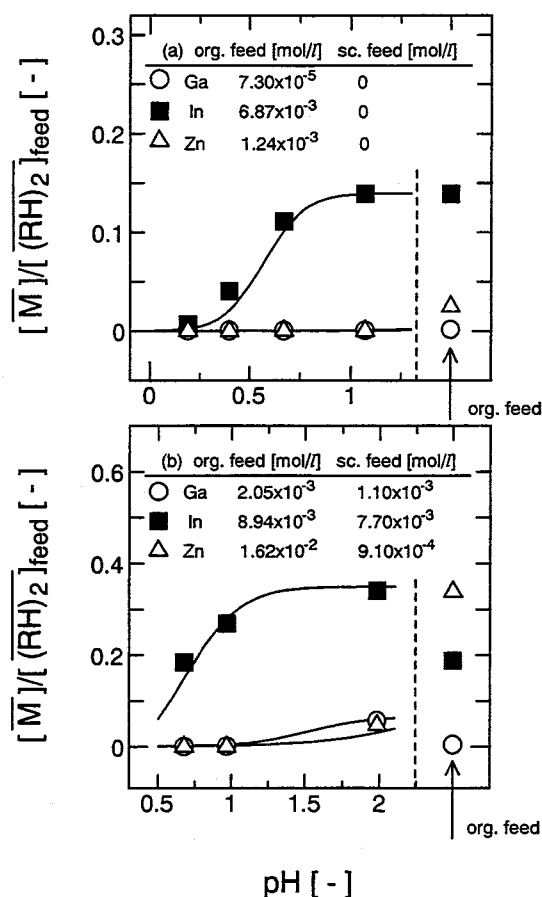
Figure 1-14 Effect of scrubbing with (a) metal-free and (b) metal-containing solutions. Comparison of observed data with prediction shown by solid lines. $[\overline{(RH)_2}]_{feed} = 5.0 \times 10^{-2}$ mol/l.

3.2.3.5 Reduction of Zn Content.

A liquor containing 2.7×10^{-3} mol/l Ga, 9.2×10^{-3} mol/l In, and 2.3×10^{-1} mol/l Zn was prepared as the feed solution for the recovery of Ga and In. The quantity of Zn in the feed solution is much larger than that for both Ga and In, with mole concentration ratios for $[Zn]_{feed}/[Ga]_{feed} = 8.5 \times 10$ and for $[Zn]_{feed}/[In]_{feed} = 2.5 \times 10$. The order of extractability is In > Ga > Zn, as apparently shown in Figure 1-13. Most of the Ga and In are thus to be extracted into the organic phase, leaving as much Zn as possible in the raffinate, in order to reduce the Zn content. The feed liquor was treated by a single extraction, using extractants of differing concentrations. The observed data are shown in **Figure 1-15**. In the case of 1.0×10^{-2} mol/l

extractant concentration, about 40 % of In is extracted at pH = 1.8, leaving most of the Ga and

Zn in the raffinate. In the case of 2.0 × 10^{-2} mol/l extractant concentration, about 10 % of Ga

and 65 % of In together with 1 % of Zn are extracted at pH = 1.6, leaving 90 % Ga and 99 %

Zn in the raffinate. These are caused by the saturation of the extractant by In, the most

extractable component. In the case of 5.0 × 10^{-2} mol/l extractant concentration, about 90 % of

Ga and 99 % of In are extracted together with 9 % Zn, leaving 91 % Zn in the raffinate. This

higher concentration of the extractant is thus used primarily to reduce the Zn content.

The solid prediction lines shown in Figure 1-15 are calculated using the extraction

scheme, as determined at a constant ionic strength of 1.0 mol/l, facilitated by adding (Na,H)Cl.

The observed data were obtained from the aqueous feed solution with an ionic strength of 7.6

× 10^{-1} mol/l. The agreement between the observed data and calculated values is surprisingly

good. The chloride ion concentration in the feed solution is the most important in the ionic

strength and is involved in the extraction scheme for Ga and In.
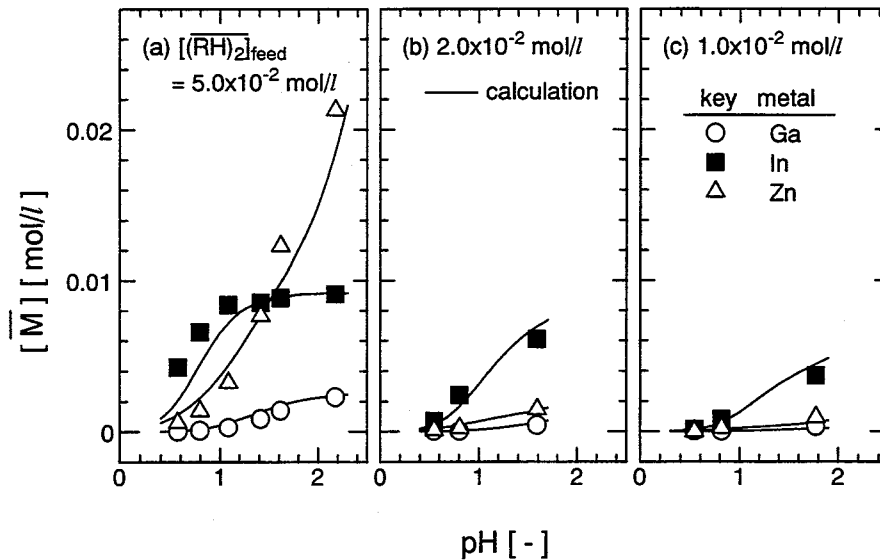
Figure 1-15 Effect of aqueous pH value on the concentration of Ga, In, and Zn in the organic phase. Comparison of observed data with prediction shown by solid lines. $[\overline{(RH)_2}]_{feed}$ = (a) 5.0 × 10^{-2} mol/l, (b) 2.0 × 10^{-2} mol/l, and (c) 1.0 × 10^{-2} mol/l, and $[Ga]_{feed}$ = 2.7 × 10^{-3} mol/l, $[In]_{feed}$ = 9.2 × 10^{-3} mol/l, and $[Zn]_{feed}$ = 2.3 × 10^{-1} mol/l.

An ionic strength of less than 1.0 mol/l is considered to have little effect on the extraction of the metals in the present system. The proposed scheme and formulations can, therefore, be used for the simulation work for the separation and recovery of the two rare metals from zinc refinery residue.

3.2.4 Simulation Work for the Separation and Recovery of Ga and In from Zinc Refinery Residue.

3.2.4.1 Procedures.

A simulation of the separation and recovery of Ga and In from zinc refinery residue was carried out based on the equilibrium studies with D2EHPA. A schematic flowsheet for a counter-current mixer-settler cascade is shown in **Figure 1-16.** The equilibrium relationship for Ga, In, and Zn in any extraction stage p is expressed by Eq. (1-36).

$$[\overline{M_i}]_p = [M_i]_p \cdot D_{i,p} \qquad (i = Ga, In, Zn) \tag{1-36}$$

Org. output soln.   Feed soln. (F)

$[\overline{M_i}]_P$ $[M_i]_{feed}$

Extr. stage P

$[\overline{M_i}]_{P-1}$ $[M_i]_P$

$[\overline{M_i}]_p$ $[M_i]_{p+1}$

Extr. stage p

$[\overline{M_i}]_{p-1}$ $[M_i]_p$

$[\overline{M_i}]_1$ $[M_i]_2$

Extr. stage 1

$[\overline{M_i}]_0$ $[M_i]_1$

Org. soln. (E)   Raffinate
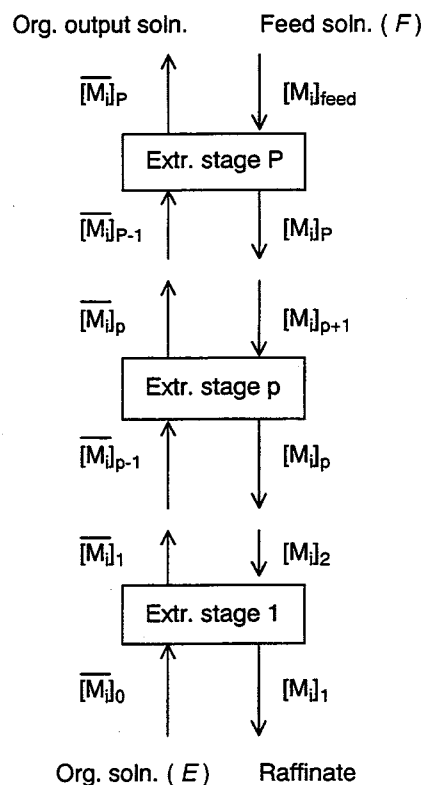
Figure 1-16 Schematic flowsheet for counter-current mixer-settler cascade.

where $D_{i,p}$, the distribution ratio of each metal in stage p, is a function of the equilibrium pH value in the stage. The mass balances for each metal species (i), chloride ion, and hydrogen ion in extraction stage p are given by Eqs. (1-37)-(1-41), respectively.

$$F \cdot [M_i]_{p+1} = F \cdot [M_i]_p + E \cdot [\overline{M_i}]_p - E \cdot [\overline{M_i}]_{p-1} \tag{1-37}$$

$$F \cdot [Cl]_{p+1} = F \cdot [Cl]_p + E \cdot [\overline{Cl}]_p - E \cdot [\overline{Cl}]_{p-1} \tag{1-38}$$

$$F \cdot [H^+]_{p+1} = F \cdot [H^+]_p - E \cdot \Delta[H^+]_p \tag{1-39}$$

$$[\overline{Cl}]_p = [\overline{Ga_4R_8Cl(OH)_3}]_p + [\overline{In_2R_4Cl(OH)}]_p + [\overline{InZnR_4Cl}]_p \tag{1-40}$$

$$\Delta[H^+]_p = 3\left([\overline{GaR_3(RH)}]_p + [\overline{InR_3(RH)}]_p - [\overline{GaR_3(RH)}]_{p-1} - [\overline{InR_3(RH)}]_{p-1}\right)$$

$$+ 2\left([\overline{Ga_4R_8Cl(OH)_3}]_p + [\overline{ZnR_2(RH)_2}]_p + [\overline{Zn_2R_4}]_p + [\overline{InZnR_4Cl}]_p \right.$$

$$\left. - [\overline{Ga_4R_8Cl(OH)_3}]_{p-1} - [\overline{ZnR_2(RH)_2}]_{p-1} - [\overline{Zn_2R_4}]_{p-1} - [\overline{InZnR_4Cl}]_{p-1}\right)$$

$$+ \left([\overline{In_2R_4Cl(OH)}]_p - [\overline{In_2R_4Cl(OH)}]_{p-1}\right) \tag{1-41}$$

The overall mass balances of the each metal and chloride are as given in Eqs. (1-42) and (1-43).

$$F \cdot [M_i]_{feed} + E \cdot [\overline{M_i}]_0 = F \cdot [M_i]_1 + E \cdot [\overline{M_i}]_P \tag{1-42}$$

$$F \cdot [Cl]_{P+1} + E \cdot [\overline{Cl}]_0 = F \cdot [Cl]_1 + E \cdot [\overline{Cl}]_P \tag{1-43}$$

3.2.4.2 Zn Reduction Section.

The calculation results based on the feed concentration of 3.0×10^{-3} mol/l Ga, 9.0×10^{-3} mol/l In, and 2.3×10^{-1} mol/l Zn are listed in **Table 1-4** as Ex. #1. Overall fractional recoveries, $\rho_{M_i,Ex\#1} = (E \cdot [\overline{M_i}]_{P+1})/(F \cdot [M_i]_{feed})$, of 9.07×10^{-1}, 9.93×10^{-1} and 8.39×10^{-2} were obtained, respectively, for Ga, In, and Zn. For stripping of a metal-loaded organic solution, the use of lower concentrations of hydrochloric acid is preferable, because the separation of Ga and In is affected by the chloride ion concentration, as shown in the extraction equilibrium formulations. A high ratio of organic solution to stripping solution is also preferable, because the metal concentrations are increased in the stripping stage. Effective stripping can be carried out with 3.98×10^{-1} mol/l of hydrochloric acid, a flow ratio of $F/E = 1/3$, and a counter-current cascade of 2 stages. Numerical values pertinent to this simulation are summarized in Table 1-4 as St. #1. The resultant stripping solution following Zn reduction is then suitable to be used for the separation of In from Ga and Zn.

Table 1-4 Simulated gallium, indium and zinc concentrations

Section	$F:E$	Stage number	$\overline{[(RH)_2]}_{feed}$ [mol/l]	pH	[Ga] [mol/l]	[In] [mol/l]	[Zn] [mol/l]	$\overline{[Ga]}$ [mol/l]	$\overline{[In]}$ [mol/l]	$\overline{[Zn]}$ [mol/l]	ρ_{Ga}	ρ_{In}	ρ_{Zn}
Zinc Reduction													
Ex. #1 input	1:1	1	5.0×10^{-2}		3.00×10^{-3}	9.00×10^{-3}	2.30×10^{-1}						
Ex. #1 output				2.20	2.78×10^{-4}	6.20×10^{-5}	2.11×10^{-1}	2.72×10^{-3}	8.94×10^{-3}	1.93×10^{-2}	9.07×10^{-1}	9.93×10^{-1}	8.39×10^{-2}
St. #1 input	1:3	2	5.0×10^{-2}	0.401	0	0	0	2.72×10^{-3}	8.94×10^{-3}	1.93×10^{-2}			
St. #1 output				0.400	8.16×10^{-3}	2.67×10^{-2}	5.79×10^{-2}	1.56×10^{-6}	5.67×10^{-5}	1.49×10^{-6}	9.07×10^{-1}	9.89×10^{-1}	8.39×10^{-2}
Indium Recovery													
Ex. #2 input	1:1	10	5.0×10^{-2}	1.48	8.16×10^{-3}	2.67×10^{-2}	5.79×10^{-2}	0	0	0			
Ex. #2 output				1.00	7.92×10^{-3}	1.84×10^{-5}	5.75×10^{-2}	2.39×10^{-4}	2.67×10^{-2}	3.79×10^{-4}	2.66×10^{-2}	9.89×10^{-1}	5.49×10^{-4}
Sc. #1 input	1:1	1	5.0×10^{-4}	1.91	0	0	0	2.39×10^{-4}	2.67×10^{-2}	3.79×10^{-4}			
Sc. #1 output				1.10	2.36×10^{-4}	3.87×10^{-3}	3.78×10^{-4}	2.92×10^{-6}	2.28×10^{-2}	1.26×10^{-6}	3.24×10^{-4}	8.44×10^{-1}	1.83×10^{-6}
Gallium Recovery													
Ex. #3 input	1:1	10	1.0×10^{-2}	1.99	7.92×10^{-3}		5.75×10^{-2}	0		0			
Ex. #3 output				1.77	1.89×10^{-5}		5.75×10^{-2}	7.91×10^{-3}		7.58×10^{-5}	8.79×10^{-1}		1.10×10^{-4}

3.2.4.3 In Recovery Section.

The recovery of In from the resulting solution following the Zn reduction operation was also investigated. **Figure 1-17** shows the organic phase concentration profiles obtained for each metal based on the countercurrent cascade.

Figure 1-17 Simulation of In recovery by 5.0×10^{-2} mol/l D2EHPA and counter-current extraction with 10 stages and phase ratio $F : E = 1 : 1$.

The input and output concentration values and operating phase ratio condition are summarized in Table 1-4 as Ex. #2. Ga and Zn extracted at stages 1-3 into the organic phase are returned to the aqueous phase at higher stage numbers of the cascade. This is because the decreased concentration of free D2EHPA caused by the extraction of In acts to reduce the extraction of Ga and Zn. This exchange reaction is in accordance with the results shown in Figure 1-14(b). The effective recovery of In is carried out with an overall fractional recovery,

$\rho_{In,Ex\#2} = \rho_{In,St\#1}(E \cdot [\overline{In}]_{P+1})/(F \cdot [In]_{feed})$, of 9.89×10^{-1}.

The scrubbing effect using a dilute acid solution was also investigated. The simulation show that Ga and Zn in the organic phase are scrubbed effectively, such that In with

34

a purity, $[In]/([Ga]+[In]+[Zn])$, of 1.00 is obtained, but in which overall fractional recovery is lowered to $\rho_{In,Sc\#1}(=\rho_{In,Ex\#2}\cdot[\overline{In}]_{P+1}/[\overline{In}]_{feed})$ = 8.44 × 10^{-1}. The numerical results are shown in Table 1-4, as Sc. #1.

3.2.4.4 Ga Recovery Section.

The separation of Ga from Zn by the countercurrent cascade with 10 stages and 1.0 × 10^{-2} mol/l D2EHPA was investigated. In this case, a lower concentration of extractant is preferable. The concentration profiles for Ga and Zn in the organic phase are shown in **Figure 1-18**.
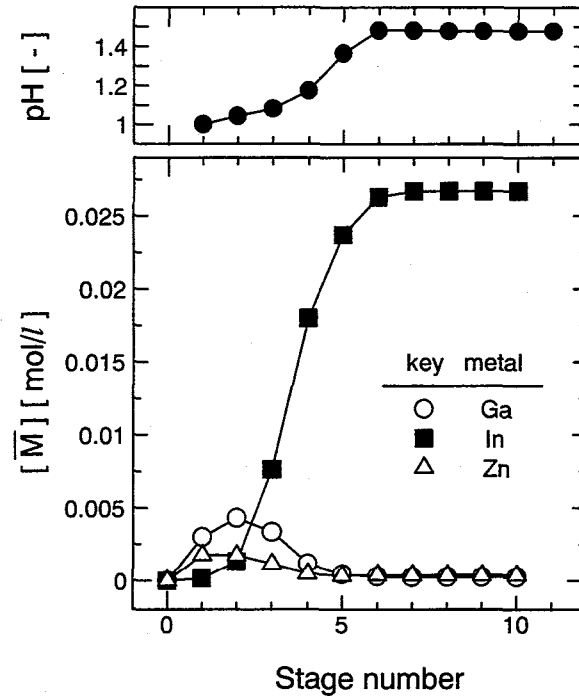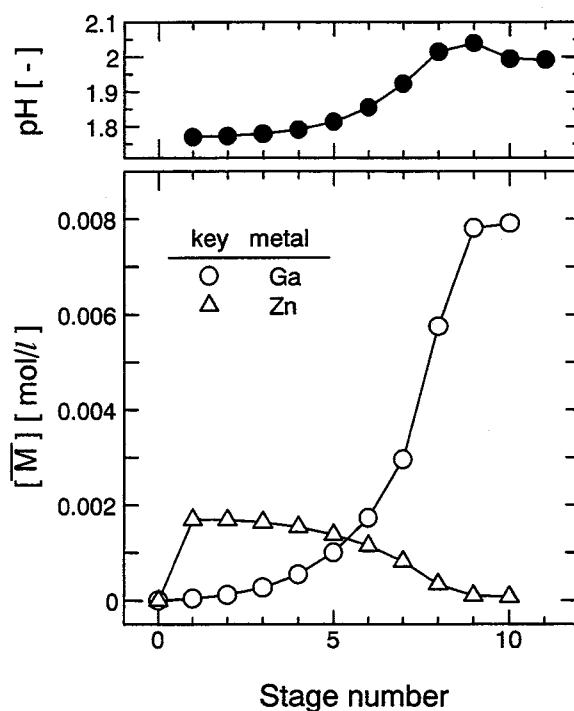

Figure 1-18 Simulation of Ga recovery by 1.0 × 10^{-2} mol/l D2EHPA and counter-current extraction with 10 stages and phase ratio $F : E$ = 1 : 1.

The extracted Zn is excluded to the aqueous phase by the progressive extraction of Ga. An effective recovery of Ga with high purity was met, with an overall fractional recovery of

$$\rho_{Ga,Ex\#3}\left(=\frac{(\rho_{Ga,St\#1}-\rho_{Ga,Ex\#2})(E\cdot\overline{[Ga]}_{P+1})}{F\cdot[Ga]_{feed}}\right)=8.79\times10^{-1}$$ and a purity of 9.91×10^{-1}. The

results obtained are summarized in Table 2 as Ex. #3.

The proposed recovery process is a simple process, consisting of the extraction stage using TBP and D2EHPA, which are familiar extractants used in the extractive separation processes. The process makes use of the property of the extractant that the apparent exchange reaction between more extractable and less extractable components becomes notable at high loadings of the extractant. Zn after recovering Ga and In could also be recovered with high purity.

4. Summary

The separation and recovery process of the rare metals with the liquid-liquid extraction system can be designed using the simulation method, based on the extraction equilibrium formulations up to high loading ratios and the material balance. The formulations must cover the extraction behavior from low loading to high loading to meet the inlet to outlet of the counter-current mixer-settler cascade. The interaction between the metals in the binary metal system should be also included in the formulations. The separation and recovery of Ga and In from zinc refinery residue was investigated as a case study, with following results.

(1) Extraction equilibrium formulations of Ga and In are established, employing D2EHPA, EHPNA, and PIA-226 as extractants and kerosene as diluent. For both metals, the extract entity is $\overline{MR_3(RH)}$ with D2EHPA and EHPNA, while $\overline{MR_2Cl(RH)}$ with PIA-226 at low loading ratios. At high loading ratios, the extract entities, or at least the stoichiometric relations of the metals, are $\overline{Ga_4R_8Cl(OH)_3}$ and $\overline{In_2R_4Cl(OH)}$ with the three extractants. In the case of a binary metal system with EHPNA and PIA-226, the mixed complex, containing both Ga and In with mole ratio of 1 : 1, must be taken into account. In is more extracted than Ga with the three extractants. D2EHPA is most suitable for the separation of Ga and In.

(2) Extraction equilibrium formulations for the ternary system containing Ga, In and Zn are now well established, when D2EHPA is employed as the extractant and kerosene as the diluent.

(3) The scrubbing effect of a metal-loaded organic solution with both metal-free and

metal-containing solutions was investigated. This showed that both Ga and Zn in the organic phase may be scrubbed off effectively into the aqueous phase with both types of scrubbing solutions. The scrubbing effect can also be expressed by the proposed extraction scheme.

(4) The separation and recovery process for Ga and In with D2EHPA has been evaluated by simulation work based on the equilibrium studies and an equilibrium countercurrent extraction stage formulation. The process consists of three sections: (i) Zn reduction, (ii) In recovery, and (iii) Ga recovery. Ga and In are shown to be capable of effective recovery with purities of 9.91×10^{-1} and 1.00, respectively.

5. Nomenclature

D	= distribution ratio	[-]
E	= flow rate of the organic phase in counter-current cascade	[l/min]
F	= flow rate of the aqueous phase in counter-current cascade	[l/min]
K_{ex}	= extraction equilibrium constant	
K_a	= overall formation constant	
M	= metal	
$(RH)_2$	= dimeric species of extractant	
S	= concentration of free dimeric extractant	[mol/l]
ρ	= overall fractional recovery	[-]
[ ]	= concentration of the species in the brackets	[mol/l]

\<Subscripts\>

aq	= aqueous phase
feed	= aqueous or organic feed solution
i	= component (Ga, In, or Zn)
org	= organic phase
p	= extraction stage number
P	= total number of extraction stages
t	= total value

\<Superscript\>

$^{-}$	= organic phase species

Chapter II

Liquid-Liquid Extraction Process Combined with the Masking Reaction
~ Separation of Rare Earth Metals ~

1. Introduction

For the effective separation of rare earth metals, various modifications of the extraction system are needed. One of the effective methods for improving the separation is to modify the aqueous phase by adding a water-soluble complexing agent. In the presence of the water-soluble complexing agent, a part of the metals in the aqueous phase is complexed and thus hindered in the extraction by a masking effect with the agent. The magnitude of the masking depends on complex formation constants, the agent concentration, and pH value of the aqueous phase. The separation of the metals should thus be improved, when the above conditions can be properly combined in the extraction system. The most popular water-soluble complexing agents are amino poly acetates, such as ethylenediaminetetraacetic acid (EDTA) and diethylenetriaminepentaacetic acid (DTPA).

There are several reports concerning this extraction system, especially for the rare earth metals, when combined with a masking reaction with amino poly acetates at the equilibrium state. Hirai et al. have reported the separation of rare earth metals with tri-n-octylmethylammonium nitrate (TOMAN) and TOMAN/α-acetyl-m-dodecylacetophenone (LIX54) in the presence of EDTA.[61] In this case, the separation is improved by adding EDTA, since the extractability of the rare earth metals with TOMAN decreases with atomic number. The extraction behavior can be expressed using an extraction equilibrium formulations, determined on the assumptions that (1) all the EDTA in the aqueous phase forms a 1 : 1 complex with the rare earth metals and (2) the complexed rare earth metal is inactive in the subsequent extraction.

Recently, crown ethers have been studied as the ion size selective masking reagents acting in the aqueous phase in separation of alkaline earths and rare earths.[62,63] 1-Phenyl-3-methyl-4-benzoylpyrazol-5-one (HPMBP)/tri-n-octylphosphine oxide (TOPO) was used for the separation of alkaline earth metals and D2EHPA/TOPO for the separation of rare earth metals, in the presence of 18-crown 6-ether (18C6) or 15-crown 5-ether (15C5). A combined effect

between the chelating extractants and crown ethers can be obtained in the rare earth metal system, since the stability of the complex formed, between the crown ethers and the metal ions, decreases with increasing atomic number. Sasaki et al. have synthesized sulfonated crown ethers, which are more hydrophilic than the conventional crown ethers,[64,65] since for the conventional crown ethers, such as 18C6, the distribution of the ether into the organic phase is not negligible.

It is known that the rate of extraction is decreased by the addition of DTPA or EDTA to the extraction system.[66] A separation process, under non-equilibrium state, can therefore be constructed, using this property. Minagawa et al. have investigated a non-equilibrium separation process for Y from other rare earth metals, using acidic organophosphorus compounds.[67] Matsuyama et al. have also investigated the effect of the addition of an organic acid, such as citric acid or lactic acid, on the non-equilibrium separation of Y/Er, using Cyanex 272 (bis(2,4,4-trimethylpentyl)phosphinic acid).[68] Under these conditions, rate of extraction is increased considerably, although the selectivity (ratio between the extraction rates) is decreased from 5.8 to ca. 3.5.

One of the problems encountered in an extraction system concerns the recovery of both the complexed metals and the agents from the raffinate aqueous solution. It is well known that the metal-EDTA complex is dissociated in high acidic solution, since EDTA exists as the H_4L form in such solution. The recovery of metals complexed with EDTA in the raffinate solution, following dissociation of the metal, can therefore be achieved, using TBP, which is active in such high acidic region.[61] In addition, the protonated EDTA (H_4L) also tends to precipitate, under such conditions, which thus enables the EDTA to be recovered. Matsuyama et al. have synthesized new hydrophilic chelating polymers, functionalized with EDTA,[69] and have applied them to the extractive separation of heavy rare earth metals, using Cyanex 272.[70] The chelating polymers synthesized are precipitated in the presence of rare earth metals, suggesting that the recovery of the agent from the extraction system is thus feasible.

The extractability of rare earth metals with acidic extractants, such as acidic organophosphorus compounds, generally increases with increasing atomic number of the rare earth metals and the complex formation constants for most complexing agents also increase accordingly.[71] The combined effect between extractant and complexing agent is, therefore,

hardly obtained in an extraction system with such acidic extractants. The extractability of Y with acidic organophosphorus compounds, however, lies between the values for Ho and Er, whilst the magnitude of the complex formation constant for Y with EDTA is the lowest of the three metals. Y, therefore, may be expected to be selectively extracted from Ho/Y/Er mixture by combining complex formation with EDTA into the extraction system. In addition, the separation of heavy rare earth metals is expected to be improved by adding DTPA, because the complex formation constants from Dy to Lu decrease with increasing atomic number.[71]

In this chapter, the liquid-liquid extraction process, combined with the masking reaction with water-soluble complexing agent at the equilibrium state, is investigated. The selective separation of rare earth metals in the presence of EDTA or DTPA is carried out as a case study. First, the extraction equilibrium formulations of rare earth metals with EHPNA or 2-ethyl-2-methylheptanoic acid (VA-10) in the presence of the agent are investigated up to high loadings, which is practical importance. The simulation work for the separation of rare earth metals with counter-current mixer-settler cascade is then carried out based on the formulations determined.

2. Experiment

2.1 Reagents.

2-Ethylhexyl phosphonic acid mono-2-ethylhexyl ester (EHPNA, marketed as PC-88A by Daihachi Chemical Industry Co., Ltd., purity: 95.9 wt%) and 2-ethyl-2-methylheptanoic acid (VA-10, marketed by Shell Chemical Co.) were used as received. The extractants were diluted in kerosene. All the inorganic chemicals were supplied by Wako Pure Chemical Industries as analytical grade reagents. Ethylenediaminetetraacetic acid (EDTA, disodium salt) and diethylenetriaminepentaacetic acid (DTPA) were supplied by Dojin Chemical Industries. Deionized water was purified by simple distillation prior to use. The aqueous rare earth chloride solutions were prepared by dissolving the oxides in heated hydrochloric acid followed by removing the excess acid by evaporation. The ionic strength of the aqueous solution was held constant at 5.0×10^{-1} mol/l by adding (Na,H)Cl. The organic solutions were prepared by diluting each extractant in the diluent.

2.2 Procedure.

The aqueous feed solutions were prepared by adding appropriate concentration of

complexing agent and NaOH to rare earth chloride solution, in order to achieve a required equilibrium pH value. The organic solutions were prepared by diluting the extractant with kerosene, and the resultant extractant concentration was determined by potentiometric titration using an automatic titration apparatus (Hiranuma Comtite-550). Organic and aqueous solutions having volume ratios of 1 : 1 were shaken and equilibrated at 298 K. Weighed organic samples were stripped with HCl with an O/A volume ratio of 0.5. The resulting aqueous samples were analyzed by using a Nippon Jarrell-Ash ICAP-575 Mark II emission spectrometer. The aqueous phase pH value was measured with an Orion 920A pH meter equipped with a glass combination electrode.

3. Results and Discussion

3.1 Extraction Equilibrium Formulations in the Absence of the Water-Soluble Complexing Agent.

3.1.1 EHPNA System.

The extraction equilibrium formulations for rare earth metals with EHPNA at low loading region has been reported by several investigators as shown in Eq. (2-1).

$$Ln^{3+} + 3\overline{(RH)_2} \leftrightarrow \overline{LnR_3(RH)_3} + 3H^+ \qquad ; K_{ex,1} \qquad (2-1)$$

Figure 2-1 shows the relationship between the loading ratio of the organic phase and the apparent extraction equilibrium constants, $K_{ex,1}$, assuming the concentration of free dimeric extractant $S = [\overline{(RH)_2}]_{feed} - 3[\overline{Ln}]$. The apparent values remain constant up to the loading ratio of about 0.25, indicating that monomeric species, $\overline{LnR_3(RH)_3}$, exist at loading ratios less than 0.25. The values then increase with increase in the loading ratio, and the loading ratios approach 0.4. This indicate that a complex containing the dimeric extractant and rare earth metal with mole ratio of 5 : 2 is formed at high loadings. Thus, the formation of aggregated species, $\overline{(LnR_3)_2(RH)_4}$, in the organic phase is assumed, as shown by Eq. (2-2).
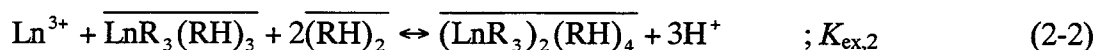
$$Ln^{3+} + \overline{LnR_3(RH)_3} + 2\overline{(RH)_2} \leftrightarrow \overline{(LnR_3)_2(RH)_4} + 3H^+ \qquad ; K_{ex,2} \qquad (2-2)$$

The most likely values of $K_{ex,1}$ and $K_{ex,2}$ are determined by the nonlinear least square method to fit the experimental results, and these are summarized in **Table 2-1**.

41
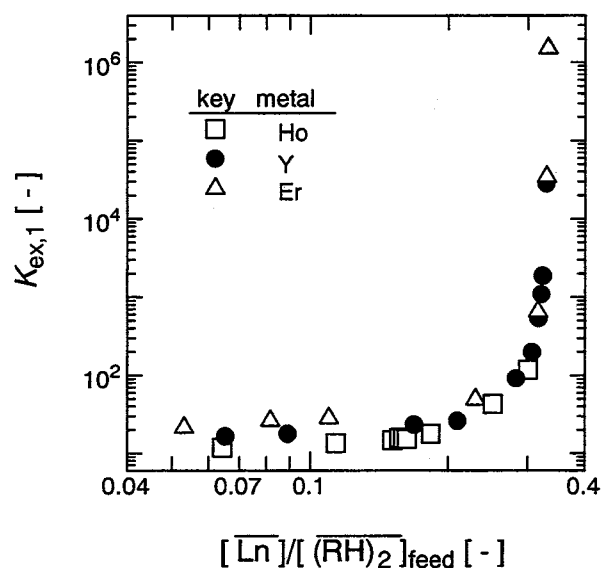
Figure 2-1 Relationship between loading ratio of organic phase and apparent extraction equilibrium constants, $K_{ex,1}$. $[\overline{(RH)_2}]_{feed} = 5.0 \times 10^{-2}$ mol/l and $[Ln]_{feed} = 1.0 \times 10^{-1}$ mol/l.

Table 2-1 Rare earth metals extraction equilibrium constants

	Ho	Y	Er
$K_{ex,1}$	1.05×10	1.62×10	2.26×10
$K_{ex,2}$	8.12	6.26	9.23

With these constants and by use of material balance equation for the dimeric extractant, the concentration of free extractant concentration can be calculated, enabling the distribution ratio to be calculated.   The experimental distribution ratios are plotted versus equilibrium pH value in **Figure 2-2**, and compared with the predicted values shown by solid lines.   The behaviors of single rare earth extraction by using EHPNA are successfully expressed up to high loading ratios by the proposed scheme.

42
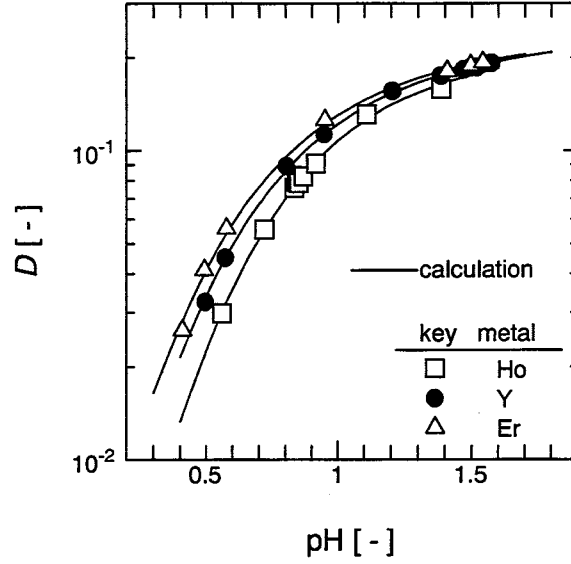
Figure 2-2   Effect of equilibrium pH values on distribution ratio of rare earth metals in single metal systems. Comparison of observed data with prediction shown by solid lines. $\overline{[(RH)_2]}_{feed} = 5.0 \times 10^{-2}$ mol/l and $[Ln]_{feed} = 1.0 \times 10^{-1}$ mol/l.

The results obtained with single metal extraction are then extended to the extraction from Ho/Y/Er ternary solution. If an interaction among the three metals is negligible, the concentration of each rare earth metal in the organic phase is expressed as Eq. (2-3).

$$\overline{[Ln_i]}_t = \overline{[Ln_i R_3(RH)_3]} + 2\overline{[(Ln_i R_3)_2(RH)_4]}$$

$$= \frac{K_{ex,1,i}[Ln_i^{3+}]S^3}{[H^+]^3} + 2\frac{K_{ex,1,i}K_{ex,2,i}[Ln_i^{3+}]^2 S^5}{[H^+]^6} \tag{2-3}$$

The concentration of feed dimeric extractant is expressed as Eq. (2-4).

$$\overline{[(RH)_2]}_{feed} = 3\sum_i \overline{[Ln_i R_3(RH)_3]} + 5\sum_i \overline{[(Ln_i R_3)_2(RH)_4]} + \overline{[(RH)_2]}$$

$$= 3\sum_i \left(\frac{K_{ex,1,i}[Ln_i^{3+}]S^3}{[H^+]^3} \right) + 5\sum_i \left(\frac{K_{ex,1,i}K_{ex,2,i}[Ln_i^{3+}]^2 S^5}{[H^+]^6} \right) + S \tag{2-4}$$

With the extraction equilibrium constants determined in the single metal systems and by using Eq. (2-4), the concentration of free dimeric extractant, S, can be calculated, enabling the distribution ratio to be calculated by using Eq. (2-3). Experimental distribution ratios are

plotted in **Figure 2-3**, as a function of pH, together with the above predicted values, shown by the solid lines. The data are seen to agree well with the prediction, thus indicating that the extraction equilibrium formulations obtained in each of the single metal system can also be used in the ternary metal system, in the absence of EDTA.
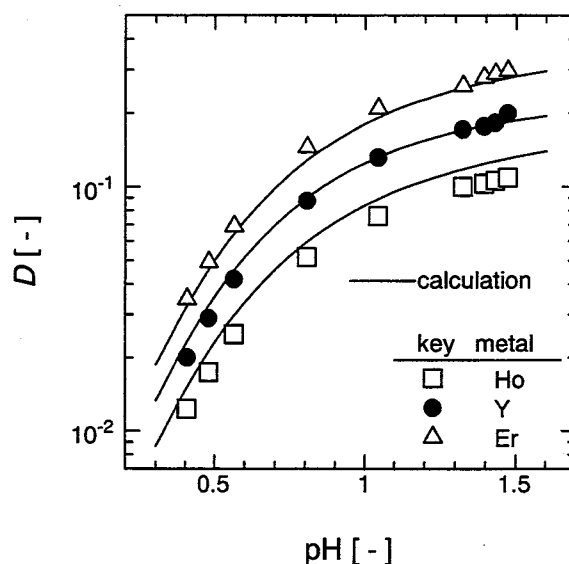
Figure 2-3   Effect of pH on distribution ratios for rare earth metals in the ternary system. Comparison of experimental data with prediction, as shown by solid lines. $[\overline{(RH)_2}]_{feed} = 5.0 \times 10^{-2}$ mol/l and $[Ln_i]_{feed} = 3.0 \times 10^{-2}$ mol/l.

3.1.2 VA-10 System.

The extraction equilibrium of heavy rare earth metals (Y, Er, Lu, and Yb) at low loadings is formulated as Eq. (2-5) by using the slope analysis method.

$$Ln^{3+} + 3\overline{(RH)_2} \leftrightarrow \overline{LnR_3(RH)_3} + 3H^+ \qquad ; K_{ex,1} \qquad (2-5)$$

This formulation is consistent with that reported previously.[14] The high loadings of the extractant were brought about by increasing the feed metal concentration and by raising the equilibrium pH value. The maximum loading ratios approach about 0.66, suggesting that a complex containing the metal and the dimeric extractant with a mole ratio of 2 : 3 is likely to be formed at the extreme conditions of maximum loading ratios of the extractant. Therefore,

the formation of aggregated species, $(LnR_3)_2$, in the organic phase is assumed, as shown in Eq. (2-6).

$$Ln^{3+} + \overline{LnR_3(RH)_3} \leftrightarrow \overline{(LnR_3)_2} + 3H^+ \qquad ; K_{ex,2} \qquad (2-6)$$

The extraction equilibrium constants are determined by the nonlinear least square method, and are summarized in **Table 2-2**. The distribution ratios are then predicted with these constants and by using the material balance equations for the concentration of rare earth metal in the organic phase and the feed concentration of the dimeric extractant, as previously shown in EHPNA system.

Table 2-2 Extraction equilibrium constants for rare earth metals

|	Y	Er	Yb	Lu
$K_{ex,1}$	2.92×10^{-14}	5.30×10^{-14}	5.11×10^{-14}	9.09×10^{-14}
$K_{ex,2}$	1.84×10^{-16}	4.59×10^{-16}	1.85×10^{-14}	1.95×10^{-14}
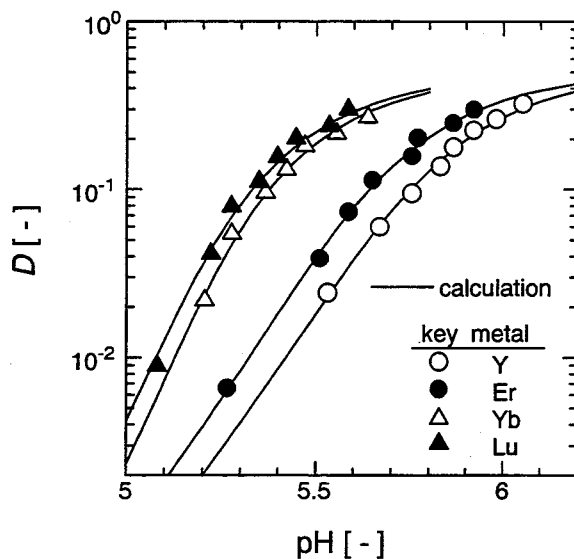
Figure 2-4 Effect of equilibrium pH values on the distribution ratios in single metal systems. Comparison of observed data with prediction shown by solid lines. $[\overline{(RH)_2}]_{feed} = 2.5 \times 10^{-2}$ mol/l and $[Ln]_{feed} = 5.0 \times 10^{-2}$ mol/l.

The experimental distribution ratios are plotted in **Figure 2-4**, together with the predicted lines. The extraction behavior of these rare earth metals in single metal systems can be expressed up to high loadings by the proposed extraction scheme.

The results obtained in single metal systems are extended to the extraction in Y/Er and Yb/Lu binary systems. The experimental distribution ratios of each metal in each binary system are plotted in **Figure 2-5 (a)**. If the interaction between the two metals is negligible, the distribution ratios of each metal can be calculated using the extraction equilibrium constants determined in the single metal systems. The predicted distribution ratios are shown in Figure 2-5 (a) by solid lines. The experimental data except for the low loading region are seen to cluster on the predicted values, indicating that the extraction scheme obtained in the single metal system also describes the binary metal system.
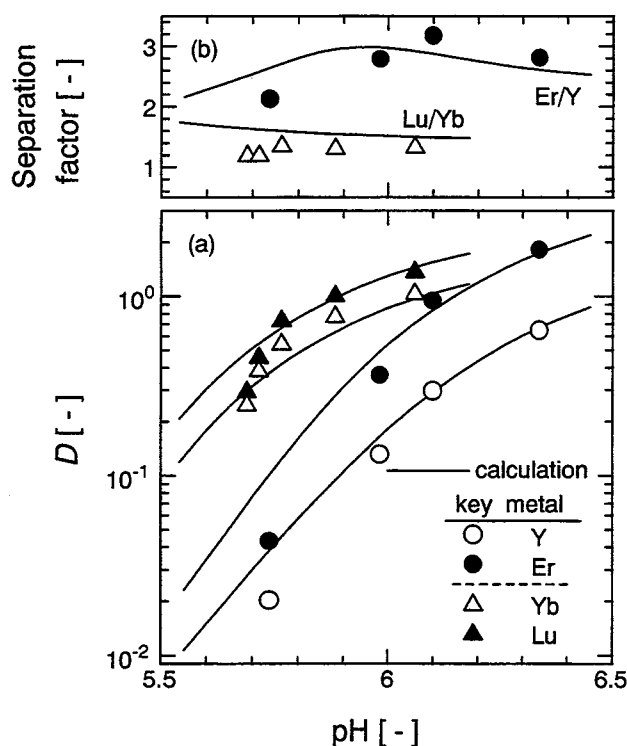
Figure 2-5 Effect of equilibrium pH values on (a) distribution ratios and (b) separation factor in binary systems (Y/Er and Yb/Lu). Comparison of observed data with prediction shown by solid lines. $[\overline{(RH)_2}]_{feed} =$ 2.0 $\times 10^{-2}$ mol/l and $[Ln_i]_{feed} = 1.0 \times 10^{-2}$ mol/l.

46

The deviation between the experimental and predicted values at low loadings may be due to limitations of the ICP-AES analytical, caused by the interaction between the two metals during analysis. The experimental and predicted separation factors, defined as the ratio of distribution ratios, are also shown in Figure 2-5 (b). In the case of the Y/Er system, the ratio of $K_{ex,2}$ for the two metals is larger than the ratio of $K_{ex,1}$, thus enhancing the separation factor with increasing loading ratio. In the case of the Yb/Lu system, however, the separation factor is almost independent of the loading ratio, because the ratio of $K_{ex,2}$ for the two metals is slightly lower than the ratio of $K_{ex,1}$.

3.2 Extraction Equilibrium Formulations in the Presence of the Water-soluble Complexing Agent.

3.2.1 EHPNA System in the Presence of EDTA.

It is known that the ability of EDTA (H_4L) to complex with rare earth metals depends on the pH value of the aqueous solution, since only the dissociated ligand of EDTA (L^{4-}) forms a complex with the rare earth metal. The formation of the dissociated ligand of EDTA, as a function of pH, and the corresponding overall formation constants are expressed by Eqs. (2-7)-(2-10).[71]

$$H^+ + L^{4-} \leftrightarrow HL^{3-} \qquad ; \beta_1 = 10^{10.17} \qquad (2\text{-}7)$$

$$2H^+ + L^{4-} \leftrightarrow H_2L^{2-} \qquad ; \beta_2 = 10^{16.28} \qquad (2\text{-}8)$$

$$3H^+ + L^{4-} \leftrightarrow H_3L^- \qquad ; \beta_3 = 10^{18.96} \qquad (2\text{-}9)$$

$$4H^+ + L^{4-} \leftrightarrow H_4L \qquad ; \beta_4 = 10^{20.96} \qquad (2\text{-}10)$$

The complex formation reaction between any rare earth metal, Ln_i, and EDTA is expressed by Eq. (2-11).

$$Ln_i^{3+} + L^{4-} \leftrightarrow Ln_iL^- \qquad ; K_{f,i} \qquad (2\text{-}11)$$

The concentrations for total EDTA and for the total rare earth metals are expressed by Eqs. (2-12) and (2-13), respectively, for the case of three rare earth metals (Ho, Y, and Er) and EDTA, contained in aqueous solution.

$$[EDTA] = [L^{4-}] + [HL^{3-}] + [H_2L^{2-}] + [H_3L^-] + [H_4L] + \sum_i [Ln_iL^-]$$

$$= (1 + \beta_1[H^+] + \beta_2[H^+]^2 + \beta_3[H^+]^3 + \beta_4[H^+]^4 + \sum_i K_{f,i}[Ln_i^{3+}])[L^{4-}] \quad (2\text{-}12)$$

$$[Ln_i]_t = [Ln_i^{3+}] + [Ln_iL^-] \qquad (2\text{-}13)$$

The concentrations of the individual free rare earth metals are expressed by Eq. (2-14).

$$[Ln_i^{3+}] = \frac{[Ln_i]_t}{1 + K_{f,i}[L^{4-}]} \qquad (2\text{-}14)$$

Literature values for the complex formation constants, $K_{f,i}$, for Ho, Y, and Er are given by $10^{18.60}$, $10^{18.08}$, and $10^{18.83}$, respectively.[71] Using these constants in combination with the use of Eqs. (2-12) and (2-14), the concentration of the dissociated ligand of EDTA, $[L^{4-}]$, can be calculated, also enabling the concentration of the free and complexed rare earth metal to be determined using Eqs. (2-13) and (2-14).

With EDTA, the rare earth metal, when complexed with EDTA as Ln_iL^-, is assumed not to take part in the extraction, and, thus, the distribution of each rare earth metal between aqueous and organic phases is determined only by the free rare earth metals in the aqueous phase, Ln_i^{3+}. The material balance of each rare earth metal in the extraction system in the presence of EDTA is expressed as Eq. (2-15).

$$[Ln_i]_{feed} = [Ln_i]_t + [\overline{Ln_i}]_t$$
$$= [Ln_i^{3+}] + [Ln_iL^-] + [\overline{LnR_3(RH)_3}] + 2[\overline{(LnR_3)_2(RH)_4}] \qquad (2\text{-}15)$$

The distribution ratio for each rare earth metal in the presence of EDTA is also expressed as Eq. (2-16).

$$D_i = \frac{[\overline{Ln_i}]_t}{[Ln_i]_t} = \frac{[\overline{Ln_i}]_t}{[Ln_i^{3+}] + [Ln_iL^-]} \qquad (2\text{-}16)$$

Based on the above assumption, an apparent distribution ratio, $D_{a,i}$, defined as $[\overline{Ln_i}]/[Ln_i^{3+}]$, can be calculated, enabling a predicted value of the distribution ratio, D_i, in the presence of EDTA to be calculated. The effect of pH on the distribution ratios for Ho, Y, and Er in the ternary system, in the presence of EDTA, is plotted in **Figure 2-6**, together with the calculated distribution ratios, as shown by the solid lines. The experimental data are seen to cluster on the respective predicted lines, thus indicating that the proposed extraction scheme can be used to describe the extraction system, in the presence of EDTA. As shown in Figure 2-6 (a) for [EDTA] = 5.0 × 10^{-3} mol/l, the distribution ratios for Ho and Er are suppressed more than for Y with a masking effect occurring at the high pH region. With an increased concentration of 1.0 × 10^{-2} mol/l EDTA (Figure 2-6 (b)) reversed, as compared to Figure 2-3, and enhances the

48

selective extraction of Y.
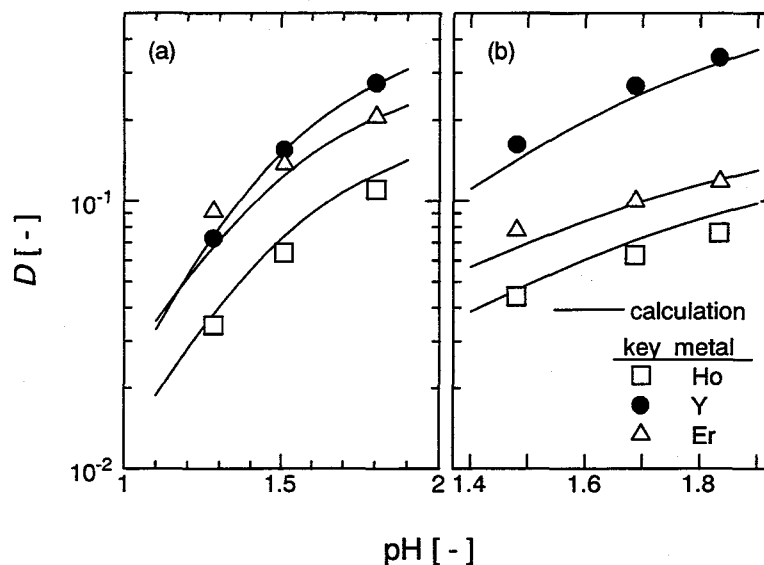
Figure 2-6 Effect of pH on distribution ratios for the rare earth metals in the ternary system in the presence of EDTA. Comparison of experimental data with prediction, as shown by solid lines. $[\overline{(RH)_2}]_{feed} = 1.0 \times 10^{-2}$ mol/l and $[Ln_i]_{feed} = 5.0 \times 10^{-3}$ mol/l, and [EDTA] = (a) 5.0×10^{-3} mol/l and (b) 1.0×10^{-2} mol/l.

3.2.2 VA-10 System in the Presence of DTPA.

In the case of DTPA, it is also generally known that a rare earth metal forms a 1 : 1 complex with the dissociated ligand of DTPA (L^{5-}) as shown in Eq. (2-17).

$$Ln^{3+} + L^{5-} \leftrightarrow LnL^{2-} \qquad ; K_f \qquad (2-17)$$

The literature values of the complex formation constants of DTPA, K_f, for Y, Er, Yb, and Lu are $10^{22.05}$, $10^{22.74}$, $10^{22.62}$, and $10^{22.44}$, respectively.[71] **Figure 2-7** shows the distribution ratios of Y in the presence of DTPA or EDTA. In the presence of the complexing agent, the distribution ratios become lower than those in the absence of the agent as expected. The distribution ratios in the presence of the complexing agent are predicted by combining the extraction equilibrium expression and the complex formation reaction between the agent and rare earth metals in the aqueous phase. The predicted distribution ratios are also shown as lines in Figure 2-7.
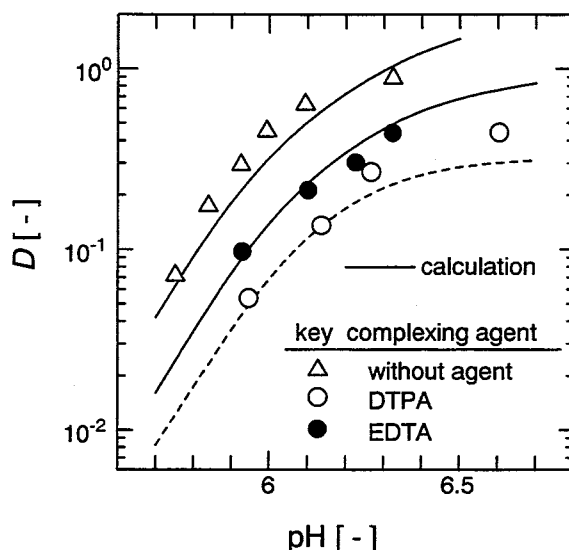
Figure 2-7 Effect of equilibrium pH values on the distribution ratios of Y in a single metal system in the presence of DTPA or EDTA. Comparison of observed data with prediction shown by lines. Solid line: based on 1 : 1 complex, dotted line: based on 1.5 : 1 complex. $[\overline{(RH)_2}]_{feed}$ = 2.0 × 10^{-2} mol/l, $[Y]_{feed}$ = 2.0 × 10^{-2} mol/l, and [complexing agent] = 1.0 × 10^{-2} mol/l.

In the EDTA system, the experimental data are seen to cluster on the predicted values based on the assumption of a 1 : 1 complex. In the DTPA system, however, the experimental values are lower than those predicted based on the assumption of a 1 : 1 complex. The predicted values for the DTPA system should be equal to those for the EDTA system, because both complexing agents are completely dissociated and form a 1 : 1 complex with rare earth metals in this pH region. The deviation of experimental values from predicted values in the DTPA system may be caused by a change in the molar ratio of rare earth metal and DTPA in the complex. Several calculation runs were carried out assuming various molar ratios of rare earth/DTPA in the complex. The predicted values based on the molar ratio of rare earth to DTPA of 1.5 are shown in Figure 2-7 by the dotted line. The experimental data are seen to cluster on the predicted line based on a 1.5 : 1 complex at pH < 6.15, but are located between the predicted lines based on the ratios of 1 : 1 and 1.5 : 1 at pH > 6.15. In the case of binary systems (Y/Er and Yb/Lu), most of experimental data also fall between the predicted values with the ratios of 1 : 1 and 1.5 : 1, suggesting that the average of the molar ratio of rare earth to

DTPA in the extraction system with DTPA varies between 1 and 1.5. **Figure 2-8** shows the distribution ratios of each rare earth metal in the binary systems (Y/Er and Yb/Lu) in the presence of DTPA.
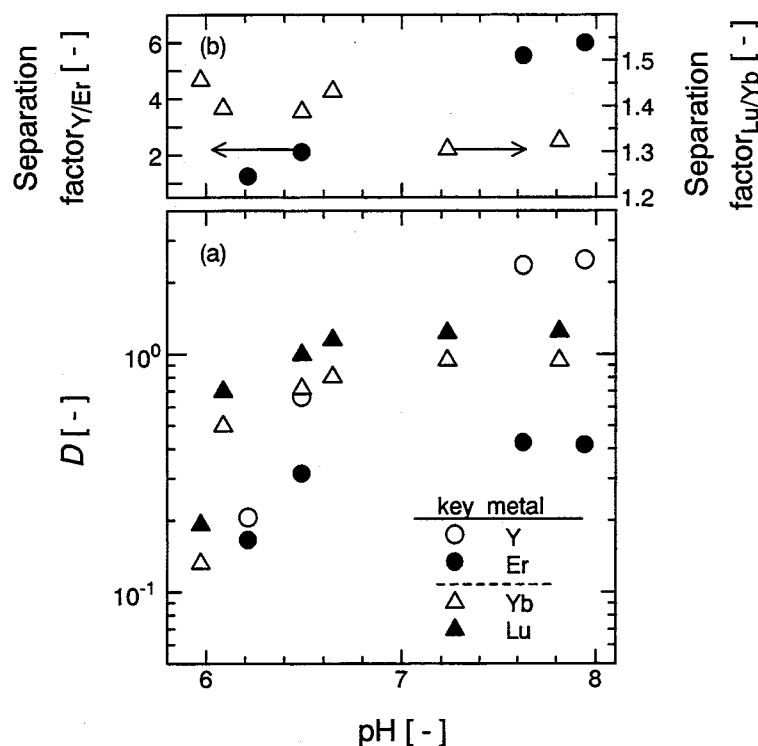
Figure 2-8 Effect of equilibrium pH on (a) distribution ratios and (b) separation factor in binary systems (Y/Er and Yb/Lu) in the presence of DTPA. $[\overline{(RH)_2}]_{feed}$ = 2.0 × 10^{-2} mol/l, $[Ln_i]_{feed}$ = 1.0 × 10^{-2} mol/l, and [DTPA] = 1.0 × 10^{-2} mol/l.

In the case of the Y/Er system, the order of extraction between Y and Er is reversed by the masking effect with DTPA. The effect increases with increase in the equilibrium pH value, making the distribution ratio of Er decrease, and thus improves the selective extraction of Y. In the case of the Yb/Lu system, however, the separation is hardly changed by the presence of DTPA, although this is expected by the masking of Yb, which is the less extractable component. This is due to the fact that the ratio of rare earth metal and DTPA changes from 1 : 1 to 1.5 : 1. In this system, thus, the masking effect with DTPA is hardly expected, and the separation factor decreases with increase in the loading ratios. The following investigation

51

was carried out in only EHPNA/EDTA system, because the extraction equilibrium formulations in VA-10/DTPA system cannot be determined quantitatively.

3.3 Scrubbing Effect of Metal-Loaded Organic Solution.

The metal-loaded organic solution was then contacted with an aqueous scrubbing solution. The resulting loading ratios are plotted against pH values in **Figure 2-9**.
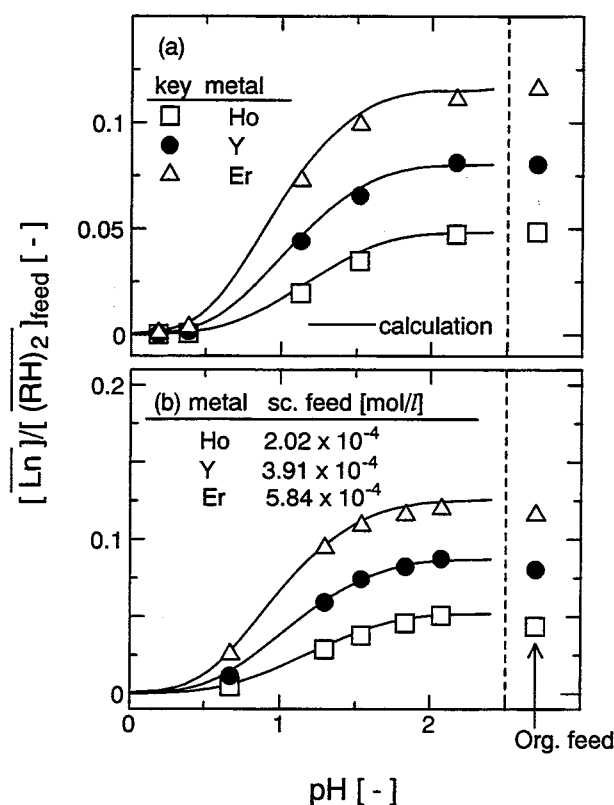
Figure 2-9   Effect of pH values on the loading ratios of rare earth metals after scrubbing of organic phase with (a) metal-free and (b) metal-containing scrubbing solution. Comparison of observed data with prediction shown by solid lines. $[\overline{(RH)_2}]_{feed} = 5.0 \times 10^{-2}$ mol/l.

The experimental values are seen to cluster on the prediction shown by solid lines, based on the extraction equilibrium formulations, in both systems with metal-free and metal-containing scrubbing solution, indicating that the metal exchange reaction is also expressed by the proposed extraction scheme. For both systems, the effect of scrubbing is not obvious, since the amount of heavier metals is too small to enhance the separation. **Figure 2-10** shows that

52

the loading ratios following scrubbing treatment with EDTA containing aqueous solution, together with the prediction shown by solid lines based on the established extraction equilibrium formulations.
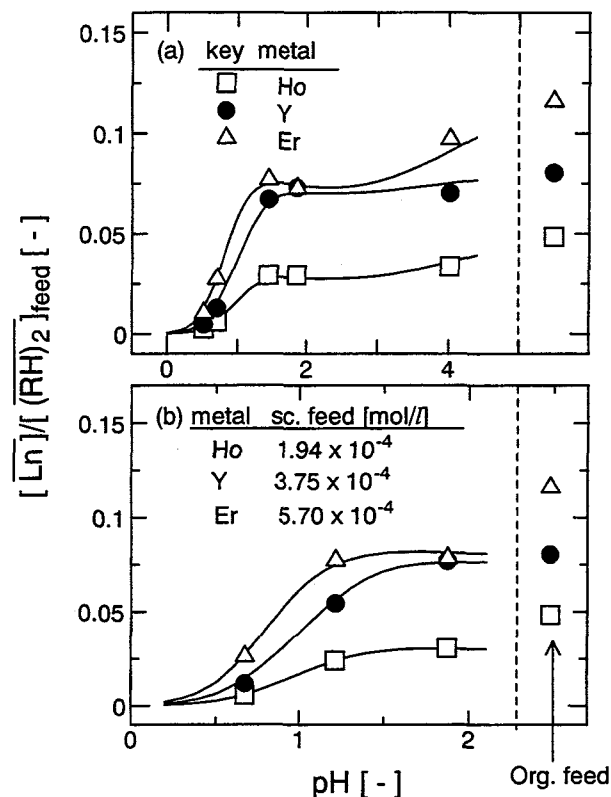
Figure 2-10 Effect of pH values on the loading ratios of rare earth metals after scrubbing of organic phase with (a) metal-free and (b) metal-containing scrubbing solution in the presence of EDTA. Comparison of observed data with prediction shown by solid lines. $[(RH)_2]_{feed} = 5.0 \times 10^{-2}$ mol/l and [EDTA] = 5.0 × 10^{-3} mol/l.

The experimental data are seen to cluster on the respective prediction lines, indicating that the scrubbing with EDTA containing aqueous solution is also expressed by the proposed extraction scheme. The loading ratios of each metal after scrubbing with EDTA containing solution much decreased than those with EDTA absent solution because of complex formation reaction. In both cases, Er and Ho are effectively scrubbed off into the aqueous phase with remaining Y in the organic phase, especially at high pH region. Therefore, separation of Y from Ho/Y/Er

mixture solution is expected to be attained with the selective extraction of Y and effective scrubbing of Ho and Er by adding EDTA in the aqueous phase.

3.4 Separation Process of Rare Earth Metals in the Presence of EDTA.

Based on the above equilibrium studies, a simulation study of the separation of Y from aqueous solution containing Ho/Y/Er at identical concentrations of 1.0×10^{-2} mol/l was carried out. Firstly, the effect of the aqueous feed solution concentration of EDTA, on the selective extraction of Y, was investigated. **Figure 2-11** shows the effect of EDTA concentration on the calculated distribution ratios obtained for each metal and the corresponding separation factors between Y/Ho and Y/Er at an equilibrium pH value of 1.5.
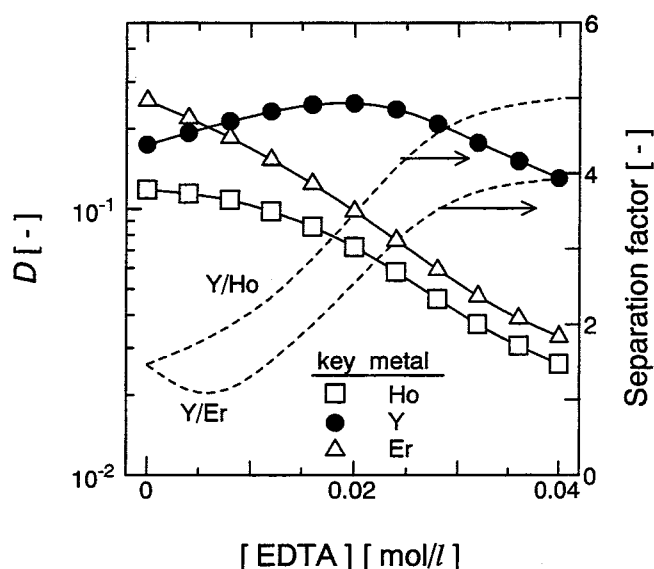
Figure 2-11 Effect of EDTA concentration on distribution ratio and the separation factor in the ternary system. $[\overline{(RH)_2}]_{feed} = 2.0 \times 10^{-2}$ mol/l and $[Ln_i]_{feed} = 1.0 \times 10^{-2}$ mol/l, and pH = 1.5.

The separation factors for Y/Ho and Y/Er both increase with EDTA concentration due to the enhanced masking effect for Ho and Er. The distribution ratio for Y, however, decreases for EDTA concentration greater than 2.0×10^{-2} mol/l. An EDTA concentration of 2.0×10^{-2} mol/l was, therefore, used thereafter.

A simulation of the separation of Y from Ho/Y/Er mixture solution by counter-current

mixer-settler cascade can be carried out, using the extraction equilibrium formulations and the material balance formulations for the each component. A schematic flowsheet for a counter-current mixer-settler cascade is shown in **Figure 2-12**.
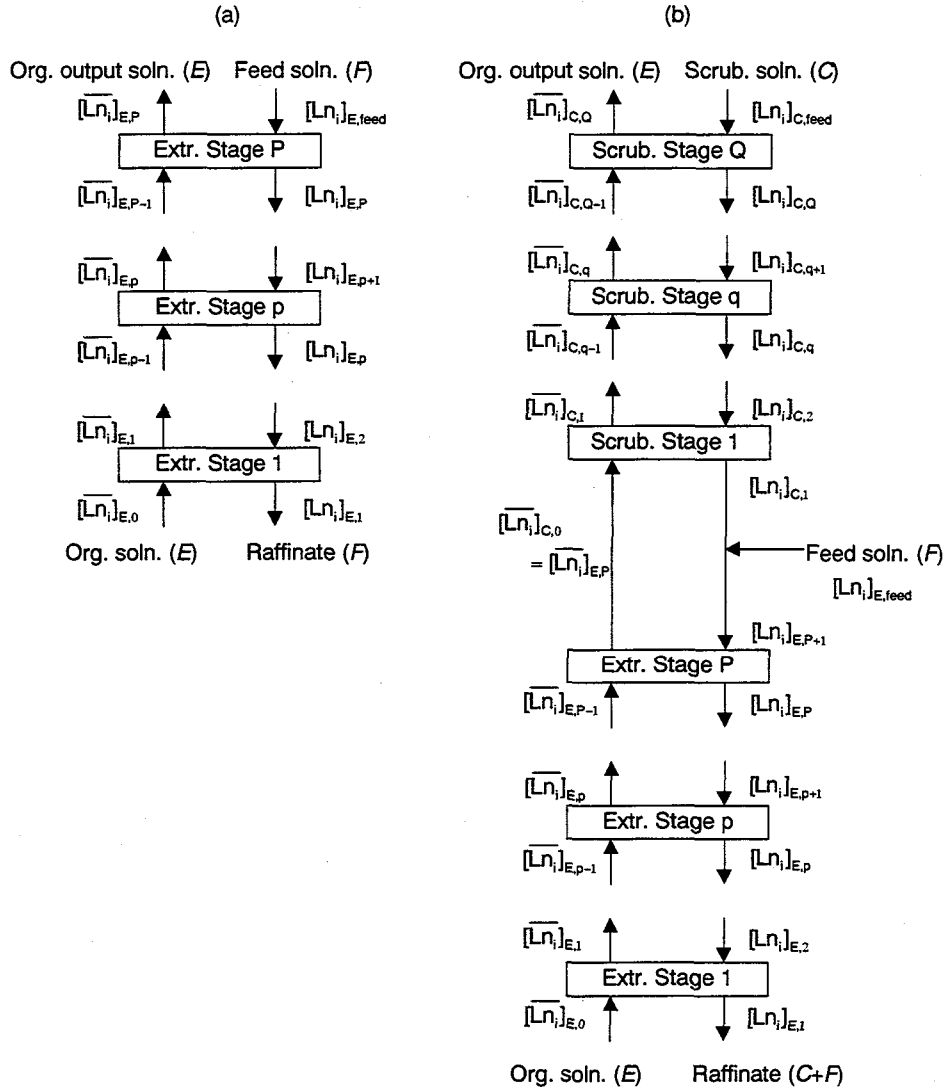
Figure 2-12 Schematic flowsheets for the counter-current mixer-settler cascade with (a) extraction only and (b) combined extraction and scrubbing sections.

Firstly, separation with only an extraction section (Figure 2-6 (a)) was carried out. In this simulation, the input values of F (= 1 l/min), E (= 1 l/min), $[Ln_i]_{E,feed}$ (= 1.0×10^{-2} mol/l), $\overline{[Ln_i]}_{E,0}$ (= 0 mol/l), $[H^+]_{E,1}$, [EDTA] (= 2.0×10^{-2} mol/l), and $\overline{[(RH)_2]}_{feed}$ (= 2.0×10^{-2} mol/l)

were applied. The calculation was done as described in Chapter I, as follows. When temporary values of $[Ln_i]_{E,1}$ and $[H^+]_{E,1}$ are given, $D_{i,1}$ is calculated using Eqs. (2-14)-(2-16), and then $[\overline{Ln_i}]_{E,1}$ is calculated. The values of $[Ln_i]_{E,2}$ and $[H^+]_{E,2}$ are thus calculated based on the material balance formulations in each stage. These calculations are carried out in a similar way from stage 1 to P repeatedly, until the resulting value of $[Ln_i]_{E,feed}$ becomes equal to the given $[Ln_i]_{E,feed}$ by changing the value of $[Ln_i]_{E,1}$ based on the material balance formulations in the cascade.

Figure 2-13 Simulation studies for separation of Y from a Ho/Y/Er mixture by a counter-current mixer-settler extraction cascade with 10 extraction stages for the conditions: $F : E = 1 : 1.$ $[\overline{(RH)_2}]_{feed} = 2.0 \times 10^{-2}$ mol/l, $[Ln_i]_{E,feed} = 1.0 \times 10^{-2}$ mol/l, and $[EDTA]_E = 2.0 \times 10^{-2}$ mol/l.

Figure 2-13 shows the resulting organic phase rare earth concentrations for the case of a ten-stage extraction cascade. With an aqueous feed pH value of 1.57 (Figure 2-13 (a)), the pH values in stages 5-10 hardly deviate from the feed value and the overall fractional recovery of Y,

56

$\rho_Y = E \cdot [\overline{Y}]_{E,P} / F \cdot [Y]_{feed}$, obtained is of low order. For a feed pH value of 2.92 (Figure 2-13

(b)), the pH values increase with increasing stage number, and an effective overall fractional

recovery of $\rho_Y = 4.91 \times 10^{-1}$ can be obtained. In addition, the masking effect for Ho and Er

increases with the increasing pH, making the concentrations for Ho and Er in the organic phase

decrease slightly with increasing stage number for stages 3-10. However, the overall

decontamination factor, $f = \rho_Y / (\rho_{Ho} + \rho_{Er})$, is not increased drastically, thus indicating that a

scrubbing section is needed in the extraction cascade in order to achieve an effective separation

for Y.

The effect of an additional scrubbing section was therefore investigated. Figure 2-12

(b) shows the schematic flowsheet for both extraction and scrubbing sections. In this

simulation, values of F (= 1 l/min), E (= 1 l/min), C (= 1 l/min), $[Ln_i]_{E,feed}$ (=2.0 × 10^{-2} mol/l),

$[Ln_i]_{C,feed}$ (= 0 mol/l), $[\overline{Ln_i}]_{E,0}$ (= 0 mol/l), $[H^+]_{E,1}$, $[EDTA]_E$ (= 4.0 × 10^{-2} mol/l), $[EDTA]_C$ (=

8.0 × 10^{-3} mol/l), and $[\overline{(RH)_2}]_{feed}$ (= 2.0 × 10^{-2} mol/l) apply. The calculated rare earth metal

concentrations in the organic phase for a cascade of ten-stage extraction stages and a single

scrubbing stage are shown in **Figure 2-14**. In this simulation, the pH value at the output of

the scrubbing section, $[H^+]_{C,0}$, was set equal to that at the input to the extraction section,

$[H^+]_{E,11}$. Although the fractional recovery value, ρ_Y (= $E \cdot [\overline{Y}]_{C,Q} / (F \cdot [Y]_{E,feed} + C \cdot [Y]_{C,feed})$),

was decreased to 1.11 × 10^{-1}, the recovery efficiencies for Ho and Er were decreased

substantially to 3.99 × 10^{-3} and 5.40 × 10^{-3}, respectively, due to the scrubbing effect obtained

with the EDTA containing solution and resulted in an effective separation with the overall

decontamination factor f = 1.18 × 10. With increasing in scrubbing stage number from one to

two, the separation of Y is much improved with f = 6.33 × 10, while the recovery decreased

with ρ_Y = 4.90 × 10^{-2} (where pH$_{C,3}$ = 1.675).

pH [-]

4
3
2

[Ln] [mol/l]

0.006

0.004

$f = 1.18 \times 10^1$

key metal p [-]
□ Ho 3.99 × 10^{-3}
● Y 1.11 × 10^{-1}
△ Er 5.40 × 10^{-3}

0.002

0

0   5   10   0   1   2

Extraction stage   Scrubbing stage

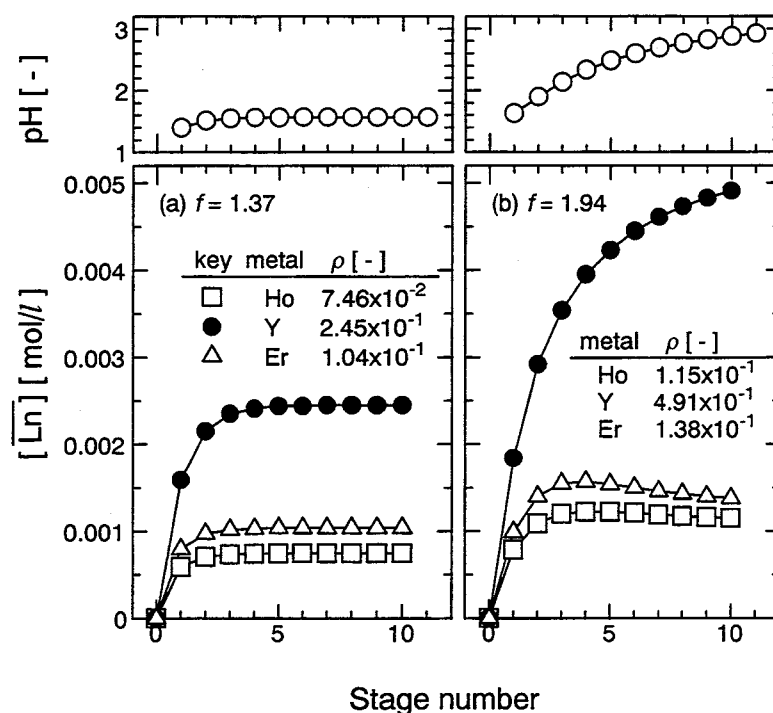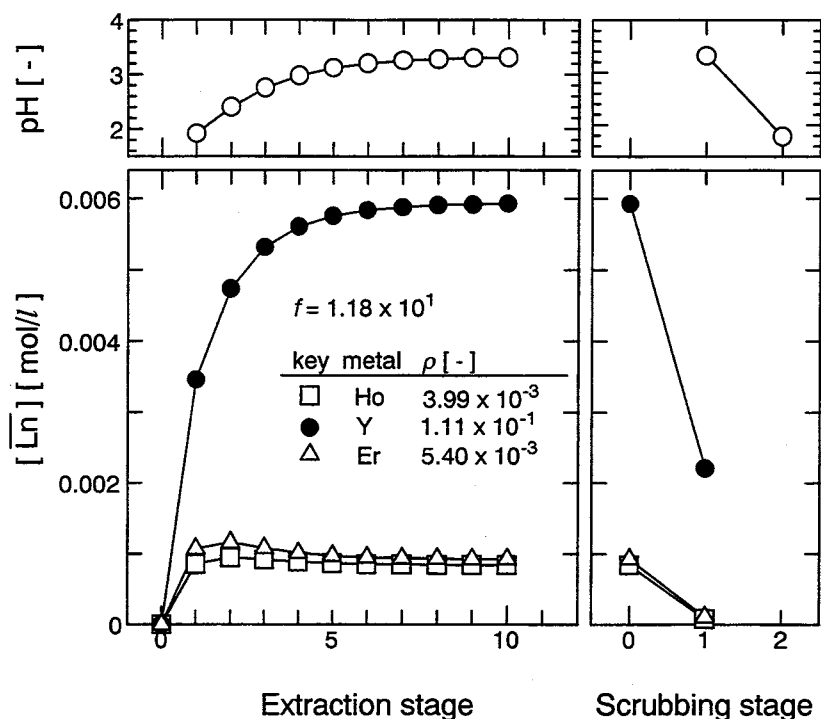**Figure 2-14** Simulation studies for separation of Y from a Ho/Y/Er mixture by a counter-current mixer-settler cascade with 10 extraction stages and a single scrubbing stage for the conditions: $F : E : C = 1 : 1 : 1$. $[\overline{(RH)_2}]_{feed} = 2.0 \times 10^{-2}$ mol/l, $[Ln_i]_{E,feed} = 2.0 \times 10^{-2}$ mol/l, $[EDTA]_E = 4.0 \times 10^{-2}$ mol/l, $[Ln_i]_{C,feed} = 0$ mol/l, and $[EDTA]_C = 8.0 \times 10^{-3}$ mol/l.

4. Summary

The liquid-liquid extraction system, combined with the masking reaction with water-soluble complexing agent at the equilibrium state, was investigated. The extraction equilibrium in the presence of the agent is formulated up to high loading ratios by taking the complexing reaction between the metals and the agents into account. The extraction process combined with the masking reaction can be designed using the simulation method, based on the extraction equilibrium formulation and the material balance. The separation process of heavy rare earth metals in the presence of EDTA or DTPA was investigated as a case study, with following results.

(1) Extraction equilibrium formulations for rare earth metals with EHPNA and VA-10

are established and extraction equilibrium constants are determined employing kerosene as diluents. $\overline{\text{LnR}_3(\text{RH})_3}$ is mainly formed at low loading ratios in both extractant systems, and then the aggregated species, $\overline{(\text{LnR}_3)_2(\text{RH})_4}$ in EHPNA systems and $\overline{(\text{LnR}_3)_2}$ in VA-10 system, appear with increasing loading ratio of organic phase.

(2) In EHPNA system, the extraction behavior in the presence of EDTA can be expressed satisfactorily, by assuming that the rare-earth metals when complexed with EDTA do not take part in the extraction. The extraction of Ho and Er in the presence of EDTA is suppressed compared to Y by a masking effect and the selective extraction of Y enhanced.

(3) In VA-10 system, the distribution ratios of each metal are decreased by the masking effect. In the Y/Er system, the order of the extractabilities of Y and Er is reversed and the selective extraction of Y is improved especially at high pH values, while the separation is little changed in the Yb/Lu system. The ratio of rare earth metal and DTPA in the rare earth-DTPA complex is not 1 : 1, but varies between 1 : 1 and 1.5 : 1 in the extraction system.

(4) Based on equilibrium extraction studies, a simulation study for the separation of Y from a Ho/Y/Er mixture of initially identical concentration using a countercurrent mixer-settler cascade was carried out. This showed that an organic solution with an overall decontamination factor of 11.8 can be obtained using a cascade of 10 extraction stages and single scrubbing stage using an aqueous feed solution with equal concentrations of all three metals. Increasing the number of the scrubbing stages from 1 to 2 enabled the separation of Y to be improved, with an overall decontamination factor of 6.33 × 10 being achieved, although the recovery of Y obtained decreased.

5. Nomenclature

C	= flow rate of the aqueous phase in the scrubbing section	[l/min]
D	= distribution ratio	[-]
E	= flow rate of the organic phase	[l/min]
f	= overall decontamination factor, $\rho_Y/(\rho_{Ho} + \rho_{Er})$	[-]
F	= flow rate of the aqueous phase in the extraction section	[l/min]
K_{ex}	= extraction equilibrium constant	
K_f	= complex formation constant	

59

L	= dissociate ligand of EDTA or DTPA	
Ln	= rare earth metal	
P	= total number of extraction stages	
Q	= total number of scrubbing stages	
$(RH)_2$	= dimeric species of extractant	
S	= concentration of free dimeric extractant	[mol/l]
S.F.	= separation factor	[-]
β	= overall formation constant	
ρ	= overall fractional recovery	[-]
[ ]	= concentration of the species in the brackets	[mol/l]

\<Subscripts\>

aq	= aqueous phase
C	= scrubbing section
E	= extraction section
feed	= aqueous or organic feed solution
i	= component
org	= organic phase
t	= total value

\<Superscript\>

| ‾ | = organic phase species |

Chapter III

Liquid-Liquid Extraction Systems Combined with the Photochemical Reduction and Its Application for Hydrometallurgical Processes

1. Introduction

Generally, the ions with different valences behave like different metals with respect to their extractability.[35] There are several reports, concerning the difference in the extraction behavior between metals with different valences, for example, Fe(II/III),[72,73] Cu(I/II),[74,75] Co(II/III),[76] Eu(II/III),[13] Ce(III/IV),[77] Np(IV/VI),[78] and Pu(III/IV/V).[79] Selective extraction (stripping) can be carried out, in which the redox reaction is accompanied during the actual extraction (stripping) process. There are three possible ways, for producing the redox reaction, which progresses in an aqueous or organic phase. These are (1) chemical reaction, (2) electrochemical reaction, and (3) photochemical reaction.

In the case of the redox reaction in the aqueous phase, the most simple method is the chemical reaction using the chemical reagent.[74,75,80-86] This type of the redox reaction, however, makes the extraction system further contaminated by the reagents, and thus, other procedures to the redox reaction, such as electro- or photo- chemical reaction, are favored. Several reports concern the case of the extraction system combined with in situ electrochemical redox reaction. These include for V(IV/V),[87] Ce(III/IV),[88,89] Eu(II/III),[90] and Am(III/IV/VI).[91,92] In most of these extraction systems, a two-compartment cell separated by a cation exchange membrane was used as a laboratory reactor. Industrial scale electrochemical reactors have also described.[93,94] In the case of a photochemical redox reaction in the aqueous phase, a weak chemical redox reagent is sometimes needed.[95,96] Hirai et al. have investigated the separation of Eu from Sm/Eu/Gd mixture by photoreductive stripping of the Eu in D2EHPA/xylene system.[97] The photochemical reduction of Eu in the organic phase does not progress in this case, as the diluent, xylene, shows a large absorption band in the UV region, in which the charge-transfer (C-T) band of Eu is included. The use of a two-compartment type cell was, therefore, required in order for the Eu to be photoreduced in the aqueous phase.

A redox reaction for the extracted species in the organic phase is also as effective as

for the metal ions in the aqueous phase. There are several reports concerning the effect of the auto-oxidation of the extracted species on the distribution ratio for Co,[98-100] Mg,[101,102] and Ce[103,104] with chelating extractants. Oxidation of the Co(II) to Co(III), in the organic phase, is especially important, as the oxidized Co(III) complex is inert for stripping by the mineral acid solution and known commonly as so-called cobalt-poisoning. There are no reports, however, applied the oxidation reaction of the extracted species in the organic phase for the separation process. The reduction reaction, especially photochemical reduction, is very effective for the separation of rare metals with high selectivity. Hirai et al. have investigated the photoreductive stripping of Eu from Sm/Eu/Gd mixture in the D2EHPA system.[105,106] The photochemical reduction of Eu in the organic phase proceeds well when cyclohexane or hexane are used as diluent, but does not proceed in the organic phase with xylene as the diluent system.[97] A high selective separation with a Eu purity of about 99 % can be carried out from a Sm/Eu/Gd aqueous mixture of equal metal concentrations by the single extraction-photoreductive stripping process. Hirai et al. have also investigated the separation of V/Mo with photoreductive stripping of V in TOMAC system.[107-109] A quantitative expression for the difference in the distribution ratio of the metal ions has not been so far obtained. In recent years, however, a relativistic density functional study for Pu(II/IV/VI)-Htta has been presented.[110] Further investigations, in this field, may throw light on the difference in the extractability of such metal ions. There are also relatively few reports concerning the mechanism for extraction, when combined with a photochemical reaction.

In this chapter, the liquid-liquid extraction systems combined with the photochemical reduction of the target metal are investigated. The photoreductive stripping of Fe(III) and photoreductive extraction of V(V) are carried out as case studies. The properties of the photochemical reduction of the metals in the separate aqueous or organic solutions are firstly investigated. The reaction is then combined into the extraction system, and the distribution ratios of the metals are controlled. The mechanism of the systems are investigated based on the kinetic study. The effect of wavelength of the irradiated light on the reaction and the possibility for the reuse of the organic phase were also investigated. The extraction systems, combined with the photochemical reduction for the target metal, are then applied for the separation of Fe(III) and the cobalt-poisoning problem.

2. Experiment

2.1 Reagents.

2-Ethylhexyl phosphonic acid mono-2-ethylhexyl ester (EHPNA, marketed as PC-88A by Daihachi Chemical Industry Co., Ltd., purity 95.9 wt%), bis(2-ethylhexyl)phosphoric acid (D2EHPA, marketed as DP-8R by Daihachi Chemical Industry Co., Ltd., purity 96.6 wt%), 2-hydroxy-5-nonylacetophenone oxime (marketed as LIX-84I by Henkel Hakusui Co., Ltd.), and 2-hydroxy-5-nonylbenzophenone oxime (marketed as LIX-65N by Henkel Hakusui Co., Ltd.) were used as extractants without any further purification. All of the inorganic chemicals, n-dodecane, and formic acid (90 %) were supplied by Wako Pure Chemical Industries as analytical-grade reagents. Deionized water was purified by simple distillation, prior to use. In the cases of Fe and Co systems, an aqueous feed solution was prepared by dissolving each metal chloride into the diluted HCl solution. In the case of V system, the aqueous feed solution was prepared by dissolving either $NaVO_3$ or $VOSO \cdot nH_2O$ into the diluted H_2SO_4. The organic solution was prepared by diluting the extractants with either n-dodecane or kerosene.

2.2 Procedure.

The extraction equilibrium data were obtained by the conventional procedure, at an organic/aqueous (O/A) volume ratio of 1, at 298 K. The photochemical reaction of metals in both single aqueous and organic solutions and the photoreductive stripping or extraction were carried out using a beaker-type glass bottle (32 mm in diameter). A 500 W xenon lamp (Ushio, UXL-500D-0) with irradiation intensity of 580 kW/m^2 was used as the light source in the case of Fe and V systems, and a 500 W halogen lamp (Eikohsha Co., Ltd., EHC-500) with irradiation intensity of 706 kW/m^2 was used in the case of Co system. The wavelength of irradiated light was adjusted by virtue of the Pyrex glass material of the reaction bottle (greater than 300 nm) or by using appropriate cutoff filters. The concentrations of metals in the aqueous solutions were analyzed using an inductively coupled argon plasma atomic emission spectrometer (Nippon Jarrell-Ash ICAP-575 Mark II). The absorption spectra were measured using an UV-vis spectrophotometer (Hewlett-Packard HP 8452A). The water concentration in the organic phase was determined by Karl Fischer titration using a Kyoto Electronics MKS-1. The photointensity was measured by thermopile (The Eppley Laboratory, Inc.).

3. Results and Discussion

3.1 Extraction Equilibrium Formulations.

Figure 3-1 shows the effect of the equilibrium pH value on the distribution ratios of Fe with EHPNA in n-dodecane and V with D2EHPA in n-dodecane. In the case of Fe, the distribution ratio for Fe(II) is much lower than that for Fe(III) in all pH range investigated in accordance with the valences, which are identical to positive charge. This extraction behavior, therefore, indicates that the selective stripping of Fe may be expected to progress by combining reduction during the stripping process. The slope analysis method revealed the extraction equilibria for Fe(III) and Fe(II) being expressed as Eqs. (3-1) and (3-2), respectively.

$$Fe^{3+} + 3\overline{(RH)_2} \leftrightarrow \overline{FeR_3(RH)_3} + 3H^+ \tag{3-1}$$

$$Fe^{2+} + 2\overline{(RH)_2} \leftrightarrow \overline{FeR_2(RH)_2} + 2H^+ \tag{3-2}$$
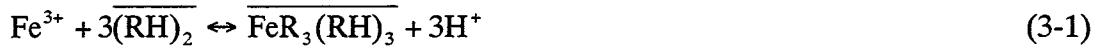
In the case of V, however, the distribution ratio for V(V) is smaller than that for V(IV), which is contrary to the valences. This may be because V(V) and V(IV) exist as VO_2^+ and $VO^{2+,}$ in such acidic solution with pH value of 0-2.[111]
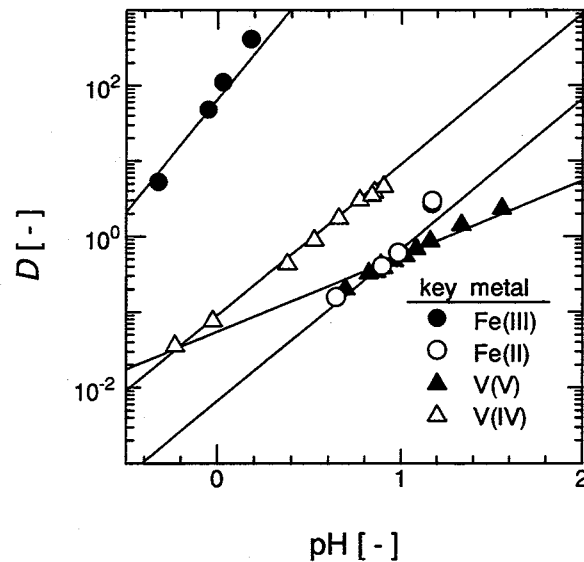
Figure 3-1 Effect of the aqueous pH on the distribution ratio for Fe with EHPNA and V with D2EHPA. $[\overline{(RH)_2}]_{feed} = 5.0 \times 10^{-1}$ mol/l and $[M]_{feed} = 1.0 \times 10^{-2}$ mol/l.

The selective extraction of V is thus expected by combining reduction during extraction, especially at high pH region. The slope analysis method revealed the extraction equilibria for these metals being expressed as Eqs. (3-3) and (3-4).

$$VO_2^+ + \overline{(RH)_2} \leftrightarrow \overline{VO_2R(RH)} + H^+ \qquad ; K_{ex,V(V)} = 1.12 \times 10^{-1} \qquad (3-3)$$

$$VO^{2+} + 2\overline{(RH)_2} \leftrightarrow \overline{VOR_2(RH)_2} + 2H^+ \qquad ; K_{ex,V(IV)} = 3.79 \times 10^{-1} \qquad (3-4)$$

3.2 Photochemical Reduction of the Metals in the Aqueous or Organic Solutions.

3.2.1 In the Aqueous Solution.

The photochemical reduction of Fe(III) in an aqueous solution using a xenon lamp was performed in the presence of formic acid, as a radical scavenger. Formic acid is known to scavenge the hydroxyl radical produced by the photochemical reduction of V[108] and Eu.[106] **Figure 3-2** shows the effect of photoirradiation on the absorption spectra for the aqueous solution containing Fe(III), hydrochloric acid, and formic acid.
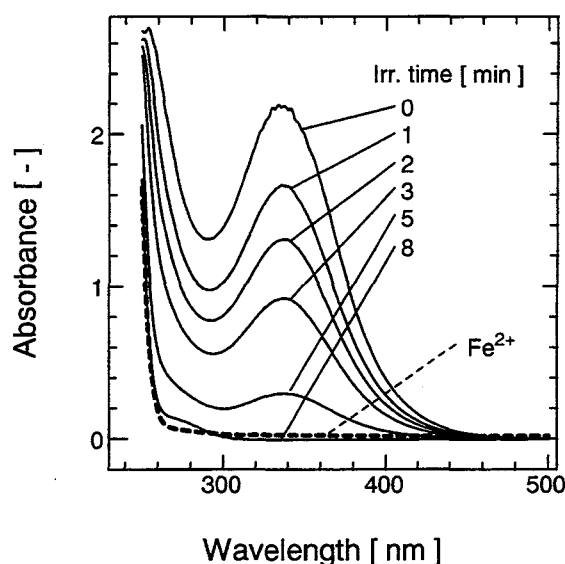
Figure 3-2 Absorption spectra for an aqueous solution containing 1.0×10^{-3} mol/l Fe(III) before and after photoirradiation. The dotted line is the spectrum of the solution containing 1.0×10^{-3} mol/l Fe(II). [HCl] = 1.1 mol/l and [HCOOH] = 1.4 mol/l. Reference: air.

The absorption band at 335 nm appears in the presence of hydrochloric acid, and this band may show the charge-transfer (C-T) band between Fe(III) and chloride ion. The absorbance of the

band decreased with photoirradiation time. The absorption spectrum of an Fe(II) aqueous solution containing hydrochloric acid and formic acid is also shown in Figure 3-2 by the dotted line. These spectra indicate that in an aqueous solution Fe(III) is photoreduced to Fe(II). Without formic acid, no change in the absorption spectra of Fe(III) was observed during the photoirradiation. Thus, the mechanism of the photochemical reduction of Fe(III) in an aqueous solution is shown to occur by electron donation from water, with the hydroxyl radical produced being scavenged by formic acid. This is shown in Eqs. (3-5) and (3-6), which is identical with that of the photochemical reduction of Eu, as found in other studies.[112]

$$Fe^{3+} + H_2O \rightarrow Fe^{2+} + H^+ + \cdot OH \tag{3-5}$$

$$\cdot OH + HCOOH \rightarrow H_2O + \cdot COOH \tag{3-6}$$

In the case of V(V), the photochemical reduction occurs without radical scavenger, and an absorption at around 768 nm appears, which is attributable to V(IV).[107] The rate of photochemical reduction of V was then investigated, following Ar bubbling in order to purge dissolved oxygen. **Figure 3-3** shows a pseudo-first-order kinetic plot for the variation in the aqueous concentration of V(V), with respect to irradiation time.
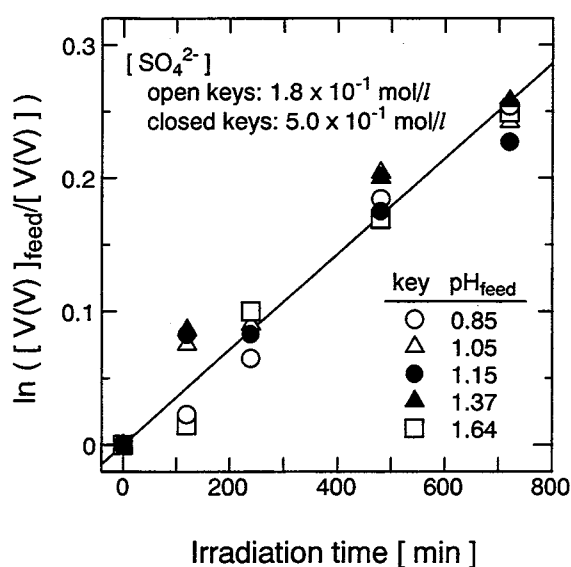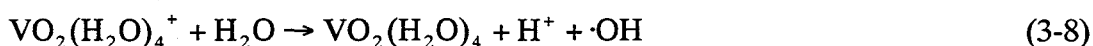

Figure 3-3   Pseudo-first-order plot for the concentration of V(V) in the aqueous solution during photoirradiation. $[NaVO_3]_{feed} = 1.0 \times 10^{-2}$ mol/l.

A linear relationship is observed between the ordinate value of and photoirradiation time and which is also independent of both pH and sulfuric ion concentration. The rate of photochemical reduction of V(V) in aqueous solution is therefore first order with respect to V(V) concentration, and can be expressed as Eq. (3-7) below, where $k_{a,V} = 3.58 \times 10^{-4}$ min^{-1}.

$$r_{a,V} = -\frac{d[V(V)]}{dt} = k_{a,V}[V(V)] \qquad (3\text{-}7)$$

The aqueous phase photochemical reduction of V(V) is likely to occur by electron donation from the water, as indicated in by Eqs. (3-8)-(3-10).

$$VO_2(H_2O)_4^+ + H_2O \rightarrow VO_2(H_2O)_4 + H^+ + \cdot OH \qquad (3\text{-}8)$$

$$VO_2(H_2O)_4 + 2H^+ \rightarrow VO(H_2O)_5^{2+} \qquad (3\text{-}9)$$

$$\cdot OH \rightarrow \frac{1}{2}H_2O + \frac{1}{4}O_2 \qquad (3\text{-}10)$$

The overall reaction is thus shown by Eq. (3-11) which is identical to that found by Jeliazkowa et al.[113]

$$VO_2(H_2O)_4^+ + \frac{1}{2}H_2O + H^+ \rightarrow VO(H_2O)_5^{2+} + \frac{1}{4}O_2 \qquad (3\text{-}11)$$
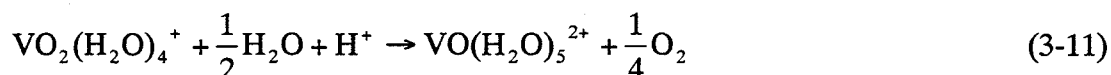
If the reduction of V(V) is the rate-determining step as shown by Eq. (3-8), then the overall reaction rate may also be expressed by means of Eq. (3-7).

3.2.2 In the Organic Solution.

The photochemical reduction of Fe(III) in the single organic solution was investigated using an ESR spectrometer. Fe(II) is known to be ESR silent at room and liquid-nitrogen temperature owing to its short spin-lattice relaxation time.[114] **Figure 3-4** shows the ESR spectra of Fe(III) when extracted with EHPNA/n-dodecane. A signal at g = 1.97 is observed with an intensity which is nearly proportional to the Fe concentration. The ESR spectrum for 3.0×10^{-3} mol/l Fe(III) in EHPNA/n-dodecane after photoirradiation for 5 h is also shown in Figure 3-4 by means of a dotted line. When compared with the spectrum for 3.0×10^{-3} mol/l Fe(III) without photoirradiation, it is noted that the intensity is not changed, thus indicating that the Fe(III) concentration in an organic solution is not affected by photoirradiation. It is therefore established that no photochemical reduction of Fe(III) occurs in an organic solution, and this is probably due to the lack of an electron donor, such as water.
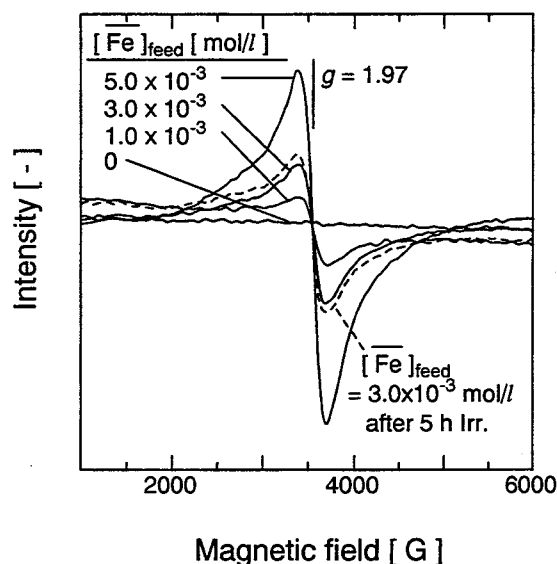
Figure 3-4 ESR spectra for Fe(III) loaded on EHPNA in *n*-dodecane. The dotted line is the spectrum for 3.0×10^{-3} mol/l Fe(III) following photoirradiation. $[\overline{(RH)_2}]_{feed} = 1.0 \times 10^{-1}$ mol/l.

The photochemical reduction of V(V) in organic solution was also investigated. V(V) is photochemically reduced in the organic solution, and again an absorption at around 768 nm, attributable to V(IV), appears. The rate of photochemical reduction of V was then investigated, following Ar bubbling in order to purge dissolved oxygen. **Figure 3-5** shows the corresponding pseudo-first-order plot for the concentration of V(V) in organic solution as a function of irradiation time. A linear relationship is again observed between and the photoirradiation time, which is independent of extractant concentration, thus indicating that the rate of photochemical reduction of V(V) in organic solution is first order with respect to V concentration. The rate of photochemical reduction is therefore expressed as Eq. (3-12) where $k_{o,V} = 9.84 \times 10^{-2}$ min^{-1}.

$$r_{o,V} = -\frac{d[\overline{V(V)}]}{dt} = k_{o,V}[\overline{V(V)}]$$ (3-12)

The photochemical reduction of V(V) in organic solution is likely to occur via electron donation from water dissolved in the organic solution.

68

Figure 3-5   Pseudo-first-order plot for the concentration of V(V) in the organic solution during photoirradiation.
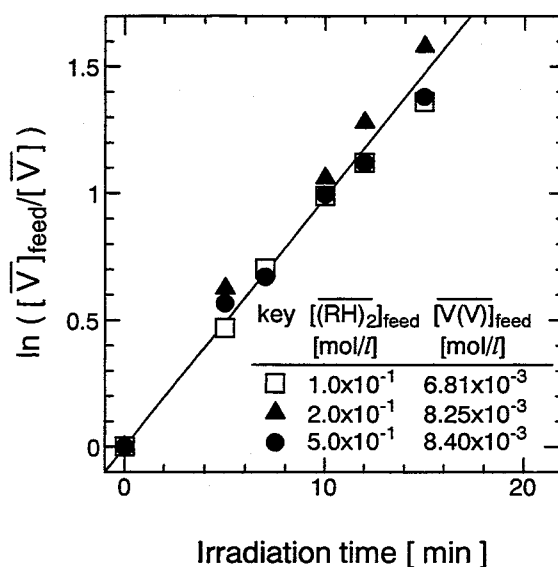
A plot of the concentration of the dissolved water versus the concentration of the extracted V(V) or Fe(III) is shown in **Figure 3-6**. In the case of V(V)/D2EHPA system, the quantity of water in the organic solutions much larger than that of V(V), and thus the photochemical reduction progresses in the separate organic solution. In the case of Fe(III)/EHPNA system, however, the quantity of water is smaller than that in the V system. This difference in the quantity of water is likely to affect the ability of photochemical reduction in the organic solution between the two metals, together with the redox potential. The overall reaction is shown by Eqs. (3-13) and (3-14).

$$\overline{VO_2R(RH)} + \overline{H_2O} \rightarrow \overline{VO_2R(RH)^-} + \overline{H^+} + \overline{\cdot OH}$$ (3-13)

$$\overline{VO_2R(RH)^-} + \overline{(RH)_2} + \overline{H^+} \rightarrow \overline{VOR_2(RH)_2} + \overline{H_2O}$$ (3-14)
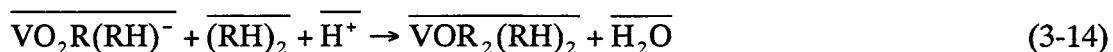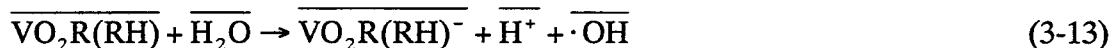
If the reduction of V(V) as shown by Eq. (3-13) is the rate-determining step, the overall rate equation can be expressed simply by means of Eq. (3-12). The hydroxyl radical produced in the reaction is likely to be scavenged by the diluent, as was found previously.[109] The photochemical reduction of V in the extraction system is expected to progress mainly in the organic phase, since the rate constant for photochemical reduction in the organic phase is much greater than that for the aqueous phase ($k_o/k_a = 275$).
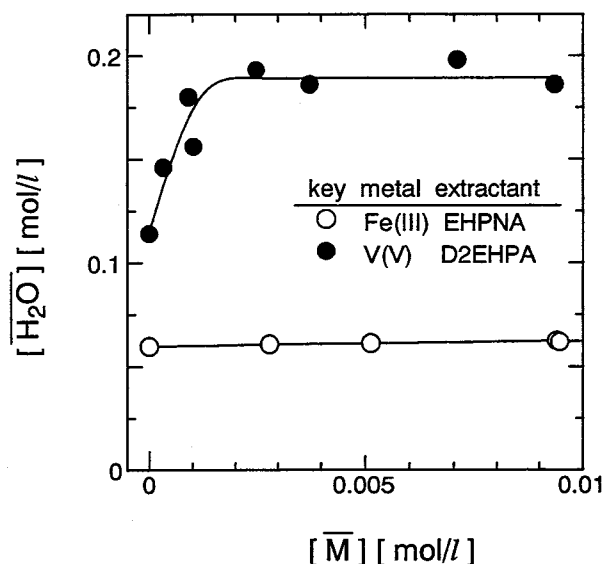
Figure 3-6   Effect of the concentration of Fe(III) and V(V) extracted on the concentration of water in the organic phase. $[\overline{(RH)_2}]_{feed}$ = 5.0×10^{-1} mol/l.

3.3 Mechanism of the Extraction Systems Combined with the Photochemical Reduction.

3.3.1 Photoreductive Stripping of Fe(III).

The photoreductive stripping of Fe(III) was then carried out. In this, EHPNA in n-dodecane containing Fe(III) was contacted with the 2.4×10^{-1} mol/l HCl solution (pH = 0.79) at a volume ratio O/A = 1, where the stripping of Fe(III) was not expected, as shown in Figure 3-1. The mixture was then photoirradiated by the xenon lamp with agitation produced by a magnetic stirrer.   **Figure 3-7** shows the time-course variation in the aqueous phase Fe concentration. Photoreductive stripping of Fe into the hydrochloric acid solution is seen to progress without a radical scavenger.   For the case of zero bubbling treatment, the photoreductive stripping of Fe(III) was delayed and only started following an induction period of 120 min.   In the case of bubbling O_2, this induction period was prolonged to 540 min, whereas in the case of Ar bubbling, photoreductive stripping was seen to start immediately.   Donohue has reported that in the case of the photochemical reduction of Yb or Sm in a methanol solution no reaction was found to occur until most or all of the oxygen was excluded.[115]   Moreover, Fe(II) is easily oxidized to Fe(III) by the dissolved oxygen.[116]

70

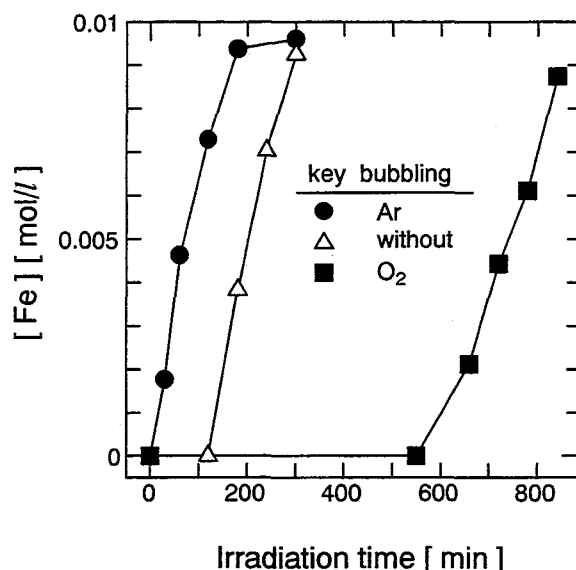**Figure 3-7** Effect of Ar or O_2 gas bubbling on the photoreductive stripping of Fe(III) in EHPNA/n-dodecane system. $[\overline{(RH)_2}]_{feed} = 2.4 \times 10^{-1}$ mol/l, $[\overline{Fe(III)}]_{feed} = 1.0 \times 10^{-2}$ mol/l, and $[HCl]_{feed} = 2.4 \times 10^{-1}$ mol/l.

In addition, following the initial induction period, no difference was seen in the rate of stripping for all three cases studied here. Therefore, during the induction period, the dissolved oxygen suppresses Fe(III) to be reduced to Fe(II), and the stripping only starts to progress when all of the oxygen in the extraction system has been consumed.

It is necessary to establish at which phase the photochemical reduction of Fe(III) occurs. In this case, the rate of agitation with the magnetic stirrer was kept at 500 rpm in order to maintain a flat interface. In addition, each phase was shielded separately from the photoirradiation by aluminum foil. Photoreductive stripping hardly occurred in the case of irradiation to the aqueous phase alone. In the case of irradiation to the organic phase alone, however, photoreductive stripping was seen to occur, and the reaction progressed at a rate that was almost identical with that in the case of irradiation to both phases. Because photochemical reduction is found not to occur in the organic solution, Fe(III) is likely to be photoexcited in the organic phase and to be reduced at the interface by electron donation from water. Thus, Fe(III) is photoreduced at the interface according to the same reaction scheme as

shown by Eq. (3-5), and the reduced Fe is then stripped into the aqueous phase. The hydroxyl radical produced will then be scavenged by the diluent, as found in the case of V.[109]

A kinetic study of the photoreductive stripping of Fe(III) was carried out, using dilute HCl solution as the stripping agent, to suppress the stripping efficiency without photoirradiation less than 5 %. The initial Fe(III) concentration in the organic phase was kept constant at 1.0×10^{-2} mol/l, and the aqueous and organic solutions were agitated by a magnetic stirrer with an agitation rate of over 4000 rpm. The photointensity was held constant at 5.80 $\times 10^5$ W/m^2. The rate of photoreductive stripping was independent of the agitation rate and the photo intensity in this range.

Figure 3-8 shows the pseudo-first-order plot for the variation in the concentration of Fe(III) in the organic phase with respect to irradiation time.
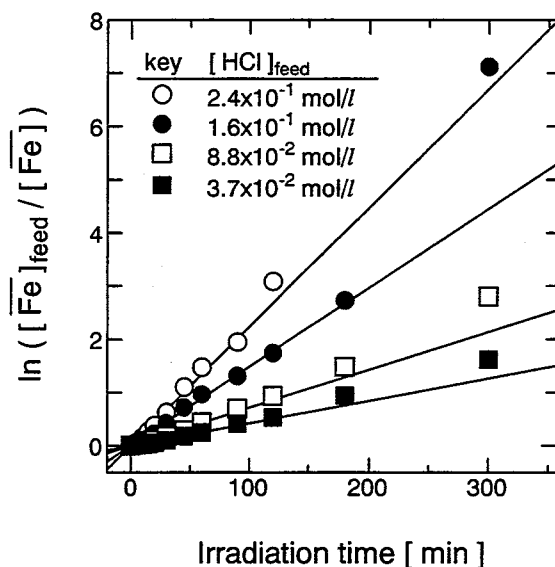
Figure 3-8   Pseudo-first-order plot for the concentration of Fe in the organic phase in the EHPNA/n-dodecane system. $[\overline{(RH)_2}]_{feed} = 1.0 \times 10^{-1}$ mol/l and $[\overline{Fe(III)}]_{feed} = 1.0 \times 10^{-2}$ mol/l.

At the start of photoreductive stripping, a linear relationship is observed between $\ln([\overline{Fe}]_{feed}/[\overline{Fe}])$ and photoirradiation time, indicating that the rate of photoreductive stripping is of first order with respect to the Fe(III) concentration in the organic phase. The rate of

photoreductive stripping can, therefore, be expressed as shown in Eq (3-15), using an apparent rate constant, k_{Fe}'.

$$r_{Fe} = -\frac{d[\overline{Fe}]}{dt} = k_{Fe}'[\overline{Fe}] \tag{3-15}$$

The deviations between the experimental data and the straight lines at 180-300 min are caused by the change in the photointensity of transmitted light during the photoirradiation, which will be described later in this section. The effects of the initial hydrogen ion concentration and the free dimeric EHPNA concentration, on the apparent rate constant k_{Fe}' are shown in parts a and b of **Figure 3-9**, respectively. In this, only the experimental values obtained before 120 min were used, because the values at 180-300 min deviated from the straight lines. Linear relationships are shown between both $\ln[H^+]$ and $\ln k_{Fe}'$, and $\ln[\overline{(RH)_2}]$ and $\ln k_{Fe}'$, with slopes of 1 and -0.5, respectively. These results thus indicate that the rate of photoreductive stripping of Fe(III) in the EHPNA/n-dodecane system can be expressed as

$$r_{Fe} = -\frac{d[\overline{Fe}]}{dt} = k_{Fe}\frac{[\overline{Fe}][H^+]}{[\overline{(RH)_2}]^{0.5}} \tag{3-16}$$

where $k_{Fe} = 2.75 \times 10^{-2}\ l^{0.5}mol^{-0.5}min^{-1}$.
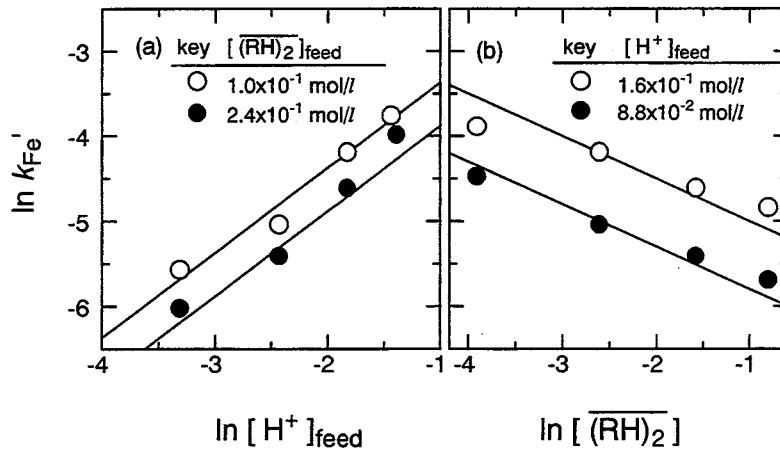
Figure 3-9   Effects of (a) initial hydrogen ion and (b) initial free dimeric EHPNA concentration on the apparent rate constant, k_{Fe}' for Eq. (3-15).

Figure 3-10 (a) shows the effect of photoirradiation time on the concentration of Fe in the aqueous phase as compared with the calculated value based on Eq (3-16). The changes of the concentrations of free dimeric extractant and hydrogen ion during the reaction were taken into account in the calculation, using the stoichiometric relationship based on Eqs. (3-1) and (3-2), respectively. The magnitude of the experimental values agrees well with the calculated values during the initial part of the run but with increasing irradiation time become greater than the calculated value. This deviation becomes notable in the run with the solution of lower hydrochloric acid concentration.
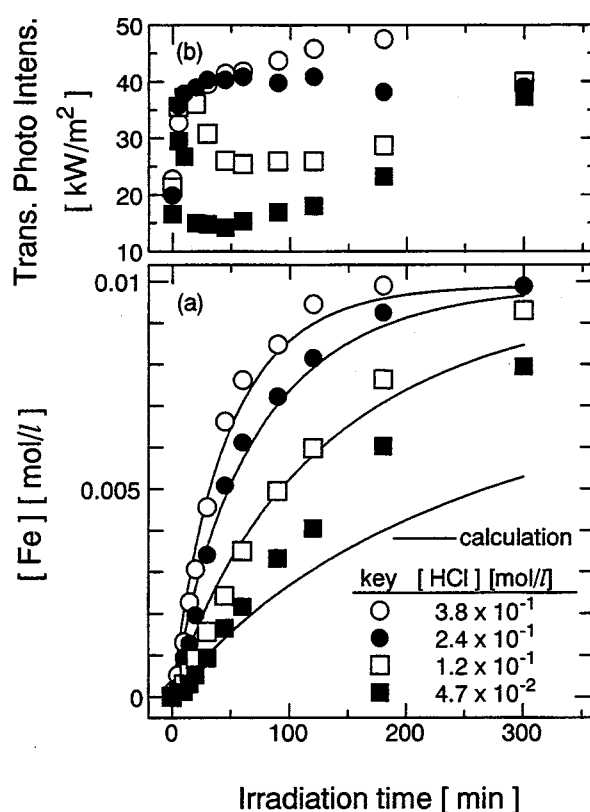
Figure 3-10 Effect of photo-irradiation time on (a) the concentration of Fe(III) in the aqueous phase and (b) the transmitted photo intensity in the EHPNA/n-dodecane system. Comparison of the observed data with prediction is shown by the solid lines. $[\overline{(RH)_2}]_{feed} = 1.0 \times 10^{-1}$ mol/l, $[\overline{Fe(III)}]_{feed} = 1.0 \times 10^{-2}$ mol/l.

74

Figure 3-10 (b) shows the time-course variation in the photointensity of transmitted light. In the case of low hydrochloric acid concentration at 4.7 × 10^{-2} mol/l, the transmitted light intensity increased as the photoreductive stripping of Fe(III) progressed, and the photoreaction progressed more effectively than that predicted based on the initial photoreductive stripping rate. Parts a and b of **Figure 3-11** show the time course variations for the aqueous Fe concentration for the D2EHPA in n-dodecane and kerosene systems, respectively. Assuming the rate of photoreductive stripping to be expressed by the same equation as that for the EHPNA system, rate constants were calculated as 1.30 × 10^{-2} $l^{0.5}$mol$^{-0.5}$min^{-1} for the n-dodecane diluent system and 1.66 × 10^{-2} $l^{0.5}$mol$^{-0.5}$min^{-1} for the kerosene diluent system. The corresponding calculated values for aqueous Fe concentration are as shown in parts a and b of Figure 3-11 by the solid lines and such that the experimental values agree well with the calculation, thus indicating that the rate of photoreductive stripping of Fe in the D2EHPA system can also be expressed by Eq. (3-16).
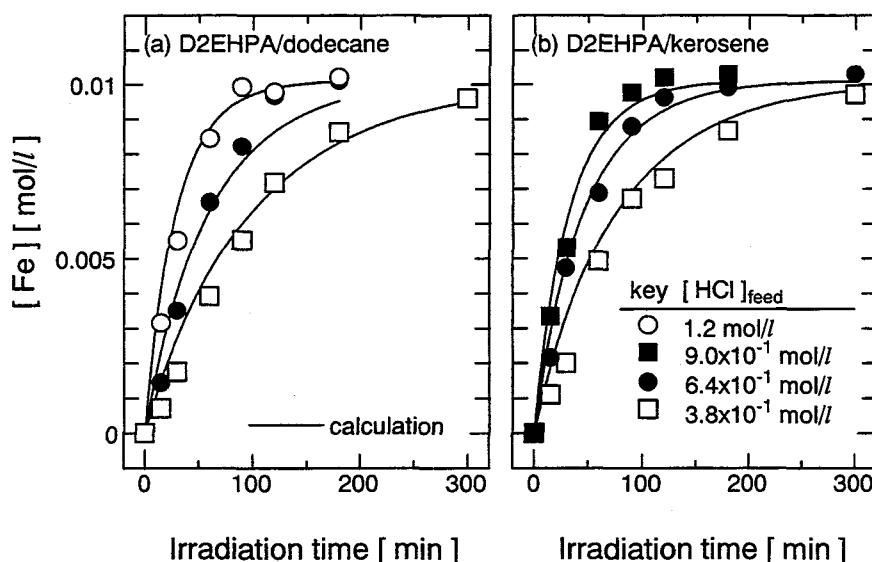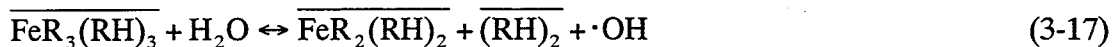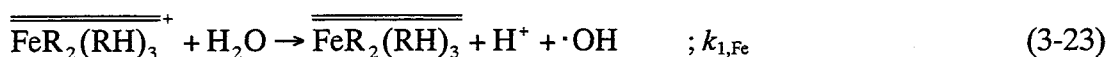
Figure 3-11 Effect of photoirradiation time on the concentration of Fe in the aqueous phase in (a) the D2EHPA/n-dodecane system and (b) the D2EHPA/kerosene system. The comparison of the observed data with prediction shown by the solid lines. $[\overline{(RH)_2}]_{feed}$ = 1.0 × 10^{-1} mol/l and $[\overline{Fe(III)}]_{feed}$ = 1.0 × 10^{-2} mol/l.

The overall reaction mechanism for the photoreductive stripping of Fe(III) can be divided into two reaction stages, the photochemical reduction of Fe(III) to Fe(II) in the organic phase, followed by the stripping of Fe(II) into the aqueous phase, as follows.

$$\overline{FeR_3(RH)_3} + H_2O \leftrightarrow \overline{FeR_2(RH)_2} + \overline{(RH)_2} + \cdot OH \tag{3-17}$$

$$\overline{FeR_2(RH)_2} + 2H^+ \leftrightarrow Fe^{2+} + \overline{2(RH)_2} \tag{3-18}$$

This reaction scheme is deduced on the assumptions that the rate-determining step is the photochemical reduction of Fe(III), as shown by Eq. (3-17), and that the rate of distribution of the reduced Fe(II) is fast.

The Fe(III)-extractant complex is found to be excited in the organic phase and to be donated an electron from the water at the aqueous/organic interface. Assuming the extractant to exist as a monomeric species at the interface, as was found in the case of D2EHPA,[117] the elementary reaction of Eq. (3-17) can be expressed in more detail as Eqs. (3-19)-(3-24).

$$\overline{(RH)_2} \leftrightarrow \overline{2RH} \qquad\qquad ; K_{1,Fe} \tag{3-19}$$

$$\overline{FeR_3(RH)_3} \leftrightarrow \overline{FeR_3(RH)_3}* \qquad\qquad ; K_{2,Fe} \tag{3-20}$$

$$\overline{FeR_3(RH)_3}* \leftrightarrow \overline{FeR_3(RH)_3}* \qquad\qquad ; K_{3,Fe} \tag{3-21}$$

$$\overline{FeR_3(RH)_3}* + H^+ \leftrightarrow \overline{FeR_2(RH)_3}^+ + \overline{RH} \qquad\qquad ; K_{4,Fe} \tag{3-22}$$

$$\overline{FeR_2(RH)_3}^+ + H_2O \rightarrow \overline{FeR_2(RH)_3} + H^+ + \cdot OH \qquad ; k_{1,Fe} \tag{3-23}$$

$$\overline{FeR_2(RH)_3} \rightarrow \overline{FeR_2(RH)_2} + \overline{RH} \tag{3-24}$$

If the rate-determining step is the photochemical reduction of Fe(III) as shown by Eq. (3-23), the overall reaction rate equation can be expressed by Eq. (3-25).

$$r_{Fe} = -\frac{d[\overline{Fe}]}{dt} = k_{1,Fe}[\overline{FeR_2(RH)_3}^+]$$

$$= \frac{k_{1,Fe}K_{2,Fe}K_{3,Fe}K_{4,Fe}}{K_1^{0.5}} \frac{[\overline{FeR_3(RH)_3}][H^+]}{[\overline{(RH)_2}]^{0.5}} = k_{Fe}\frac{[\overline{Fe}][H^+]}{[\overline{(RH)_2}]^{0.5}} \tag{3-25}$$

This agrees with the result from the kinetic study, as shown by Eq (3-16).

3.3.2 Photoreductive Extraction of V(V).

The photoreductive extraction of V was also carried out. In this, the extractant D2EHPA in n-dodecane was contacted with the aqueous solution, containing $NaVO_3$, at a

volume ratio of O/A = 1. The mixture was then photoirradiated following Ar bubbling with agitation by magnetic stirrer. **Figure 3-12** shows the effect of photoirradiation time on the distribution ratio for V under conditions of vigorous stirring at over 4000 rpm.
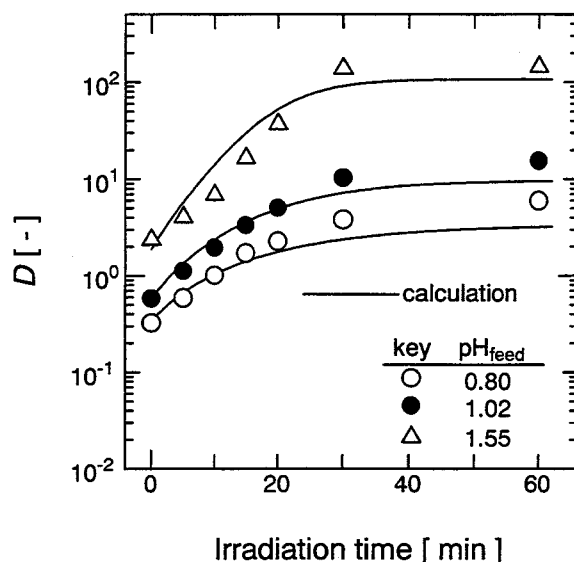
Figure 3-12 Effect of photoirradiation time on the distribution ratio for V. Comparison of the observed data with predicted values, shown by the solid lines. $[\overline{(RH)_2}]_{feed} = 5.0 \times 10^{-1}$ mol/l and $[NaVO_3]_{feed} = 1.0 \times 10^{-2}$ mol/l.

In the extraction system, the time-course variation of the distribution ratio can be predicted, when assuming that the rate of the reaction is dominated by the photochemical reduction of V in the aqueous and organic phases, and the distribution of both V(V) and V(IV) between the two phases is attained immediately. Such predictions, however, lead to much lower values for the distribution ratio than for the experimental results. This difference may be caused by photochemical reduction of V at the interface between the aqueous and organic phases, as was also found in the case for the photoreductive stripping of Fe(III). The photochemical reduction of V(V) at the interface may be thought to be expressed by the mechanisms indicated in Eqs. (3-26)-(3-29).

$$\overline{VO_2R(RH)} \leftrightarrow \overline{\overline{VO_2R(RH)}} \qquad ; K_{i,V} \qquad (3\text{-}26)$$

$$\overline{VO_2R(RH)} + H_2O \rightarrow \overline{VO_2R(RH)}^- + H^+ + \cdot OH \qquad ; \ k_{i,v}' \qquad (3\text{-}27)$$

$$\overline{VO_2R(RH)}^- + \overline{(RH)_2} + H^+ \rightarrow \overline{VOR_2(RH)_2} + H_2O \qquad (3\text{-}28)$$

$$\overline{VOR_2(RH)_2} \rightarrow \overline{VOR_2(RH)_2} \qquad (3\text{-}29)$$
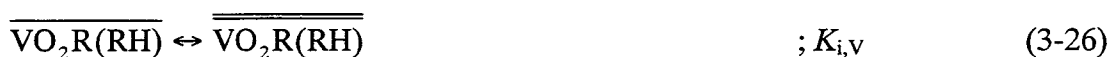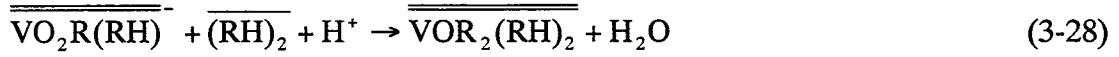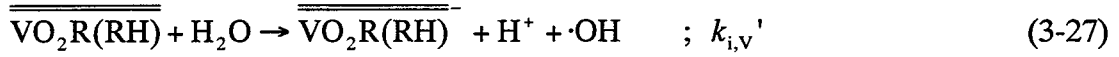
If the rate of photochemical reduction at the interface is first order with respect to the concentration of V(V) at the interface, as in the case of reduction in aqueous and organic solutions, then the interfacial surface rate equation can be expressed by Eq. (3-30),

$$r_{i,v}' = -\frac{Q}{A}\frac{d[\overline{V(V)}]}{dt} = k_{i,v}'[\overline{V(V)}] = K_{i,v}k_{i,v}'[\overline{V(V)}] \qquad (3\text{-}30)$$

where Q and A are the volume of organic phase and the area of interface, respectively. Assuming the interface area to be constant, the overall rate equation at the interface can be expressed as Eq. (3-31).

$$r_{i,v} = \frac{A}{Q}r_{i,v}' = k_{i,v}[\overline{V(V)}] \qquad (3\text{-}31)$$

The overall rate constant for photochemical reduction of V at the interface was determined as $k_{i,v} = 1.75 \times 10^{-1}$ min^{-1}, by nonlinear least squares fit to the experimental results. The change in the concentration of V(V) and V(IV) in the aqueous and organic phases for a time interval Δt lying between time t and $t + \Delta t$ can be calculated from a knowledge of the values of the rate constants, $k_{a,v}$, $k_{o,v}$, and $k_{i,v}$, as indicated in Eqs. (3-32)-(3-35).

$$[V(V)]_{t+\Delta t} = \frac{[V(V)]_t}{e^{k_{a,v}\Delta t}} \qquad (3\text{-}32)$$

$$[V(IV)]_{t+\Delta t} = [V(IV)]_t + \{[V(V)]_t - [V(V)]_{t+\Delta t}\} \qquad (3\text{-}33)$$

$$[\overline{V(V)}]_{t+\Delta t} = \left(\frac{1}{e^{k_{o,v}\Delta t}} + \frac{1}{e^{k_{i,v}\Delta t}} - 1\right)[\overline{V(V)}]_t \qquad (3\text{-}34)$$

$$[\overline{V(IV)}]_{t+\Delta t} = [\overline{V(IV)}]_t + \{[\overline{V(V)}]_t - [\overline{V(V)}]_{t+\Delta t}\} \qquad (3\text{-}35)$$

Assuming that an equilibrium distribution of both V(V) and V(IV) between the phases is attained immediately, the distribution ratio at the new time ($t + \Delta t$) can be calculated using the extraction equilibrium formulations previously determined. Repeated calculation, until the values of the distribution ratios and the proton concentration converge, enables the apparent distribution ratio, $D = ([\overline{V(V)}] + [\overline{V(IV)}])/([V(V)] + [V(IV)])$, to be determined.

78

These predicted values according to the above method are shown in Figure 3-12 by means of the solid lines. The experimental data are seen to fall well on the prediction lines, thus indicating that the photochemical reduction of V progresses both in the aqueous phase, the organic phase, and at the interface. **Figure 3-13** shows the time-course variation in reduction yield for each phase, Y, defined as the ratio of the concentration of V(IV) reduced in the appropriate phase to that of the feed V(V) concentration. The photoreductive extraction progresses mainly via photochemical reduction at the interface and in the organic phase, with the reduction in the aqueous phase hardly contributing to the overall photoreductive extraction.
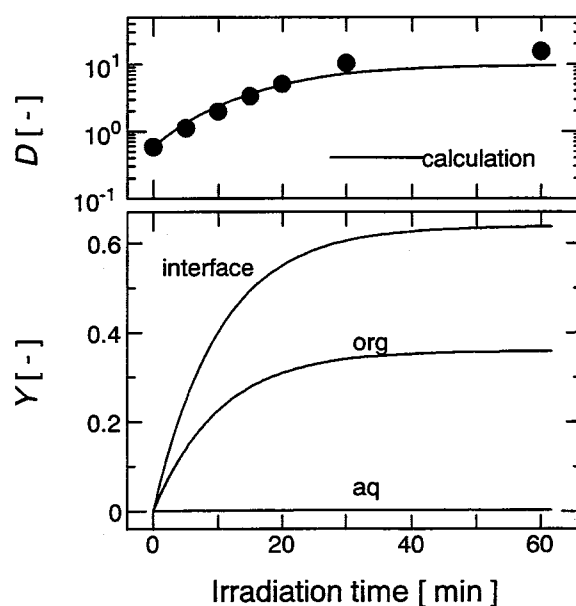
Figure 3-13 Effect of photoirradiation time on the distribution ratio and reduction yield in each phase. $[\overline{(RH)_2}]_{feed} = 5.0 \times 10^{-1}$ mol/l, $[NaVO_3]_{feed} = 1.0 \times 10^{-2}$ mol/l, and pH$_{feed}$ = 1.02.

3.4 Effect of the Wavelength of the Irradiated Light.

Figure 3-14 shows the effect of the wavelength of the irradiated light, when varied by the use of appropriate cutoff filters, on the time-course variation in the photoreductive stripping of Fe(III) and photoreductive extraction of V(V). In the case of Fe, the reaction hardly occurs when the irradiated light less than 400 nm is cut off. This may be caused by the ability for photoabsorption of the extracted species.
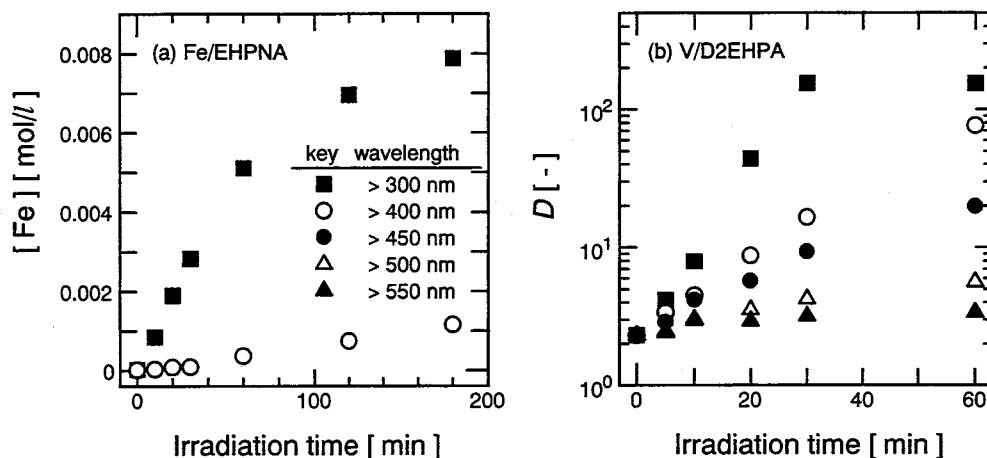
Figure 3-14 Effect of the wavelength of the light source on the time-course variation in (a) photoreductive stripping of Fe(III) and (b) photoreductive extraction of V(V). (a) Fe/EHPNA system, $[\overline{(RH)_2}]_{feed} = 1.0 \times 10^{-1}$ mol/l, $[Fe(III)]_{feed} = 8.8 \times 10^{-3}$ mol/l, and $[HCl]_{feed} = 2.4 \times 10^{-1}$ mol/l, and (b) V/D2EHPA system, $[\overline{(RH)_2}]_{feed} = 5.0 \times 10^{-1}$ mol/l, $[NaVO_3]_{feed} = 1.0 \times 10^{-2}$ mol/l, and $pH_{feed} = 1.52$.

Figure 3-15 Absorption spectrum for organic solutions containing (a) Fe(III) and (b) V(V). $[\overline{(RH)_2}]_{feed} = 1.0 \times 10^{-1}$ mol/l. Reference: air.

Figure 3-15 (a) shows the absorption spectrum for the organic solution with and without Fe(III) and indicates that the absorption band, caused by Fe(III), appears at 200-350 nm. In

the case of V, the absorption band, caused by V(V), appears at 300-500 nm, and the reaction hardly occurs when the irradiated light less than 500 nm is cut off. These resul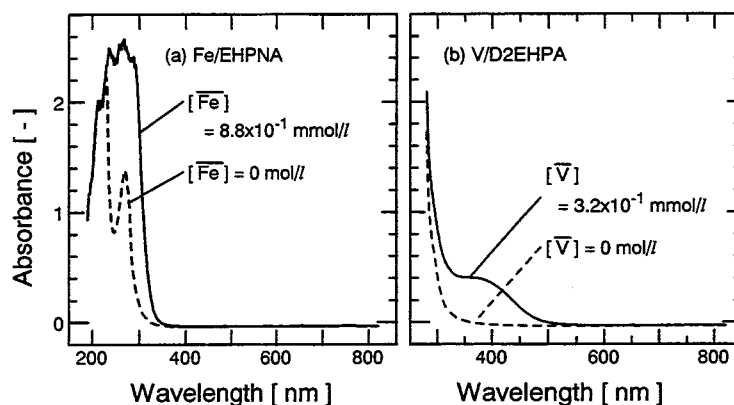ts thus indicate the photochemical reduction of the metals in the organic phase and at the interface progresses following photoabsorption at the absorption band for the metal extracted.

3.5 Reusability of the Organic Phase.

The reuse of an organic solution following photoirradiation was also investigated. In the case of Fe, the aqueous feed solution and organic solution were contacted at O/A = 1. The weighed organic solution was then contacted with 3.6×10^{-1} mol/l of HCl solution with O/A = 1 and were photoirradiated for 300 min. In the case of V, the aqueous and organic solutions were contacted at O/A = 1 and were photoirradiated for 60 min. The resultant organic solution was then stripped using 6 mol/l of HCl at O/A = 0.5. These resultant organic solutions were then used for repeated processing after washing with 3 mol/l of HCl and then water. **Figure 3-16** shows the concentration of Fe or V in the organic phase during the repeated extraction-stripping processing. The results thus show that the organic phase possesses a sufficient loading and stripping capacity for use in repeated processing and confirm the possible reuse of the organic phase following photoirradiation.
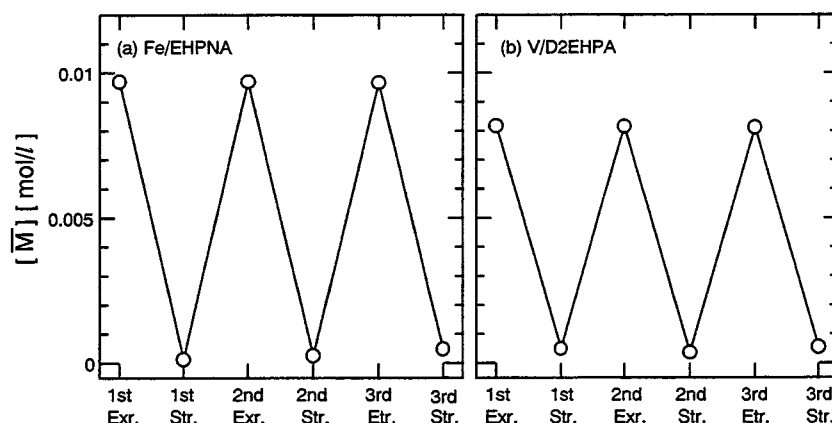

Figure 3-16 The concentration of (a) Fe and (b) V in the organic phase following the repeated extraction-stripping processing. $[\overline{(RH)_2}]_{feed}$ = (a) 1.0 × 10^{-1} mol/l and (b) 5.0 × 10^{-1} mol/l, $[M]_{feed}$ = 1.0 × 10^{-2} mol/l, and pH_{feed} = (a) 1.47 and (b) 0.86.

3.6 Application of the Extraction System Combined with the Photochemical Reduction.

3.6.1 Separation Process.

In chapter I, the separation and recovery process for Ga and In from a zinc refinery residue, containing both rare metals as minor components and Fe, Zn, and Al as major components, was studied. The proposed process consists of two parts, the removal of the major components by use of TBP and the separation and recovery of the two rare metals using D2EHPA. In the first step, all of the Al was left in the aqueous phase. Fe(II) was removed only at low hydrochloric acid concentration conditions in the aqueous phase, and a reduction of Fe(III) to Fe(II) was needed prior to the extraction with TBP. The simple Fe removal process was, therefore, investigated by combining photochemical reduction in the extraction step with D2EHPA, following the TBP extraction step, in which the Al had already effectively been removed. Two possible operations are to prevent Fe extraction in the extraction step and to strip the Fe selectively from the loaded organic solution, as established in the previous section of the present study.

Thus, photochemical reduction is here combined in the extraction step to prevent the extraction of Fe and to enhance the extraction of the two rare metals. A feed liquor containing 1.8×10^{-1} mol/l Fe(III), 3.0×10^{-3} mol/l Ga, 9.0×10^{-3} mol/l In, and 2.3×10^{-1} mol/l Zn was prepared as the feed solution, with a pH$_{feed}$ of 1.61. **Figure 3-17** shows the effect of photoirradiation time on the concentration of each metal species in the organic phase. The pH value fell from 1.61 to values of less than 0.8 in all cases, because of the extraction of metals at the very beginning part of the extraction. The extent of pH reduction obtained depended on the quantity of metals extracted and also on the use of formic acid as a radical scavenger.

For 5.0×10^{-2} mol/l dimeric D2EHPA without formic acid, the Fe concentration of the organic phase remained constant for up to 24 h (Figure 3-17 (a)). D2EHPA at 5.0×10^{-2} mol/l can extract less than half of Fe(III) in the feed solution, and therefore more than half the Fe(III) remains in the aqueous phase. The extraction and photoreductive stripping processes for Fe thus progress at the same time, because no photochemical reduction of Fe(III) occurs in the aqueous phase without the presence of radical scavenger. At 2.0×10^{-1} mol/l dimeric D2EHPA, in the absence of formic acid, the organic phase Fe concentration decreases rapidly, whereas the concentrations of the two rare metals and that of Zn increase with photo-irradiation time (Figure 3-17 (b)). In this case, most of the Fe(III) present in the aqueous feed solution is

extracted into the organic phase during the very early part of the operation and only then does photoreductive stripping progress. After 20 h of photoirradiation, most of the Fe is removed to the aqueous phase (the concentration of Fe in the organic phase being less than 1 ppm) and an effective recovery of the Ga and In is achieved.
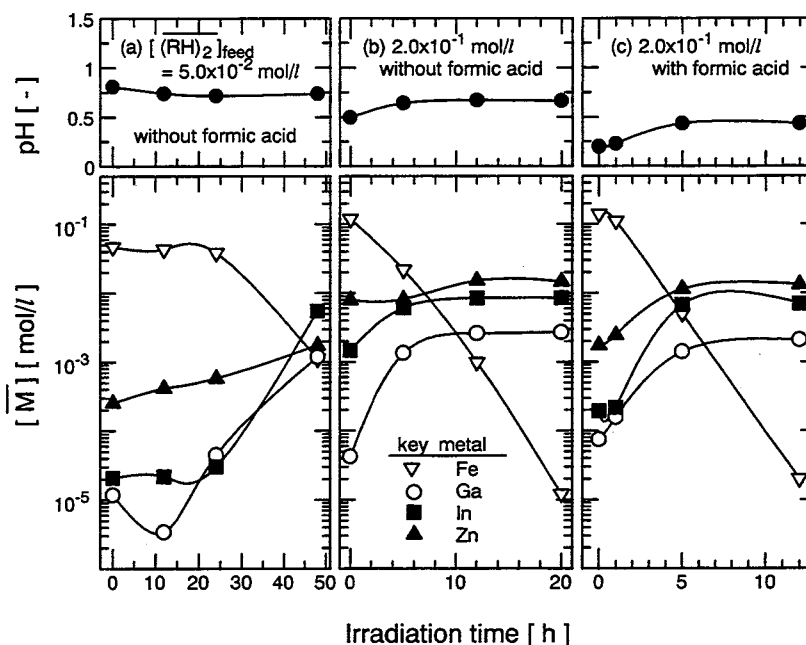
Figure 3-17 Effect of photo-irradiation time on the concentration of Fe, Ga, In and Zn in the organic phase. $[Fe(III)]_{feed} = 1.8 \times 10^{-1}$ mol/l, $[Ga]_{feed} = 3.0 \times 10^{-3}$ mol/l, $[In]_{feed} = 9.0 \times 10^{-3}$ mol/l, $[Zn]_{feed} = 2.3 \times 10^{-1}$ mol/l, pH_{feed} = (a and b) 1.61, and (c) 0.580, $[\overline{(RH)_2}]_{feed}$ = (a) 5.0×10^{-2} mol/l and (b and c) 2.0×10^{-1} mol/l, and $[HCOOH]_{feed}$ = (a and b) 0 mol/l, and (c) 3.41 mol/l.

The hydroxyl radical produced by the photochemical reduction of Fe(III) is likely to be scavenged with the diluent. The effect of the radical scavenger on the removal of Fe was then investigated, where the addition of formic acid accelerates the removal of Fe from the organic phase as shown in Figure 3-17 (c). After 12 h of photo-irradiation, most of the Fe is removed into the aqueous phase (the concentration of Fe in the organic phase being 1.1 ppm). The pH value of the aqueous feed solution was lowered by the addition of formic acid. The removal rate of Fe into the aqueous phase becomes faster with an increase in the hydrogen ion

concentration in the aqueous phase, as shown by Eq. (3-16). In addition, the rate of photochemical reduction, as shown in Eq. (3-23), may be enhanced by the reductive effect of the formic acid. The photochemical reduction of Fe(III) can, therefore, be combined both in the extraction step, and in the stripping step to achieve removal of Fe for the hydrometallurgical process. Although a long period of photoirradiation is needed for removal of the Fe, the reaction time can be shortened by using a photochemical reactor with high photoefficiency.

3.6.2 Stripping of Co Loaded on Hydroxyoxime Extractant.

It is well known that Co(II) when extracted via commercial chelating extractants, such as hydroxyoxime type extractants, is difficult for recovery by conventional stripping procedure, owing to cobalt-poisoning.[118-120] This occurs because the Co(II)-extractant complex formed is easily oxidized to the trivalent state under atmospheric air and is then stabilized in the organic phase. Effective stripping may therefore be expected to be carried out, if the oxidized Co(III) complex can be photoreduced within the organic phase.

3.6.2.1 Extraction Equilibrium Formulations.

The extraction equilibrium formulation for Co with LIX-84I or LIX-65N as extractants, when diluted with n-heptane, has been investigated and expressed according to Eq. (3-36).[121]

$$Co^{2+} + 2\overline{RH} \leftrightarrow \overline{CoR_2} + 2H^+ \qquad (3-36)$$

Figure 3-18 shows the effect of the equilibrium pH value on the distribution ratio, for the n-dodecane diluent system. Linear relationships with slope of 2 were obtained in the present systems as for the reported n-heptane system, thus indicating that only divalent Co takes part in the extraction.

Figure 3-19 shows the effect of the HCl concentration on the stripping efficiency for Co at an O/A volume ratio of 0.5. The extraction-stripping was carried out using both Ar or O_2 bubbling and also without bubbling. For both zero bubbling and bubbling with O_2, the stripping efficiency obtained with 6 mol/l HCl was at most about 80 %, and thus quantitative stripping, by the conventional method, cannot be achieved using either extractant system. In the case of Ar bubbling and thus the absence of oxygen molecules in the system during the extraction-stripping process, the stripping is substantially improved and quantitative stripping is achieved at 6 mol/l HCl. These results, thus, indicate that the Co is stabilized in the organic phase by the presence of oxygen and which thus suppresses quantitative stripping.
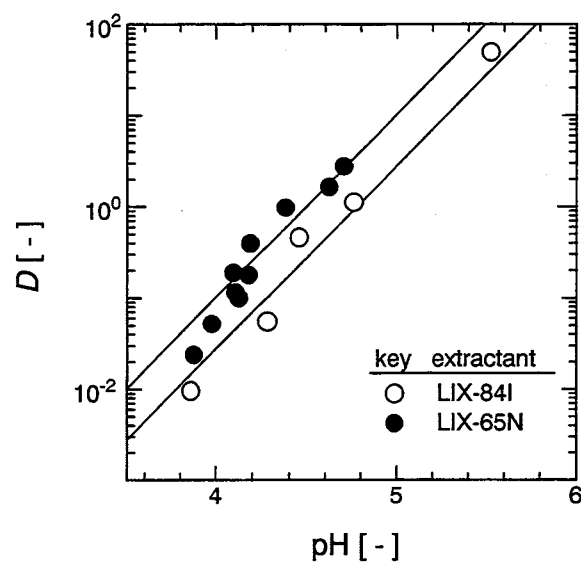
Figure 3-18 Effect of the aqueous phase pH on the distribution ratio for *n*-dodecane diluent. $[\overline{RH}]_{feed}$ = 10 vol% and $[Co^{2+}]_{feed}$ = 1.0 × 10^{-2} mol/l.
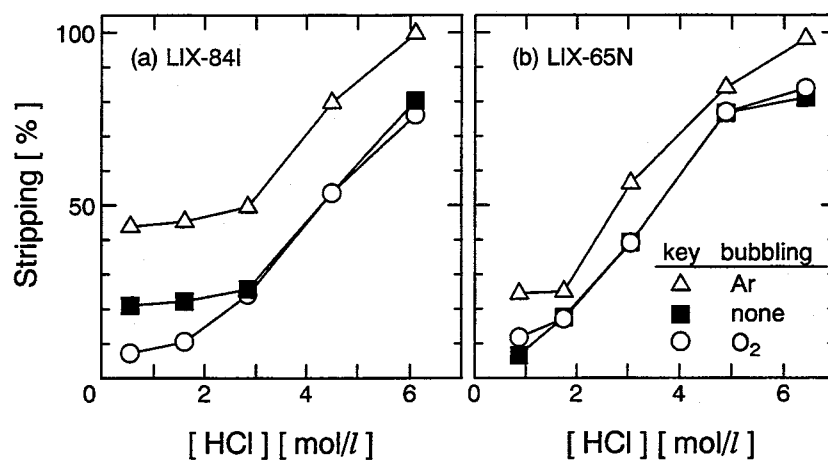

Figure 3-19 Effect of HCl concentration on the stripping efficiency in (a) LIX-84I and (b) LIX-65N systems, at O/A ratio of 0.5. $[\overline{RH}]_{feed}$ = 10 vol%, and $[\overline{Co}]_{feed}$ = (a) 6.76 mmol/l and (b) 7.13 mmol/l.

3.6.2.2 Mechanism for the Oxidation of Extracted Species.

The extracted species of Co using LIX-84I was analyzed by an ESR spectrometer. Co(III) is known to be ESR silent, because it is not paramagnetic. **Figure 3-20** shows the ESR spectra for Co-LIX-84I complexes, prepared by extraction under sets of differing conditions. In the case of Ar bubbling, a broad signal caused by Co(II)-LIX-84I complex, shown by spectrum (a), is observed. However, by contacting it with air, new split sharp signals, as shown by spectrum (b), appear. For both zero bubbling and for O_2 bubbling, only the sharp signals are observed, spectra (c) and (d), and the broad signal corresponding to the resulting Co(II)-LIX-84I complex is no longer observed.

Magnetic field [G]
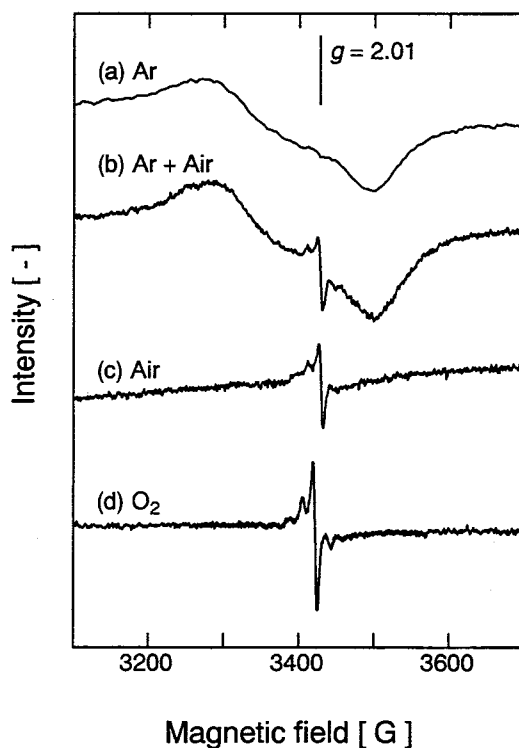
Figure 3-20 ESR spectra for Co loaded on LIX-84I in n-dodecane. The Co-LIX-84I complexes were prepared by extraction under the differing conditions with (a) Ar atmosphere, (b) Ar atmosphere but measured following exposure to air, (c) air atmosphere, and (d) O_2 atmosphere. $[\overline{RH}]_{feed} = 30\,vol\%$, and $[\overline{Co}]_{feed} =$ (a) 7.34 $\times$ $10^{-2}\,mol/l$, (b) 7.32 $\times$ $10^{-2}\,mol/l$, (c) 7.38 $\times$ $10^{-2}\,mol/l$, and (d) 7.35 $\times$ $10^{-2}\,mol/l$.

Co(II) complexes are well known to add easily to an O_2 molecule, and to be oxidized to Co(III), to form a superoxo complex as expressed by Eq. (3-37).[122-124]

$$\overline{\text{Co(II)}} + O_2 \rightarrow \overline{\text{Co(III)} - O - O \cdot} \qquad (3\text{-}37)$$

The split sharp signals are thus caused by the superoxide anion added to Co, thus indicating that the Co(II) molecule is oxidized to the trivalent state by electron attraction with O_2 in the extraction system. This superoxo complex is reported to react further with a second Co(II) to form a μ-peroxo complex, as shown by Eq. (3-38).[125]

$$\overline{\text{Co(III)} - O - O \cdot} + \overline{\text{Co(II)}} \rightarrow \overline{\text{Co(III)} - O - O - \text{Co(III)}} \qquad (3\text{-}38)$$
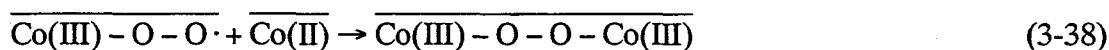
3.6.2.3 Photoreductive Stripping of Co.

The photoreductive stripping of Co was then carried out, using both extractant systems. In this, the extractant-n-dodecane solution, containing Co, was first contacted with HCl solution at an O/A volume ratio of 1. The mixture was then photoirradiated following Ar bubbling with agitation by magnetic stirrer. **Figure 3-21** shows the time-course variation in the stripping efficiency for Co, in the LIX-84I system, with 3 mol/l of HCl, under the conditions of vigorous stirring with photoirradiation at three differing wavelengths.
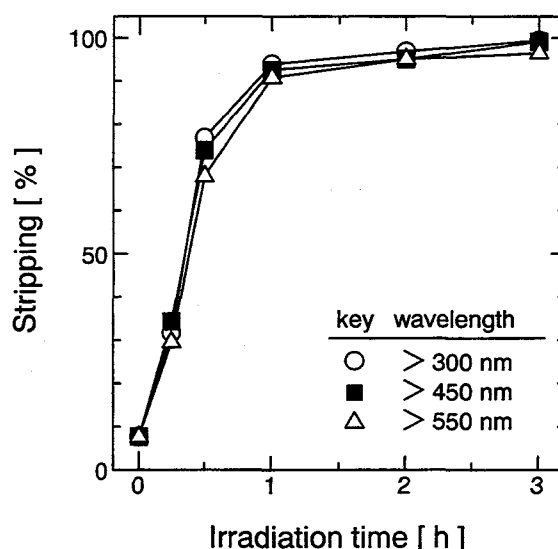

Figure 3-21 Effect of the wavelength of the light source on the time-course variation in the stripping efficiency for the LIX-84I system. $[\overline{\text{RH}}]_{feed} = 10 \text{ vol\%}$, $[\overline{\text{Co}}]_{feed} = 7.64 \text{ mmol/}l$, and $[\text{HCl}] = 3 \text{ mol/}l$.

87

The photoreductive stripping of Co into HCl solution progresses successively, with the concentration of Co in the aqueous phase increasing with irradiation time. In addition, the rate of the photoreductive stripping of Co appears to be insensitive to the wavelength of the irradiated light. **Figure 3-22** shows the absorption spectra for the organic solutions containing Co-LIX-84I complex.
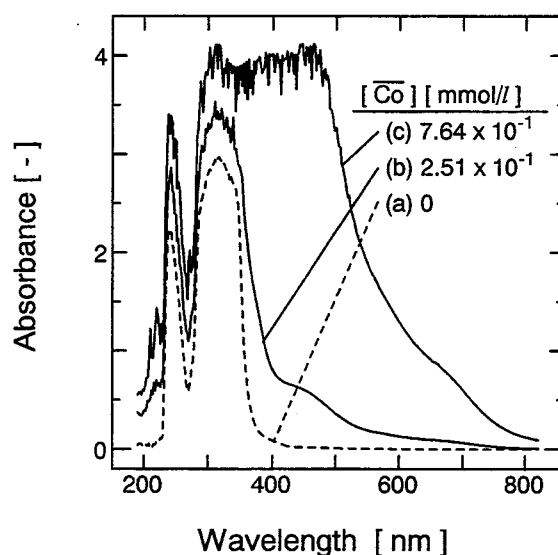
Figure 3-22 Absorption spectra for the organic solution containing LIX-84I and Co. $[\overline{RH}]_{feed}$ = 2.5 vol%, and $[\overline{Co}]_{feed}$ = (a) 0 mol/l, (b) 2.51 × 10^{-1} mmol/l, and (c) 7.64 × 10^{-1} mmol/l. Reference: air.

A large absorption band, caused by the Co-LIX-84I complex is seen at 400-800 nm. These results indicate that the photochemical reduction of Co occurs following photo-absorption at wavelengths of 400-800 nm, and thus the photoreductive stripping progresses with photoirradiation of visible light as well as of UV light.

The effect of HCl concentration on the photoreductive stripping of Co with photoirradiation of wavelength greater than 550 nm in LIX-84I and LIX-65N systems is shown in **Figure 3-23** (a) and (b), respectively. Successive stripping also progresses in the LIX-65N system as well as for LIX-84I system. The photoreductive stripping of Co is improved by increasing concentration of HCl in both systems, and a stripping efficiency of about 90 % can be achieved with 3 mol/l of HCl following photoirradiation for 3 h.

Figure 3-23 Effect of the HCl concentration on the time-course variation of photoreductive stripping in (a) LIX-84I and (b) LIX-65N systems. $[\overline{RH}]_{feed}$ = 10 vol%, and $[\overline{Co}]_{feed}$ = (a) 6.53 mmol/l and (b) 9.37 mmol/l.

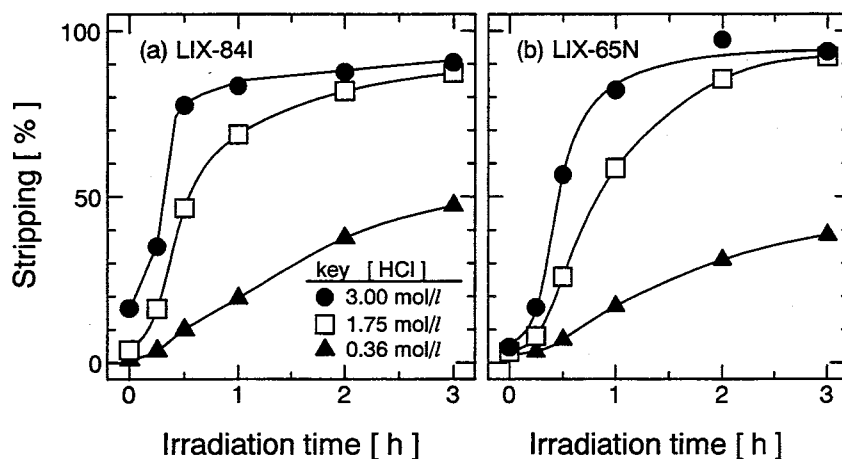**Figure 3-24** shows the effect of photoirradiation on the ESR spectra of the Co-LIX-84I complex. Spectrum (a) applies for the case without Co being present, with the appearance of the signal seeming to indicate addition of oxygen to the extractant. Spectrum (b) applies to the case of organic solution containing 8.2 × 10^{-2} mol/l Co. Here the spectrum differs from spectrum (a) in that it is split, indicating the electronic state of the oxygen to be different for the case of superoxide anion added to Co-LIX-84I complex for spectrum (b) as compared to that for oxygen added to LIX-84I in spectrum (a). Spectrum (c) applies to the case of the solution containing Co-LIX-84I, stripped with 6.0 × 10^{-1} mol/l HCl with photoirradiation for 12 h, and containing a residual 3.0 × 10^{-2} mol/l Co. In this case, the broad signal caused by Co(II) as shown by the spectrum (a) in Figure 3-20 is absent, although the conditions provide sufficient time for the Co in the organic phase to be reduced to the divalent state. Spectrum (d) applies to the case where 3 mol/l HCl was used for the stripping and most of the Co was stripped into the aqueous phase. Here the spectrum (d) shows both the absence of Co(II) and the absence of superoxide anion added to the Co(III)-LIX-84I complex, leaving only a sharp signal, of which the shape is identical to that observed for oxygen added to extractant, as in spectrum (a).

89
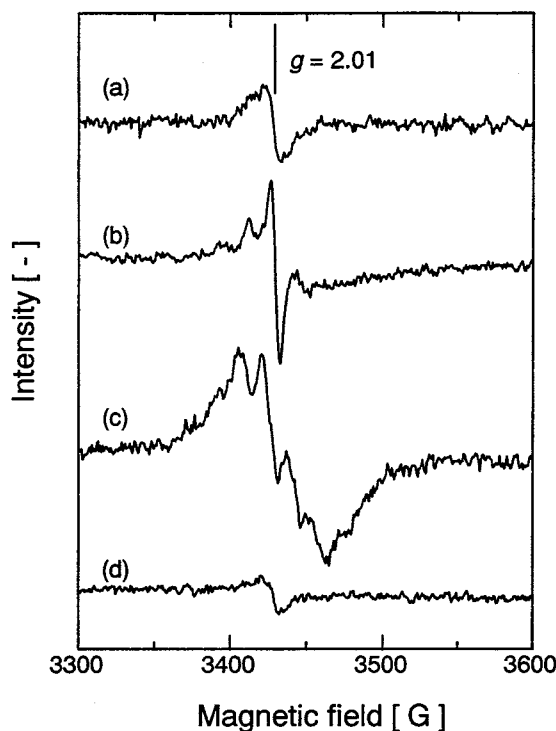
Figure 3-24 Effect of photoirradiation on the ESR spectra for Co loaded on LIX-84I in n-dodecane. $[\overline{RH}]_{feed} = 30$ vol%, $[\overline{Co}]$ = (a) 0 mol/l, (b) 8.2 $\times 10^{-2}$ mol/l, (c) 3.0 $\times 10^{-2}$ mol/l, and (d) 1.1 mmol/l, and [HCl] = (c) 6.0 $\times 10^{-1}$ mol/l and (d) 3 mol/l.

The reduced Co is, therefore, immediately re-oxidized by the oxygen in the organic phase, unless stripped into the aqueous phase.

3.6.2.4 Reusability of the Organic Phase.

The possible reuse of the organic solution following photoirradiation was also investigated for the case of the LIX-84I system. 3 mol/l HCl solution and Co-containing organic solution were contacted at an O/A volume ratio of 1 and were photoirradiated for 5 h. The resultant organic solution, after washing with water, was then used for extraction and the extracted organic solution then again used for repeated processing. **Figure 3-25** shows the concentration of Co in the organic phase for the repeated extraction-photoreductive stripping processing. The results thus show that the organic phase possesses sufficient loading and stripping capacity for use in repeated processing and confirm possible reuse of the organic phase.

key wavelength

■ > 300 nm
○ > 450 nm
△ > 550 nm

0.01

0.005

0

$[\overline{Co}]$ [mol/l]

1st Ext. | 1st Str. | 2nd Ext. | 2nd Str. | 3rd Ext. | 3rd Str.
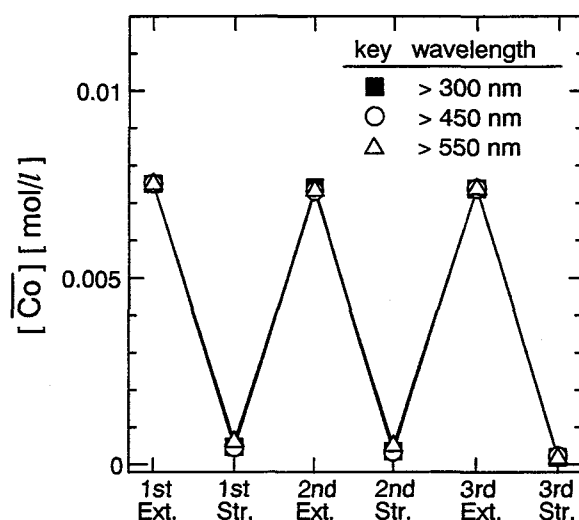
Figure 3-25 The concentration of Co, obtained in the organic phase, following the repeated extraction-photoirradiation processing. $[\overline{RH}]_{feed}$ = 10 vol% and $[Co^{2+}]_{feed}$ = 1.0 × 10^{-2} mol/l.

4. Summary

The liquid-liquid extraction system, combined with the photochemical reduction of the target metal, is investigated. The mechanism of the photoreductive stripping of Fe(III) and photoreductive extraction of V(V) were investigated as case studies, and the results were applied for the separation and purification of the metals and the stripping of Co loaded on the hydroxyoxime extractant, with following results.

(1) The extraction equilibria for Fe(III) and Fe(II) with EHPNA and D2EHPA and V(V) and V(IV) with D2EHPA are established. For Fe(III) and Fe(II), the extracted species are $\overline{FeR_3(RH)_3}$ and $\overline{FeR_2(RH)_2}$, respectively. For V(V) and V(IV), the extracted species are $\overline{VO_2R(RH)}$ and $\overline{VOR_2(RH)_2}$, respectively.

(2) The photochemical reduction of Fe(III) occurs in the aqueous solution in the presence of formic acid as a radical scavenger, but no reaction occurs in the organic solution for the Fe(III)-extractant complex.

(3) The photochemical reduction of V occurs in both aqueous and organic solutions, at a rate which is first order with respect to the concentration of V in the respective solutions.

91

The rate constant for photochemical reduction in the organic phase is much greater than that for the aqueous phase.

(4) The photoreductive stripping of Fe(III) progresses following an initial induction period because of the dissolved oxygen in the extraction system. The Fe(III)-extractant complex is photoexcited in the organic phase and is photoreduced at the interface by electron donation from water. A kinetic study of the photoreductive stripping of Fe(III) reveals that the photochemical reduction of Fe(III) is the rate-determining step.

(5) In V extraction system, reduction also occurs at the interface between the aqueous and organic phases. The photoreductive extraction is mainly contributed by the photochemical reduction at the interface and in the organic phase. The variation in the distribution ratio with respect to photoirradiation time is expressed successfully by the proposed reaction scheme, in which the photochemical reduction of V is the rate-determining step.

(6) The removal of Fe from a simulated zinc refinery residue solution can be carried out effectively by photoirradiation during the extraction step. Ga and In are recovered effectively into the organic phase, leaving almost all of the Fe in the aqueous phase.

(7) The photoreductive stripping of Co progresses by photoirradiation, using the wavelengths of visible light. The photoreductive stripping is improved by increasing concentration of HCl, and a stripping efficiency of about 90 % can be achieved following photoirradiation for 3 h.

(8) The organic solution following photoirradiation is reusable for repeated extraction-photoreductive stripping or photoreductive extraction-stripping processing.

5. Nomenclature

A	= interfacial area	$[dm^2]$
D	= distribution ratio	$[-]$
g	= g value for ESR measurement	
k_{Fe}	= rate constant	$[l^{0.5} mol^{0.5} min^{-1}]$
k_V	= rate constant	$[min^{-1}]$
$k_{1,Fe}$	= rate constant for Eq. (3-23)	$[min^{-1}]$

k_{Fe}'	= apparent rate constant for photoreductive stripping of Fe	$[\text{min}^{-1}]$
$k_{i,v}'$	= rate constant at the interface	$[\text{dm min}^{-1}]$
K	= equilibrium constants for the elementary reaction	
K_{ex}	= extraction equilibrium constant	
$K_{i,v}$	= equilibrium constant for V between organic phase and interface	
Q	= volume of the organic phase	$[l]$
r_{Fe}	= rate of photoreductive stripping	$[\text{mol } l^{-1} \text{ min}^{-1}]$
r_v	= rate of photochemical reduction	$[\text{mol } l^{-1} \text{ min}^{-1}]$
r_v'	= rate of photochemical reduction at the interface	$[\text{mol dm}^{-2} \text{ min}^{-1}]$
$(RH)_2$	= dimeric species of the EHPNA and D2EHPA	
Y	= reduction yield	$[\text{-}]$
[ ]	= concentration of the species in the bracket, mol/L	
*	= excited species	

\<Subscript\>

a	= aqueous phase
feed	= aqueous or organic feed solution
i	= interface
o	= organic phase

\<Superscripts\>

—	= organic phase species
=	= interface species

General Conclusions

This work described the separation and recovery processes of rare metals with advanced liquid-liquid extraction system. First, the design of the liquid-liquid extraction process, with the counter-current mixer-settler cascade, based on the equilibrium theory was investigated with the simulation method. Two types of the advanced extraction systems were then employed. One is the system combined with the masking reaction with a water-soluble complexing agent at the equilibrium state. The extraction process with the counter-current mixer-settler cascade were designed using the extraction equilibrium formulations, which include the complexing reaction between the metals and the agents in the aqueous phase. Another is the system combined with the photochemical reduction for the target metals. The mechanism of the extraction system was made clear, enabling the variation of the distribution ratio to be predicted.

In chapter I, the design of the liquid-liquid extraction process with the simulation method based on the extraction equilibrium formulations determined and the material balance was investigated. The separation and recovery process of Ga and In from simulated zinc refinery was carried out as a case study. The extraction equilibrium formulations of Ga and In were established, with the slope analysis method and the investigation for the analytical composition of the extracted species. In the three extractants used, D2EHPA is most suitable for the separation of Ga and In, and thus, the extraction equilibrium formulation in Ga/In/Zn ternary system was also determined. The formulation can be applied for the scrubbing treatment of metal-loaded organic solution. These experimental results on the extraction equilibrium show that the extraction equilibrium formulations determined is worthy of using to the simulation work. The separation and recovery process for Ga and In with D2EHPA was then evaluated by simulation work based on the equilibrium studies and an equilibrium countercurrent extraction stage formulation. The process consists of three sections: (i) Zn reduction, (ii) In recovery, and (iii) Ga recovery. Ga and In were shown to be capable of effective recovery with purities of 9.91×10^{-1} and 1.00, respectively.

In chapter II, the design of the extraction process combined with the masking reaction with the water-soluble complexing agent was investigated. The separation of rare earth metals in the presence of EDTA or DTPA was carried out as a case study. The extraction equilibrium formulations for rare earth metals, in the absence of the complexing agent, with

94

EHPNA and VA-10 were established. In the EHPNA system, the extraction behavior in the presence of EDTA can be expressed satisfactorily, by assuming that the rare-earth metals when complexed with EDTA do not take part in the extraction. The extraction of Ho and Er in the presence of EDTA is suppressed compared to Y by a masking effect and the selective extraction of Y enhanced. A simulation study for the separation of Y from a Ho/Y/Er mixture of initially identical concentration using a countercurrent mixer-settler cascade was carried out. This showed that an organic solution with an overall decontamination factor of 11.8 can be obtained using a cascade of 10 extraction stages and a single scrubbing stage using an aqueous feed solution with equal concentrations of all three metals. Increasing the number of the scrubbing stages from 1 to 2 enabled the separation of Y to be improved, with an overall decontamination factor of 6.33 × 10 being achieved, although the recovery of Y obtained decreased. In VA-10 system, the distribution ratios of each metal are decreased by the masking effect. In the Y/Er system, the order of the extractabilities of Y and Er is reversed and the selective extraction of Y is improved especially at high pH values, while the separation is little changed in the Yb/Lu system. The molar ratio of rare earth metal and DTPA in the rare earth-DTPA complex is not fixed at 1 : 1, but varies between 1 : 1 and 1.5 : 1 in the extraction system.

In chapter III, the liquid-liquid extraction system combined with the photochemical reduction for the target metals was investigated. The photoreductive stripping of Fe(III) and photoreductive extraction of V(V) were carried out as case studies. The photochemical reduction of Fe(III) occurs in the aqueous solution in the presence of formic acid as a radical scavenger, but no reaction occurs in the organic solution for the Fe(III)-extractant complex. The photochemical reduction of V occurs in both aqueous and organic solutions, at a rate which is first order with respect to the concentration of V in the respective solutions. The rate constant for photochemical reduction in the organic phase is much greater than that for the aqueous phase. The photoreductive stripping of Fe(III) progresses following an initial induction period because of the dissolved oxygen in the extraction system. The Fe(III)-extractant complex is photoexcited in the organic phase and is photoreduced at the interface by electron donation from water. A kinetic study of the photoreductive stripping of Fe(III) reveals that the photochemical reduction of Fe(III) is the rate-determining step and the distribution of the reduced Fe(II) is attained fast. In V extraction system, reduction also

occurs at the interface between the aqueous and organic phases. The photoreductive extraction is mainly contributed by the photochemical reduction at the interface and in the organic phase. The variation in the distribution ratio with respect to time of photoirradiation is expressed successfully by the proposed reaction scheme, in which the photochemical reduction of V is the rate-determining step. The removal of Fe from a simulated zinc refinery residue solution can be carried out effectively by photoirradiation during the extraction step. Ga and In are recovered effectively into the organic phase, leaving almost all of the Fe in the aqueous phase. The photoreductive stripping of Co progresses by photoirradiation, using the wavelengths of visible light. The photoreductive stripping is improved by increasing concentration of HCl, and the stripping efficiency of about 90 % can be achieved following photoirradiation for 3 h.

Suggestions for Future Work

The following studies are recommended to extend the results in this work.

(1) Design of the Photochemical Liquid-Liquid Reactor.

In the work of this thesis, the photochemical reduction was carried out in the beaker-type bottle cell. However, a long period of photoirradiation time is needed for the photoreductive stripping or extraction of the target metals. The investigation for the development of the photochemical liquid-liquid reactor is needed for the design of the extraction process on the industrial scale. A photochemical reactor, for the separation of the elements from high-level radioactive waste solution using the photochemical reduction with KrF excimer laser, has been reported.[126] The reaction time is expected to be shortened by using a photochemical reactor with high photoefficiency, since the rate-determining step of the system is photochemical reduction of the metals in the extraction system, as shown in Chapter III. The investigation for the design of the industrial process of the extraction system combined with the photoredox reaction using such reactor is expected as a future work.

(2) Conversion of the Liquid-Liquid Process to the Solid-Liquid Process.

One of the disadvantages in the liquid-liquid extraction process is that large amount of the organic solvent is needed for diluting the extractant. Recently, several attempts were made for the capsulation of the extractant using microcapsule with polymers.[127,128] In the microcapsule system, the liquid-liquid process can extend to the solid-liquid process, without using the organic solvent. Using this system, the recovery and concentration of the metals from the dilute aqueous solution is expected to be easily carried out. In addition, the high selective separation can be achieved with the chromatograph with the microcapsule. The design of high performance separation and recovery process of rare metals using the microcapsule system is also expected as a future work.

References Cited

1) Flett, D.S.; Spink, D.R. Solvent Extraction of Non-Ferrous Metals: A Review 1972-1974. *Hydrometallurgy* **1976**, *1*, 207.

2) Nakashio, F.; Inoue, K.; Kondo, K. Extraction of Metals by the Formation of Complexes (in Japanese). *Kagaku Kogaku* **1978**, *42*, 182.

3) Nishimura, S. Solvent Extraction in Extraction Metallurgy of Rare Metals (in Japanese). *Nippon Kinzoku Gakkai Kaiho* **1982**, *21*, 311.

4) Sekine, T.; Hasegawa, Y. Metal Complexes and Their Solvent Extraction (in Japanese). *Yukagaku* **1990**, *39*, 729.

5) Kawamoto, H.; Akaiwa, H. Chelate Extraction (in Japanese). *Bunseki* **1992**, 998.

6) Gupta, B. Extractionof Metals by Carboxylic Acids-A Review. *J. Sci. Ind. Res.* **1993**, *52*, 808.

7) Inoue, K. Recent Progress on Industrial Metal Extraction 1 (in Japanese). *Bunri Gijutsu* **1996**, *26*, 381.

8) Goto, M.; Nakashio, F. Extraction Operation (in Japanese). *Kemikaru Enjiniyaringu* **1997**, *42*, 124.

9) Inoue, K. Recent Progress on Industrial Metal Extraction 2 (in Japanese). *Bunri Gijutsu* **1997**, *27*, 205.

10) Inoue, K. Recent Progress on Industrial Metal Extraction 3 (in Japanese). *Bunri Gijutsu* **1997**, *27*, 399.

11) Yuan. C.; Ye, W.; Ma, H.; Wang, G.; Long, H.; Xie, J.; Qin, X.; Zhou, Y. Synthesis of Acidic Phosphates and Phosphonates and Their Structure-Reactivity Studies on The Extraction of Neodymium, Samarium, Ytterbium and Yttrium. *Sci. Sin. Ser. B (Engl. Transl.)* **1982**, *25*, 7.

12) Preston, J.S. Solvent Extraction of Metals by Carboxylic Acids. *Hydrometallurgy* **1985**, *14*, 171.

13) Preston, J.S.; Preez, A.C.D. The Solvent Extraction of Europium(II) by Some Organophosphorus and Carboxylic Acids. *Solv. Extr. Ion Exch.* **1991**, *9*, 237.

14) Preez, A.C.D.; Preston, J.S. The Solvent Extraction of Rare-Earth Metals by Carboxylic Acids. *Solv. Extr. Ion Exch.* **1992**, *10*, 207.

15) Takahashi, T.; Nishizawa, H.; Tsuchiya, Y.; Sato, T. Effect of Changes in Structure of Phosphoric Acid Esters on Extractability of Rare Earths-Extraction of Rare Earths by Phosphoric Acid Esters Containing Bulky Alkyl Groups I. *Shigen-to-Sozai* **1995**, *111*, 109.

16) Ishida, K.; Takeda, S.; Takahashi, T.; Sato, T. Extraction Behaviors of Rare Earth Elements in Solvent Extraction with Single and Mixed Extractant Systems-Extraction of Rare Earths by Phosphoric Acid Esters Containing Bulky Alkyl Groups II. *Shigen-to-Sozai* **1995**, *111*, 114.

17) Takahashi, T.; Sato. T. Effect of Changes in Structure of Phosphoric Acid Esters on Solvent Extraction of Cobalt(II) and Nickel(II). *Shigen-to-Sozai* **1995**, *111*, 787.

18) Inoue, S.; Zhang, Q.; Uto, M. Steric Effect of Substituents on the extraction of Lanthanoids(III) with *N-p-(n-, iso-* and *tert-*)butylbenzoyl-*N*-phenylhydroxylamine. *Talanta* **1997**, *44*, 1455.

19) Ohto, K.; Ota, H.; Inoue, K. Solvent Extraction of Rare Earths with a Calix[4]arene Compound Containing Phosphonate Groups Introduced to the Upper Rim. *Solv. Extr. Res. Dev. Jpn.* **1997**, *4*, 167.

20) Yoshizuka, K.; Kosaka, H.; Shinohara, T.; Ohto, K.; Inoue, K. Structural Effect of Phosphoric Esters Having Bulky Substituents on the Extraction of Rare Earth Elements. *Bull. Chem. Soc. Jpn.* **1996**, *69*, 589.

21) Comba, P.; Gloe, K.; Inoue, K.; Krueger, T.; Stephan, H.; Yoshizuka, K. Molecular Mechanics Calculations and the Metal Ion Selective Extraction of Lanthanoids. *Inorg. Chem.* **1998**, *37*, 3310.

22) Goto, M.; Matsumoto, S.; Uezu, K.; Nakashio, F.; Yoshizuka, K.; Inoue, K. Development and Computational Modeling of Novel Bifunctional Organophosphorus Extractants for Lanthanoid Separation. *Sep. Sci. Technol.* **1999**, *34*, 2125.

23) Yoshizuka, K.; Inoue, K.; Comba, P. Quantitative Structure-Property Relationship of Extraction Equilibria of Lanthanoid Series Using Molecular Mechanics Calculations (in Japanese). *Kagaku Kogaku Ronbunshu* **2000**, *26*, 517.

24) Honjo, T. Solvent Extraction-Utilization of Synergism (in Japanese). *Bunseki* **1980**, 800.

25) Kakoi, T.; Goto, M. Novel Extractants with High Selectivity for Valuable Metals in Seawater-Calixarene Derivatives (in Japanese). *Nippon Kaisui Gakkaishi* **1997**, *51*,

319.

26) Alexandratos, S.D.; Natesan, S. Coordination Chemistry of Phosphorylated Calixarenes and Their Application to Separation Science. *Ind. Eng. Chem. Res.* **2000**, *39*, 3998.

27) Cox, M.; Flett, D.S. Metal Extractant Chemistry. In *Handbook of Solvent Extraction*; Lo, T.C., Baird, M.H.I., Hanson, C., Eds.; John Wiley & Sons: New York, 1983.

28) Kolarik, Z.; Grimm, R. Acidic Organophosphorus Extractants-XXIV. The Polymerization Behavior of Cu(II), Cd(II), Zn(II) and Co(II) Complexes of Di(2-ethylhexyl)phosphoric Acid in Fully Loaded Organic Phases. *J. Inorg. Nucl. Chem.* **1976**, *38*, 1721.

29) Komasawa, I.; Otake, T.; Hattori, I. Extraction of Nickel and Cobalt with 2-ethylhexyl Phosphonic Acid Mono-2-ethylhexyl Ester. *J. Chem. Eng. Jpn.* **1983**, *16*, 210.

30) Xun, F.; Golding, J.A. Solvent Extraction of Cobalt and Nickel in Bis(2,4,4-tri-methylpentyl) Phosphinic Acid, "Cyanex 272". *Solv. Extr. Ion Exch.* **1987**, *5*, 205.

31) Godfrey, J.C.; Slater, M.J. Principles of Mixer-Settler Design. In *Handbook of Solvent Extraction*; Lo, T.C., Baird, M.H.I., Hanson, C., Eds.; John Wiley & Sons: New York, 1983.

32) Tanaka, M.; Koyama, K.; Shibata, J. Role of the Extraction Equilibrium Constant in the Countercurrent Multistage Solvent Extraction-Stripping Process for Metal Ions. *Ind. Eng. Chem. Res.* **1998**, *37*, 1943.

33) Bogacki, M.B. Effect of Various Phenomena in the Organic Phase on Metal Extraction with Chelating Reagents in Countercurrent and Crosscurrent Extraction Systems. *Ind. Eng. Chem. Res.* **1999**, *38*, 1611.

34) Goto, T. Calculation of Counter-Current Extraction of Lanthanides with a Digital Computer. *Proc. Int. Solv. Extr. Conf. '74* **1974**, 1011.

35) Benedict, M.; Pigford, T.; Levi, H. *Nuclear Chemical Engineering*; McGraw-Hill Book Company: New York, 1981.

36) Matsuyama, H.; Teramoto, M. Separation of Rare Earth Elements by Solvent Extraction in the Presence of Complexing Agents (in Japanese). *Hyomen* **1992**, *30*, 1053.

37) Ono, N. Sumitomo's New Process for Nickel and Cobalt Recovery from Their Sulfide Mixture (in Japanese). *Nippon Kogyo Kaishi* **1979**, *95*, 441.

38) Ritcey, G.M.; Ashbrook, A.W. *Solvent Extraction Part I; Elsevier*: New York, 1984.

39) Hala, J. Some Aspects of Synergistic Extractions with Chelating Extractants. *J. Radioanal. Chem.* **1979**, *51*, 15.

40) Akaiwa, H. Analytical Chemistry of Synergistic Extraction (in Japanese). *Bunseki* **1979**, 500.

41) Akaiwa, H.; Kawamoto, H. The Application of Synergistic Extraction to Analytical Chemistry. *Rev. Anal. Chem.* **1982**, *6*, 65.

42) Choppin, G.R. Studies of the Synergistic Effect. *Sep. Sci. Technol.* **1981**, *16*, 1113.

43) Honjo, T. Solvent Extraction-Utilization of Synergism (in Japanese). *Bunseki* **1980**, 800.

44) Kikuchi, S.; Kamagami, S. Extraction and Separation of Gallium(III), Indium(III) and Aluminum(III) from Sulfuric Acid Solution by Octylphenyl Phosphoric Acid in Benzene (in Japanese). *Nippon Kogyo Kaishi* **1988**, *104*, 601.

45) Inoue, K. Solvent Extraction of Indium(III) and Gallium(III) with Various Acidic Extractants (in Japanese). *Shigen-to-Sozai* **1989**, *105*, 751.

46) Sato, T.; Horie, J.; Nakamura T. Extraction of Gallium(III) from Hydrochloric Acid Solutions by Acid Organophosphorus Compounds. *Proc. Symp. Solv. Extr. Jpn.* **1987**, 131.

47) Takahashi, T.; Nishizawa, H.; Kakiuchi, T.; Takeuchi, H. Solvent Extraction of Gallium from Aqueous Hydrochloric Acid Solutions by an Organophosphorus Monoester in *n*-Heptane. *Kagaku Kogaku Ronbunshu* **1989**, *15*, 1006.

48) Mihaylov, I.; Distin, P.A. Gallium Solvent Extraction in Hydrometallurgy: An Overview. *Hydrometallurgy* **1992**, *28*, 13.

49) Abe, H. The Recovery of Gallium and Indium from Zinc Refinery By-Product (in Japanese). *Nippon Kogyo Kaishi* **1982**, *98*, 561.

50) Hino, A.; Hirai, T.; Komasawa, I. Acidic Phosphinates with Different Alkyl Groups as Extractants for Rare Earths. *J. Chem. Eng. Jpn.* **1996**, *29*, 1041.

51) Nagaosa, Y.; Binghua, Y. Extraction Equilibria of Some Transition Metal Ions by Bis(2-ethylhexyl)phosphinic Acid. *Talanta* **1997**, *44*, 327.

52) Naganawa, H.; Tachimori, S. High Hydrated Associate of Tributyl Phosphate in Dodecane. *Anal. Sci.* **1994**, *10*, 607.

53) Hino, A.; Hirai, T.; Komasawa, I. The Recovery of Phosphorus Value from Incineration

Ashes of Sewage Sludge Using Solvent Extraction (in Japanese). *Kagaku Kogaku Ronbunshu* **1998**, *24*, 273.

54) Nakamoto, K.; *Infrared and Raman Spectra of Inorganic and Coodination Compounds*; John Wiley & Sons: New York, 1970.

55) Inoue, K.; Baba, Y.; Yoshizuka, K. Equilibria in the Solvent Extraction of Indium(III) from Nitric Acid with Acidic Organophosphorus Compound. *Hydrometallurgy* **1988**, *19*, 393.

56) Inoue, K.; Baba, Y.; Yoshizuka, K. Solvent Extraction Equilibria of Gallium(III) with Acidic Organophosphorus Compounds from Aqueous Nitrate Media. *Solv. Extr. Ion Exch.* **1988**, *6*, 381.

57) Hogfeldt, E. *Stability Constants of Metal Ion Complexes part A: Inorganic Ligands*; Pergamon Press: Oxford, U.K., 1982.

58) Hartley, F.R.; Burgess, C.; Alcock, R.M. *Solution Equilibria*; John Wiley & Sons: New York, 1980.

59) Hanson, C. Commercial Processes for Other Metals. In *Handbook of Solvent Extraction*; Lo, T. C., Baird, M. H. I., Hanson, C., Eds.; John Wiley & Sons: New York, 1983.

60) Orlowska, B.; Ciurla, Z.; Golab, Z. Biorecovery of Gallium from Plant Wastes. In *Precious and Raremetal Technologies*; Torma, A. E., Gundiler, I. H., Eds.; Elsevier: New York, 1989.

61) Hirai, T.; Komasawa, I. Extraction and Separation of Rare-Earth Elements by Tri-*n*-Octylmethylammonium Nitrate and *β*-Diketone Using Water-Soluble Complexing Agent. *J. Chem. Eng. Jpn.* **1991**, *24*, 731.

62) Umetani, S.; Matsui, M.; Tsurubou, S. Improvement of Separation in the Solvent Extraction of Alkaline Earths by the Use of 18-Crown-6 as a Masking Reagent. *J. Chem. Soc., Chem. Commun.* **1993**, 914.

63) Tsurubou, S.; Mizutani, M.; Kadota, Y.; Yamamoto, T.; Umetani, S.; Sasaki, T.; Le, Q.T.H.; Matsui, M. Improved Extraction-Separation of Alkaline Earths and Lanthanides Using Crown Ethers as Ion Size Selective Masking Reagents: A Novel Macrocycle Application. *Anal. Chem.* **1995**, *67*, 1465.

64) Sasaki, T.; Umetani, S.; Le, Q.T.H.; Matsui, M.; Tsurubou, S. Improved Extraction-Separation of Alkaline Earths and Lanthanides with the Aid of an Ion Size-Selective

Masking Reagents. *Analyst* **1996**, *121*, 1051.

65) Sasaki, T.; Umetani, S.; Matsui, M.; Tsurubou, S.; Kimura, T.; Yoshida, Z. Complex Formation of Lanthanide Ions with Sulfonated Crown Ethers in Aqueous Solution. *Bull. Chem. Soc. Jpn.* **1998**, *71*, 371.

66) Matsuyama, H.; Okamoto, T.; Miyake, Y.; Teramoto, M. Extraction Mechanism of Rare Earth Metals in the Presence of Diethylenetriaminepentaacetic Acid in Aqueous Phase. *J. Chem. Eng. Jpn.* **1989**, *22*, 627.

67) Minagawa, Y.; Yajima, F. Selective Separation of Yttrium Ions from Other Rare Earth Ions Using Nonequilibrium Extraction. *Bull. Chem. Soc. Jpn.* **1992**, *65*, 29.

68) Matsuyama, H.; Azis, A.; Fujita, M.; Teramoto, M. Enhancement in Extraction Rates by Addition of Organic Acids to Aqueous Phase in Solvent Extraction of Rare Earth Metals in the Presence of Diethylenetriaminepentaacetic Acid. *J. Chem. Eng. Jpn.* **1996**, *29*, 126.

69) Matsuyama, H.; Miyamoto, Y.; Teramoto, M.; Goto, M.; Nakashio, F. Selective Separation of Rare Earth Metals by Solvent Extraction in the Presence of New Hydrophilic Chelating Polymers Functionalized with Ethylenediaminetetraacetic Acid. I. Development of New Hydrophilic Chelating Polymers and Their Adsorption Properties for Rare Earth Metals. *Sep. Sci. Technol.* **1996**, *31*, 687.

70) Matsuyama, H.; Miyamoto, Y.; Teramoto, M.; Goto, M.; Nakashio, F. Selective Separation of Rare Earth Metals by Solvent Extraction in the Presence of New Hydrophilic Chelating Polymers Functionalized with Ethylenediaminetetraacetic Acid. II. Separation Properties by Solvent Extraction. *Sep. Sci. Technol.* **1996**, *31*, 799.

71) Martell, E.; Smith, R.M. *Critical Stability Constants Volume 1; Amino Acids*; Plenum Press: New York, USA, 1974.

72) Mickler, W.; Reich, A.; Uhlemann, E. Extraction of Iron(II) and Iron(III) with 4-Acyl-5-pyrazolones in Comparison with Long-Chain 1-Phenyl-1,3-(cyclo)alkanediones. *Sep. Sci. Technol.* **1998**, *33*, 425.

73) Nasu, A.; Takagi, H.; Ohmiya, Y.; Sekine, T. Solvent Extraction of Iron(II) and Iron(III) as Anionic Thiocyanate Complexes with Tetrabutylammonium Ions into Chloroform. *Anal. Sci.* **1999**, *15*, 177.

74) Nasu, A.; Yamaguchi, S.; Sekine, T. Solvent Extraction of Copper(I) and (II) as Thiocyanate Complexes with Tetrabutylammonium Ions into Chloroform and with Trioctylphosphine Oxide into Hexane. *Anal Sci.* **1997**, *13*, 903.

75) Nasu, A.; Kato, K.; Sekine, T. Solvent Ectraction of Copper(I) and Copper(II) from Aqueous Halide Solutions with Tetrabutylammonium Ions into Chloroform. *Bull. Chem. Soc. Jpn.* **1998**, *71*, 2141.

76) Przeszlakowski, S.; Wydra, H. Extraction of Nickel, Cobalt and Other Metals [Cu, Zn, Fe(III)] with a Commercial β-diketone Extractant. *Hydrometallurgy* **1982**, *8*, 49.

77) Soldenhoff, K.H. Options for the Recovery of Cerium by Solvent Extraction. *Proc. Int'l Solv. Extr. Conf. '96* **1996**, 469.

78) Kolarik, Z.J.; Horwitz, E.P. Extraction of Neptunium and Plutonium Nitrates with n-Octyl(phenyl)-N,N-diisobutyl-Carbamoylmethylphosphine Oxide. *Solv. Extr. Ion Exch.* **1988**, *6*, 247.

79) Gehmecker, H.; Traumann, N.; Herrmann, G. Extraction of Pu^{3+}, Pu^{4+} and PuO_2^{2+} from Various Mineral Acid Solutions by Tri-n-butylphosphate and Di-(2-ethylhexyl)-orthophosphoric Acid. *Radiochim. Acta* **1986**, *40*, 11.

80) Gaunand, A.; Bouboukas, G.; Renon, H. Iron Elimination in Cupric Chloride Hydrometallurgical Processes by Oxidizing Extraction. *Chem. Eng. Sci.* **1987**, *42*, 1221.

81) Morita, Y.; Kubota, M. Extraction of Neptunium with Di-Isodecyl Phosphoric Acid from Nitric Acid Solution Containing Hydrogen Peroxide. *Solv. Extr. Ion Exch.* **1988**, *6*, 233.

82) Hirai, T.; Komasawa, I. Separation and Purification of Vanadium and Molybdenum by Solvent Extraction Followed by Reductive Stripping. *J. Chem. Eng. Jpn.* **1990**, *23*, 208.

83) Takahashi, N.; Asano, S. Solvent Extraction of Europium with Crown Ether (in Japanese). *Nippon Kinzoku Gakkaishi* **1995**, *59*, 271.

84) Tochiyama, O.; Nakamura, Y.; Katayama, Y.; Inoue, Y. Equilibrium of Nitrous Acid-Catalyzed Oxidation of Neptunium in Nitric Acid-TBP Extraction System. *J. Nucl. Sci. Technol.* **1995**, *32*, 50.

85) Preston, J.S.; Preez, A.C.D. The Separation of Europium from a Middle Rare Earth Concentrate by Combined Chemical Reduction, Precipitation and Solvent-

Extraction Methods. *J. Chem. Technol. Biotechnol.* **1996**, *65*, 93.

86) Chitnis, R.R.; Wattal, P.K.; Ramanujam, A.; Dhami, P.S.; Gopalakrishman, V.; Mathur, J.N.; Murali, M.S. Separation and Recovery of Uranium, Neptunium, and Plutonium from High Level Waste Using Tributyl Phosphate: Countercurrent Studies with Simulated Waste Solution. *Sep. Sci. Technol.* **1998**, *33*, 1877.

87) Hirai, T.; Komasawa, I. Electro-Reductive Stripping of Vanadium in Solvent Extraction Process for Separation of Vanadium and Molybdenum Using Tri-*n*-octylmethylammonium Chloride. *Hydrometallurgy* **1993**, *33*, 73.

88) Horbez, D.; Strock, A. Coupling between Electrolysis and Liquid-Liquid Extraction in an Undivided Electrochemical Reactor: Applied to the Oxidation of Ce^{3+} to Ce^{4+} in an Emulsion Part I. Experimental. *J. Appl. Electrochem.* **1991**, *21*, 915.

89) Kedari, C.S.; Pandit, S.S.; Ramanujam, A. In Situ Electro-Oxidation and Liquid-Liquid Extraction of Cerium(IV) from Nitric Acid Medium Using Tributyl Phosphate and 2-Ethylhexyl Hydrogen 2-Ethylhexyl Phosphonate. *J. Radioanal. Nucl. Chem.* **1997**, *222*, 141.

90) Hirai, T.; Komasawa, I. Separation of Europium from Samarium and Gadolinium by Combination of Electrochemical Reduction and Solvent Extraction. *J. Chem. Eng. Jpn.* **1992**, *25*, 644.

91) Karalova, Z.I.; Lavrinovich, E.A.; Myasoedov, B.F. Use of Actinide in Uncommon Oxidation States for Their Extraction and Separation from Alkaline Solutions. *J. Radioanal. Nucl. Chem., Articles* **1992**, *159*, 259.

92) Adnet, J.M.; Donnet, L.; Brossard, P.; Bourges, J. The Selective Extraction of Americium from High Level Liquid Wastes. *Proc. Int'l Solv. Extr. Conf. '96* **1996**, 1297.

93) Petrich, G.; Galla, U.; Goldacker, H.; Schmieder, H. Electro Reduction Pulsed Column for the PUREX Process: Operational and Theoretical Results. *Chem. Eng. Sci.* **1986**, *41*, 981.

94) Schmieder, H.; Galla, U. Electrochemical Processes for Nuclear Fuel Reprocessing. *J. Appl. Electrochem.* **2000**, *30*, 201.

95) Ohki, A.; Takagi, M. Liquid-Liquid Extraction of Group IB Metal Ions by Thioethers. *Anal. Chim. Acta* **1984**, *159*, 245.

96) Hirai, T.; Komasawa, I. Separation of Ce from La/Ce/Nd Mixture by Photooxidation and

Liquid-Liquid Extraction. *J. Chem. Eng. Jpn.* **1996**, *29*, 731.

97) Hirai, T.; Onoe, N.; Komasawa, I. Separation of Europium from Samarium and Gadolinium by Combination of Photochemical Reduction and Solvent Extraction. *J. Chem. Eng. Jpn.* **1993**, *26*, 64.

98) Guesnet, P.; Sabot, J.L.; Bauer, D. Kinetics of Cobalt Oxidation in Solvent Extraction by 8-Quinolinol and KELEX 100. *J. Inorg. Nucl. Chem.* **1980**, *42*, 1459.

99) Sekine, T.; Ishii, T.; Sato, A.; Abdurahman, A. Oxidation of Cobalt(II) during Its Solvent Extraction with Acetylacetone. *Anal. Sci.* **1992**, *8*, 599.

100) Sekine, T.; Abdurahman, A.; Dung, N.T.K.; Tebakari, M. Oxidation of Cobalt(II) in Solvent Extraction Systems with β-Isopropyltropolone in the Presence of *p*-Benzoquinone. *Anal. Sci.* **1994**, *10*, 955.

101) Sekine, T.; Fujimoto, Y. Oxidation and Reduction of Manganese Acetylacetonate Complexes in Solvent Extraction Systems and in Organic Solvents by Atmospheric Oxygen. *Solv. Extr. Ion Exch.* **1986**, *4*, 121.

102) Sekine, T.; Ishii, T.; Fukaya, T. Oxidation of Metal Ions during Solvent Extraction of Manganese(II) with Benzoylacetone and Dibenzoylmethane. *Anal. Sci.* **1990**, *6*, 115.

103) Sekine, T.; Dung, N.T.K. Oxidation of Cerium(III) during Solvent Extraction with Benzoyltrifluoroacetone into Carbon Tetrachloride in the Absence and Presence of Tetrabutylammonium Ions. *Anal. Sci.* **1993**, *9*, 361.

104) Hokura, A.; Dung, N.T.K.; Sekine, T. Oxidation and Reduction of Cerium during Solvent Extraction with Benzoyltrifluoroacetone into Nonpolar Organic Solvents in the Absence and Presence of Trioctylphosphine Oxide. *Proc. Int'l Solv. Extr. Conf. '96* **1996**, 81.

105) Hirai, T.; Onoe, N.; Komasawa, I. High-Performance Separation Process of Eu from a Sm/Eu/Gd Mixture by Liquid-Liquid Extraction Combined with a Photoredox Reaction (in Japanese). *Bunseki Kagaku* **1993**, *42*, 681.

106) Hirai, T.; Komasawa, I. Separation of Eu from Sm/Eu/Gd Mixture by Photoreductive Stripping in Solvent Extraction Process. *Ind. Eng. Chem. Res.* **1995**, *34*, 237.

107) Hirai, T.; Onoe, N.; Komasawa, I. Photoreductive Stripping of Vanadium in Solvent Extraction Process for Separation of Vanadium and Molybdenum. *J. Chem. Eng. Jpn.* **1993**, *26*, 416.

108) Hirai, T.; Manabe T.; Komasawa, I. The Effect of Formic Acid on Photoreductive Stripping of Vanadium in Liquid-Liquid Extraction Process of Vanadium and Molybdenum. *J. Chem. Eng. Jpn.* **1995**, *28*, 486.

109) Hirai, T.; Manabe, T.; Komasawa, I. Photoreductive Stripping of Vanadium Using 2-Propanol as Radical Scavenger in Liquid-Liquid Extraction Process of Vanadium and Molybdenum. *J. Chem. Eng. Jpn.* **1997**, *30*, 268.

110) Gagliardi, L.; Handy, N.C.; Skylaris, C.K.; Willetts, A. A Theoretical Study of Plutonium Diketone Complexes for Solvent Extraction. *Chem. Phys.* **2000**, *252*, 47.

111) Bard, A.J.; Parsons, R.; Jordan, J. *Standard Potentials in Aqueous Solutions*; Marcel Dekker: New York, 1985.

112) Donohue, T. Photochemical Separation of Europium from Lanthanide Mixtures in Aqueous Solution. *J. Chem. Phys.* **1977**, *67*, 5402.

113) Jeliazkowa, B.G.; Nakamura, S.; Fukutomi, H. Photochemical Reduction of Vanadium(V) in Aqueous Perchloric Acid Solutions. *Bull. Chem. Soc. Jpn.* **1975**, *48*, 347.

114) Boca, R.; Baran, P.; Dlhan, L.; Sima, J.; Wiesinger, G.; Renz, F.; El-Ayaan, U.; Linert, W. Complete Spin Crossover in Tris(pyridylbenzimidazole) Iron(II). *Polyhedron* **1996**, *16*, 47.

115) Donohue, T. Photoreduction of Ytterbium and Samarium. *Rare Earths Mod. Sci. Technol.* **1982**, *3*, 223.

116) Iwai, M.; Majima, H.; Izaki, T. A Kinetic Study on The Oxidation of Ferrous Ion with Dissolved Molecular Oxygen (in Japanese). *Denki Kagaku* **1979**, *47*, 409.

117) Huang, T.C.; Huang, C.T. Kinetics of the Extraction of Uranium(VI) from Nitric Acid Solutions with Bis(2-ethylhexyl)phosphoric Acid. *Ind. Eng. Chem. Res.* **1988**, *27*, 1675.

118) Skarbo, R.R. Cobalt Stripping. U.S. Patent 3,849,534, 1974.

119) Ritcey, G.M.; Ashbrook, A.W. *Solvent Extraction Part II; Elsevier*: New York, 1979.

120) Ritcey, G.M. Commercial Processes for Nickel and Cobalt. In *Handbook of Solvent Extraction*; Lo, T.C., Baird, M.H.I., Hanson, C., Eds.; John Wiley & Sons: New York, 1983.

121) Kakoi, T.; Ura, T.; Kasaini, H.; Goto, M.; Nakashio, F. Separation of Cobalt and Nickel

by Surfactant Membranes Containing a Synthesized Cationic Surfactant. *Sep. Sci. Technol.* **1998**, *33*, 1163.

122) Hoffman, B.M.; Diemente, D.L.; Basolo, F. Electron Paramagnetic Resonance Studies of Some Cobalt(II) Schiff Base Compounds and Their Monomeric Oxygen Adducts. *J. Am. Chem. Soc.* **1970**, *92*, 61.

123) Drago, R.S.; Cannady, J.P.; Leslie, K.A. Hydrogen-Bonding Interactions Involving Metal – Bound Dioxygen. *J. Am. Chem. Soc.* **1980**, *102*, 6014.

124) Wong, C.L.; Switzer, J.A.; Balakrishnan, K.P.; Endicott, J.F. Oxidation-Reduction Reactions of Complexes with Macrocyclic Ligands. Oxygen Uptake Kinetics, Equilibria, and Intermediates in Aqueous $Co^{II}(N_4)$ Systems. *J. Am. Chem. Soc.* **1980**, *102*, 5511.

125) Vaska, L. Dioxygen-Metal Complexes: Toward a Unified View. *Acc. Chem. Res.* **1976**, *9*, 175.

126) Kawamura, W.; Miyake, T.; Sato, I.; Okazaki, K. Apparatus for Separation of Elements from High-Level Radioactive Waste Solutions by Photoreduction-Solvent-Extraction Method. Japan Kokai Tokkyo Koho JP5297185, 1993.

127) Yoshizawa, H.; Uemura, Y.; Kawano, Y.; Hatate, Y. Preparation and Extraction Properties of Microcapsules Containing Tri-*n*-Octyl Amine as Core Material. *J. Chem. Eng. Jpn.* **1993**, *26*, 198.

128) Watarai, H. Microcapsule-A New Efficient Separation Medium (in Japanese). *Kagaku to Kogyo* **1994**, *47*, 1542.

List of Publications

Papers:

1 Nishihama, S.; Hirai, T.; Komasawa, I. Separation and Recovery of Gallium and Indium from Simulated Zinc Refinery Residue by Liquid-Liquid Extraction. *Ind. Eng. Chem. Res.* **1999**, *38*, 1032.

2. Nishihama, S.; Hirai, T.; Komasawa, I. Mechanism of Photoreductive Stripping of Iron(III) in a Liquid-Liquid Extraction System and Its Application for a Hydrometallurgical Process. *Ind. Eng. Chem. Res.* **1999**, *38*, 4850.

3. Nishihama, S.; Hirai, T.; Komasawa, I. Design of Liquid-Liquid Extraction Process for Separation of Metal Ions (short review, in Japanese). *Kagaku Kogaku Ronbunshu* **2000**, *26*, 497.

4. Nishihama, S.; Hirai, T.; Komasawa, I. Selective Extraction of Y from a Ho/Y/Er Mixture by Liquid-Liquid Extraction in the Presence of a Water-Soluble Complexing Agent. *Ind. Eng. Chem. Res.* **2000**, *39*, 3907.

5. Nishihama, S.; Sakaguchi, N.; Hirai, T.; Komasawa, I. Extraction and Separation of Heavy Rare Earth Metals in the Presence of Diethylenetriaminepentaacetic Acid. *Solv. Extr. Res. Dev. Japan* **2000**, *7*, 159.

6. Nishihama, S.; Hirai, T.; Komasawa, I. Mechanism of Photoreductive Extraction of Vanadium in a Liquid-Liquid Extraction System Using Bis(2-ethylhexyl)phosphoric Acid. *Ind. Eng. Chem. Res.* **2000**, *39*, 3018.

7. Nishihama, S.; Sakaguchi, N.; Hirai, T.; Komasawa, I. Photoreductive Stripping of Cobalt Loaded on Hydroxyoxime Extractant in a Liquid-Liquid Extraction System. *Ind. Eng. Chem. Res.* **2000**, *39*, 4986.

8. Nishihama, S.; Hirai, T.; Komasawa, I. High Functional Liquid-Liquid Extraction System Using Photochemical Reduction for Metal Ions. *Solv. Extr. Res. Dev. Japan* submitted.

9. Nishihama, S.; Hirai, T.; Komasawa, I. Advanced Liquid-Liquid Extraction Systems for the Separation of Metal Ions by Combination of the Conversion of the Metal Species with Chemical Reaction (review work). *Ind. Eng. Chem. Res.* submitted.

Related Works:

1. Hino, A.; Nishihama, S.; Hirai, T.; Komasawa, I. Practical Study of Liquid-Liquid Extraction Process for Separation of Rare Earth Elements with Bis(2-ethylhexyl)phosphinic Acid. *J. Chem. Eng. Japan* **1997**, *30*, 1040.

2. Nishihama, S.; Hino, A.; Hirai, T.; Komasawa, I. Extraction and Separation of Gallium and Indium from Aqueous Chloride Solution Using Several Organophosphorus Compounds as Extractants. *J. Chem. Eng. Japan* **1998**, *31*, 818.

Proceedings:

1. Nishihama, S.; Hirai, T.; Komasawa, I. Separation and Recovery Process of Gallium and Indium from Zinc Refinery Residue. *Proc. Int. Solv. Extr. Conf. (ISEC '99)* in press.

2. Nishihama, S.; Hirai, T.; Komasawa, I. Photoreductive Stripping of Iron in the Liquid-Liquid Extraction System and Its Application for Hydrometallurgical Process (in Japanese). *Chem. Eng. Symp. Ser.* **2000**, *74*, 76.

Patent:

1. Hino, A.; Komasawa, I.; Hirai, T.; Nishihama, S. Method for Separation and Recovery of Rare Earth Metal Ions. *Japan Kokai Tokkyo Koho*, JP11100622, 1999.

Acknowledgement